IFT - UNESP
INSTITUTO DE FÍSICA TEÓRICA

unesp
UNIVERSIDADE ESTADUAL PAULISTA
"JÚLIO DE MESQUITA FILHO"

Doctoral Thesis IFT-T.003/20

Probing the Unruh effect

Gabriel Cozzella

July, 2020

IFT - UNESP
INSTITUTO DE FÍSICA TEÓRICA

unesp
UNIVERSIDADE ESTADUAL PAULISTA
"JÚLIO DE MESQUITA FILHO"

Tese de doutoramento IFT–T.003/20

Sondando o efeito Unruh

Gabriel Cozzella

Tese apresentada ao Programa de Pós Graduação em Física do Instituto de Física Teórica da Universidade Estadual Paulista como parte dos requisitos para obtenção do título de Doutor em Física.

Orientador - George Emanuel Avraam Matsas

Julho, 2020

Cozzella, Gabriel.
C882p Probing the Unruh effect / Gabriel Cozzella. – São Paulo, 2020
85 f. : il.

Tese (doutorado) – Universidade Estadual Paulista (Unesp), Instituto de Física Teórica (IFT), São Paulo
Orientador: George Emanuel Avraam Matsas

1. Teoria quântica de campos. 2. Neutrinos. 3. Gravitação. I. Título

Sistema de geração automática de fichas catalográficas da Unesp. Biblioteca do Instituto de Física Teórica (IFT), São Paulo. Dados fornecidos pelo autor(a).

To my parents and to my bride.

Acknowledgments

This thesis is the result of four years of work in collaboration with multiple people who not only made writing this possible but also enriched my professional and personal life in many different ways.

First and foremost, I would like to thank my supervisor George Matsas for all our years working together. Not only you showed the utmost patience in mentoring me but also always went a great length to make me understand what being a good scientist (and a good human being in general) really means. I hope our friendship endures for as long as observers need to accelerate for perfect validity of the Unruh effect.

To all my co-authors, whose ideas improved greatly whatever initial draft I had or idea I proposed. Particularly, I would like to thank André Landulfo for his role as an informal co-supervisor of this thesis and Carlo Giunti for proposing a very interesting *impromptu* collaboration.

To my friends and colleagues at the IFT who made the time I spent there worthwhile. Particular thanks to Ernane for the TeX template used here.

To Alexssandre, Bruno, Jesuel, João and Pedro for entertaining discussions during various conferences, meetings and conversations.

To my friends of T20, Mateus and Ulisses, who always had a way of lightening up the mood in the worst of situations, especially in our (almost traditional now) annual meetings.

To my grandparents who supported me, each in their own way, along this journey.

To my childhood friends, Cauê, Edgar, Fabio, Lucas, Marcos and Ricardo. *We won!*

To my father, Marcos, who gave me the initial kick to go into this scientific path.

To my mother, Silvia, who endured so much during this period and yet always remained the most caring and loving person in the world. You were always there for me even when I did not deserve it. Thank you for everything.

Finally, to my bride, Raquel. None of these words would be written here if you were not by my side all these long years, listening, laughing, caring and loving me. We belong together according to any observer's point of view. *Te amo demais da conta, sô!*

This thesis was financially supported by *Fundação de Amparo à Pesquisa do Estado de São Paulo*, FAPESP, under grant 2016/08025-0, and *Coordenação de Aperfeiçoamento de Pessoal de Nível Superior*, CAPES.

Abstract

Quantum field theory in curved spacetimes (QFTCS) and semi-classical gravity are the best frameworks we have for understanding the interplay between gravitational physics and quantum theory. Here we study one well-known effect derived from QFTCS, namely, the Unruh effect. Our focus is on how the Unruh effect is required for the internal consistency of quantum field theories and how it may be experimentally probed in the near-future. Specifically, we focus on showing that the Unruh effect is perfectly compatible with mixing neutrinos and on how it can be observed using classical electromagnetic radiation. For completeness, we also present a spin-off work dealing with phenomenological flavor neutrino states which arose from our study of this subject in the context of the Unruh effect.

This doctoral thesis is mainly based on the following original work published by the author:

- Phys. Rev. Lett. 118, 161102 (2017) in collaboration with André G. S. Landulfo, George E. A. Matsas and Daniel A. T. Vanzella [1][I];
- Int. J. of Mod. Phys., Vol. 27, No. 11, 1843008 (2018) in collaboration with André G. S. Landulfo, George E. A. Matsas and Daniel A. T. Vanzella [2];
- Phys. Rev. D 97, 105022 (2018) in collaboration with Stephen A. Fulling, André G. S. Landulfo, George E. A. Matsas and Daniel A. T. Vanzella [3];
- Phys. Rev. D 98, 096010 (2018) in collaboration with Carlo Giunti [4].

Key-words: Quantum field theory, curved spacetimes, Unruh effect, neutrinos.
Field of knowledge: Particle physics, high-enegy physics, gravitation.

[I] Highligthed in a press report by *Science*, https://www.sciencemag.org/news/2017/04/does-space-heat-when-you-accelerate-physicists-propose-test-controversial-idea, and also by *Revista FAPESP*, https://revistapesquisa.fapesp.br/en/2018/09/05/when-vacuum-is-hot/.

Abstract in Portuguese

A teoria quântica de campos em espaços-tempos curvos (TQCEC) e a gravitação semiclássica são os melhores arcabouços teóricos que temos atualmente para entender fenômenos que envolvam a interação entre a física gravitacional e a teoria quântica. Nesta tese focamos em um fenômeno bem conhecido derivado destes arcabouços, o efeito Unruh. Nosso interesse é em como o efeito Unruh é necessário para a consistência interna de teorias quânticas de campos e como isso pode ser observado experimentalmente no futuro próximo. Mais especificamente, mostramos que o efeito Unruh é perfeitamente compatível com neutrinos com mistura de sabor e como o efeito pode ser observado utilizando radiação eletromagnética clássica. Por questão de completude, também apresentamos um estudo correlato tratando de estados fenomenológicos de neutrinos de sabor, resultado dos nossos estudos sobre este tema no contexto do efeito Unruh.

Esta tese de doutorado é baseada principalmente nos seguintes trabalhos realizados pelo autor:

- Phys. Rev. Lett. 118, 161102 (2017) em colaboração com André G. S. Landulfo, George E. A. Matsas e Daniel A. T. Vanzella [1][II];
- Int. J. of Mod. Phys., Vol. 27, No. 11, 1843008 (2018) em colaboração com André G. S. Landulfo, George E. A. Matsas e Daniel A. T. Vanzella [2];
- Phys. Rev. D 97, 105022 (2018) em colaboração com Stephen A. Fulling, André G. S. Landulfo, George E. A. Matsas e Daniel A. T. Vanzella [3];
- Phys. Rev. D 98, 096010 (2018) em colaboração com Carlo Giunti [4].

Palavras-chaves: Teoria quântica de campos, espaços-tempo curvos, efeito Unruh, neutrinos.
Áreas do conhecimento: Física de partículas, física de altas-energias, gravitação.

[II] Destacado em uma reportagem pela *Science*, https://www.sciencemag.org/news/2017/04/does-space-heat-when-you-accelerate-physicists-propose-test-controversial-idea, e também pela *Revista FAPESP*, https://revistapesquisa.fapesp.br/en/2018/09/05/when-vacuum-is-hot/.

List of Figures

2.1 The left and right Rindler wedges (LR/RR), along with the expanding/contracting degenerate Krasner universes (EDK/CDK). Figure taken from [21] with permission. 12

3.1 Feynman diagrams for the semi-classical inverse β-decay according to inertial observers. 33
3.2 Feynman diagrams for the semi-classical inverse β-decay according to Rindler observers. 38

4.1 Interaction rate per transverse momenta for different temperatures of the Rindler thermal bath. The values of the chosen parameters are explained in Sec. 4.3. 47
4.2 Experiment representation. After setting appropriate electric and magnetic fields to create the described 4-current, we inject a bunch of electrons into the cylinder with an opening in the middle, from where radiation is collected by a sphere of electromagnetic detectors. 48
4.3 Relation between the angular quantum number m seen in the Rindler frame (above) and in the Minkowski frame (below). 53
4.4 Exclusion region where the theory does not approximate the expected experimental result due to boundary effects. 54
4.5 Exclusion regions due to background sources. 55

Notations and conventions

- Except where otherwise stated, we work with units where $c = \hbar = G = k_b = 1$.
- We work in 3+1 dimensional spacetime unless stated otherwise. The metric signature is mostly minus, i.e., $(+,-,-,-)$.
- $\sqrt{-g}$ stands for the square root of minus the metric determinant $g \equiv det(g_{\mu\nu})$.
- Sums and integrals with no range explicitly shown are understood to cover the entire range of the relevant variable (e.g., $\sum_m \equiv \sum_{m=-\infty}^{+\infty}$ if $m \in \mathbb{Z}$, $\int dx \equiv \int_{-\infty}^{+\infty} dx$ if $x \in \mathbb{R}$).
- The Pauli matrices $\sigma_x, \sigma_y, \sigma_z$ are given by

$$\sigma_x = \begin{pmatrix} 0 & 1 \\ 1 & 0 \end{pmatrix}, \ \sigma_y = \begin{pmatrix} 0 & -i \\ i & 0 \end{pmatrix}, \ \sigma_z = \begin{pmatrix} 1 & 0 \\ 0 & -1 \end{pmatrix}.$$

Contents

1 Introduction **2**

2 The Unruh effect **6**
2.1 Quantum field theory and Bogoliubov transformations . . . 7
2.2 The Unruh effect in flat spacetime . . . 11
2.3 The Unruh-DeWitt detector . . . 17
2.3.1 The detector as a two-level system . . . 18
2.3.2 Excitation rate according to Minkowski observers . . . 18
2.3.3 Excitation rate according to Rindler observers . . . 20

3 The Unruh effect for mixing neutrinos **24**
3.1 The inverse beta decay . . . 25
3.2 Fermi theory and the decay rate for the inverse beta decay . . . 27
3.3 Inertial point of view . . . 28
3.4 Accelerated point of view . . . 33

4 Proposal for observing the Unruh effect with classical electrodynamics **40**
4.1 Rindler particles . . . 41
4.2 Observing the Unruh effect with electromagnetic radiation . . . 42
4.2.1 Rindler observers' proposal . . . 42
4.2.2 Inertial observers' confirmation . . . 48
4.3 Experimental proposal . . . 53

5 Conclusion **56**

Appendices **60**

A Extending the definition of flavor neutrino states **62**
A.1 Flavor states for single-neutrino processes . . . 63
A.2 Flavor states for multiple-neutrino processes . . . 66

B *Mathematica*© code used for calculating amplitudes of Chapter 3 **70**
B.1 Code used for calculating Eq. (3.24) . . . 71
B.2 Code used for obtaining the spin sums in Eq. (3.51) and subsequent similar calculations . . . 74

C Total proper time correspondence **78**

Bibliography **82**

CHAPTER 1

Introduction

A harmonious synthesis (and an understanding thereof) between quantum theory and relativity has arguably been one of the major undertakings of theoretical physics since the beginning of the 20th century. While *special* relativity and quantum mechanics together gave birth to the framework of *quantum field theory* (QFT), with astonishing experimental success, the situation regarding *general* relativity and quantum mechanics is less satisfying.

Initial attempts to apply lessons learned from quantizing the electromagnetic field to the gravitational one failed due to the issue of non-renormalizability [5]. Despite being possible to quantize linear perturbations of the gravitational field and interpret them in the framework of effective field theories (as it is done with most QFTs nowadays) [6], simple questions such as what is the spacetime resulting from a spatial superposition of a massive particle are still hard to answer due to the unique fact that the gravitational field is not simply a field living in a spacetime, but *part of spacetime itself* (along with the underlying manifold). Moreover, since it endows spacetime with a causal structure, the physical content of a fully non-perturbative quantum theory of gravity probably will be very hard to grasp [7].

Progress, we hope, can be made by better understanding phenomena at the low-energy level[I] on the interface between gravity and quantum mechanics: we begin with a quantum field theory initially defined over flat spacetime and consider it instead on a *fixed* curved background in such a way as to include at least some gravitational phenomena. This procedure gives us a *quantum field theory in curved spacetime* (QFTCS) [8, 9, 10, 11, 12, 13]. A further (and more ambitious) step, including how quantum matter fields influence the gravitational field (i.e., *back-reaction*), takes us into the realm of *semi-classical gravity* [8, 14].

While several frameworks for a theory of quantum gravity were created in the last decades [15], none has any kind of strong experimental support or can claim to be agreed by the majority of the high-energy physics community. For this reason, QFTCS and semi-classical gravity can be argued to be the safest bets in uncovering phenomena that a full theory of quantum gravity must eventually reproduce in its low energy limit. This is the case for the most preeminent example of such phenomena, Hawking radiation [16].

Along with Hawking radiation and particle creation in inflationary universes, another important discovery stemming from the framework of QFTCS is the *Unruh effect* [17]. Originally discovered in the context of better understanding Hawking radiation in curved spacetimes, the Unruh effect is applicable even in flat Minkowski spacetime, where it says that *while inertial observers see no particles when fields are in their inertial vacuum state, uniformly linearly accelerated observers (also called Rindler observers) see a thermal state of particles at a temperature T_U, proportional to their proper acceleration a*, i.e.,

$$T_U = \frac{\hbar a}{2\pi k_B c}, \tag{1.1}$$

in standard units.

[I] Compared to the Planck scale.

Pictorially, this means that while inertial observers may freeze to death at 0 K, Rindler ones may instead burn to death (at high enough accelerations)! Initially unveiled in 1976 (although already communicated previously in a talk one year before, see [18]), the Unruh effect has garnered steadily increasing attention during the ensuing years. It is easy to see why: the Unruh effect teaches us, in the simplest setting possible (Minkowski spacetime), that even for free quantum fields the vacuum is non-unique, that what a particle is turns out to be an observer-dependent concept [19], that particles can have non-zero momenta even with zero energy [20], among other fascinating things (see [21] for an extensive review).

A lot has been and still is debated about the "reality" of the particles seen by accelerated observers[II]. However, despite the counter-intuitive phenomena seen in the Rindler frame associated with the Unruh thermal bath, the Unruh effect is *as essential to the consistency of quantum field theory as inertial forces are to the consistency of classical mechanics*. Theoretical agreement between inertial and accelerated observers predictions has been shown to hold in a myriad of physical settings, from simple massless scalar fields to mixing neutrinos [3] and extensive bodies [22].

On the other hand, in contrast to inertial forces, observing the Unruh effect directly is a daunting task: from Eq. (1.1) we see that a thermal bath of 1 K requires an acceleration of order $10^{20} m/s^2$, which no macroscopic material known today would be able to withstand. For this reason, we believe that there are two reasonable strategies that can be adopted to gather experimental evidence for the Unruh effect.

The first is the use of analogue systems to probe the Unruh thermal bath (see, e.g., [23]). The advantages of this strategy are that (i) the speed of light appearing in Eq. (1.1) ceases to be the relevant speed scale, being substituted by the speed of small perturbations (commonly called *sound*) in the material medium, which, being much smaller than c, boosts T_U and (ii) higher "analogue" accelerations can be achieved in the laboratory.

The second strategy, which is more in line with the work presented here, is to find real (i.e., non-analogue) physical phenomena that can be easily and demonstrably interpreted in terms of the Unruh effect. Since the advent of analogue models is a recent development, this has been the path historically trod, an early example being interpreting depolarization of electrons' spins in storage rings in terms of the Unruh thermal bath [24].

With today's acceleration and optical technology, both these strategies present reasonable chances of claiming an experimental observation of the Unruh effect in the near and mid-term future. For this very reason, a thorough understanding of *what* the Unruh effect is, *what* it predicts[III] and what are the requirements and limitations involved in experimentally observing it is needed.

[II] The news report by *Science* mentioned in the abstract contains a small sample of different opinions on this subject.

[III] Maybe even more importantly, what it *does not*.

The purpose of this thesis is to probe different aspects of the Unruh effect, paying particular attention to how it is needed for consistency of the QFT framework and how it can be experimentally observed. Specifically, we show in this doctoral thesis that:

- The Unruh effect is perfectly compatible even with more "exotic" fields such as mixing neutrino fields [3], contrary to claims made previously in the literature (see, e.g., [25], for the work which brought our attention to this topic).

- Signs of the Unruh effect can already be seen at the classical level in Larmor radiation. Moreover, we propose a conceptually simple experiment that may evidence this in the near future [1, 2].

For completeness, we also present a spin-off work, [4], which sprung from our studies of mixing neutrinos in the context of quantum field theory, where the phenomenological definition of flavor neutrino states is generalized to more complicated interaction processes involving multiple neutrinos. The outline of this thesis is as follows:

- Chapter 2 gives a brief introduction to the relevant tools of QFTCS necessary for understanding the Unruh effect, whose derivation is shown here. We also present the Unruh-DeWitt particle detector model.

- Chapter 3 discusses the application of the Unruh effect to multiple mixing neutrino fields and sheds light over controversies recently sparked on the literature.

- Chapter 4 discusses the Unruh effect and its relation to classical electrodynamics, with the aim of presenting a conceptually simple experimental proposal whose output could be clearly interpreted in terms of the Unruh effect. We also discuss some challenges of actually carrying out the experiment.

- Chapter 5 includes our conclusions and a discussion about future work.

In Appendix A we present a generalization of flavor neutrino states discussed in chapter 3, in Appendix B we present the *Mathematica*© code used for some calculations presented in this thesis and, finally, in Appendix C we discuss the physical meaning of an important mathematical identification made in Chapter 4.

CHAPTER 2

The Unruh effect

In this introductory chapter we give a short review of the Unruh effect. To this end, we first outline relevant aspects of quantum field theory in curved spacetimes (QFTCS), mainly focusing on how the particle notion in QFT is observer dependent and, therefore, not unique [19]. Afterwards, we show the Unruh effect for a massive scalar field in 3+1 dimensional flat spacetime and then apply all concepts discussed to the important case of the Unruh-DeWitt detector, which is a simplified model of a particle detector where directional degrees of freedom may be discarded.

Besides introducing the basic physics that pervades the work presented in this thesis and also setting our notation, this chapter (especially its last section) serves the important purpose of exemplifying some recurring techniques we will use in the following chapters, but which already appear here, although in simpler settings. The first section of this chapter is based mainly on Ref. [26] and the remaining ones on Ref. [21], where the interested reader can find a more thorough discussion of the topics presented here.

We assume the reader to have basic knowledge of quantum field theory in flat spacetime and general relativity. For a good introduction to the former, see Ref. [5], and for the latter, see Ref. [7].

2.1 Quantum field theory and Bogoliubov transformations

The starting point of most quantum field theories is a classical field theory to which a suitable quantization method is applied. The classical theory is usually defined in terms of a local Lagrangian (density), $\mathscr{L}$, which preserves covariance explicitly. We consider here, without loss of generality, a minimally coupled massive scalar field, whose Lagrangian is given by

$$\mathscr{L} = \frac{1}{2}\left(\nabla_\mu \Phi \nabla^\mu \Phi - m^2 \Phi^2\right). \tag{2.1}$$

The two most common methods of quantization are the canonical one, where the field and its conjugate momentum are promoted to operators satisfying canonical commutation relations, and the path integral method, where we perform a functional integration over the exponential of the action associated with $\mathscr{L}$. Both methods give us the same results, but different physical aspects may be more easily extracted from the theory using one or the other. In particular, a particle interpretation of field excitations is very simple to obtain in the canonical quantization method and for this reason we shall use it here.

The Euler-Lagrange equation derived from the Lagrangian in Eq. (2.1) is the Klein-Gordon equation in curved spacetime, i.e.,

$$(g^{\mu\nu}\nabla_\mu \nabla_\nu + m^2)\Phi = 0, \tag{2.2}$$

whose general solution depends on the form of the metric and boundary conditions and usually has no easily expressed closed analytical form.

However, for Minkowski spacetime, on which we shall focus for now, we can write a general solution for Eq. (2.2) in terms of the well-known plane wave *normal modes* (and their complex conjugates), i.e.,

$$f_{\vec{k}}(t,\vec{x}) = \frac{e^{-i\omega t + i\vec{k}\cdot\vec{x}}}{(2\pi)^{3/2}\sqrt{2\omega}}, \tag{2.3}$$

where the vector $\vec{k} \equiv (k_x, k_y, k_z)$ indexes the mode and ω satisfies the usual dispersion relation, i.e., $\omega = +\sqrt{|\vec{k}|^2 + m^2}$. The field then is given by the Fourier expansion

$$\Phi(t,\vec{x}) = \int \frac{d^3k}{(2\pi)^{3/2}} \frac{1}{\sqrt{2\omega}} \left(a_{\vec{k}} e^{-i\omega t + i\vec{k}\cdot\vec{x}} + c.c. \right), \tag{2.4}$$

where *c.c.* stands for the *complex conjugate* of the preceding term. We choose the normal modes to be orthonormalized according to the *Klein-Gordon inner product*

$$(f,g) \equiv -i \int d\Sigma^\mu (f \nabla_\mu g^* - g^* \nabla_\mu f), \tag{2.5}$$

where $d\Sigma^\mu$ is the future-oriented volume element of a Cauchy surface. They satisfy

$$(f_{\vec{k}}, f_{\vec{k}'}) = -(f^*_{\vec{k}}, f^*_{\vec{k}'}) = \delta^3(\vec{k} - \vec{k}'), \tag{2.6}$$

$$(f_{\vec{k}}, f^*_{\vec{k}'}) = 0, \tag{2.7}$$

for all $\vec{k}$ and $\vec{k}'$. In possession of the classical field solution, we promote now the coefficients $a_{\vec{k}}$ and $a^*_{\vec{k}}$ in Eq. (2.4) to operators $\hat{a}_{\vec{k}}$ and $\hat{a}^\dagger_{\vec{k}}$ which satisfy the usual harmonic-oscillator commutation relations, i.e.,

$$\left[\hat{a}_{\vec{k}}, \hat{a}_{\vec{k}'}\right] = \left[\hat{a}^\dagger_{\vec{k}}, \hat{a}^\dagger_{\vec{k}'}\right] = 0, \tag{2.8}$$

$$\left[\hat{a}_{\vec{k}}, \hat{a}^\dagger_{\vec{k}'}\right] = \delta^3(\vec{k} - \vec{k}'), \tag{2.9}$$

and we define a vacuum state of the field, called the *Minkowski vacuum state*, $|0_M\rangle$, as the state satisfying

$$\hat{a}_{\vec{k}} |0_M\rangle = 0, \qquad \forall \vec{k}. \tag{2.10}$$

This is the usual departure point of QFT in Minkowski spacetime. Particles are obtained by the action of creation operators over this vacuum state and interactions can be studied, e.g., using perturbation theory over the free Lagrangian to calculate scattering amplitudes or decay rates. For now let us explore the free theory in more detail.

From the functional form of $f_{\vec{k}}$, we see that these modes satisfy an eigenvalue equation, namely

$$i\partial_t f_{\vec{k}} = +\omega f_{\vec{k}}\,, \tag{2.11}$$

where ∂_t is a Killing field associated with the time-translation symmetry of Minkowski space-

time and also the generator of inertial observers' trajectories[I]. For this reason they are called *positive frequency* modes with respect to ∂_t. Their complex conjugate are then called *negative frequency* modes. This division is relevant because the coefficients of the *positive* modes are the ones promoted to annihilation operators (and those of the *negative* modes to creation operators). A clear separation between positive and negative frequency modes is what allow us to have a well defined particle concept (in the sense outlined in the previous paragraph) and it is intimately linked to the existence of time-translation symmetries in spacetime.

As the coefficients associated with the normal modes give rise to particles when promoted to operators, one may ask if the field expansion given by Eq. (2.4) is unique, since it seems we could then obtain a different particle interpretation of our theory if we use another set of modes to expand our solutions of the Klein-Gordon equation[II]. Suppose that instead of $f_{\vec{k}}$ we had a different set of orthonormalized normal modes, $g_{\vec{q}}$, indexed by another set of quantum numbers, $\vec{q}$, which we can also use to Fourier expand our field. Instead of Eq. (2.4) we would obtain

$$\Phi(t,\vec{x}) = \int d^3q \left(b_{\vec{q}} g_{\vec{q}} + c.c.\right). \tag{2.12}$$

When quantizing the field now, $b_{\vec{q}}$ and its conjugate would be promoted to operators satisfying the same commutation relations as $\hat{a}_{\vec{k}}$ and $\hat{a}^\dagger_{\vec{k}}$, but the operators $\hat{b}_{\vec{q}}$, in principle, *do not* necessarily define the same vacuum state as $\hat{a}_{\vec{k}}$. Since particles are given by excitations of the vacuum state, this implies that particle definitions may differ between different constructions of the field expansion. As we shall see explicitly in the next section, different observers have different natural field constructions and, therefore, *different definitions of what particles are.*

Not everything is devoid of absolute[III] meaning, though. Since we are describing the same field Φ, it must be possible to find a relation between these different constructions. This relation is known as a *Bogoliubov transformation* [27]. Using this fact, we have that

$$\Phi(t,\vec{x}) = \int d^3k \left(a_{\vec{k}} f_{\vec{k}} + a^*_{\vec{k}} f^*_{\vec{k}}\right) = \int d^3q \left(b_{\vec{q}} g_{\vec{q}} + b^*_{\vec{q}} g^*_{\vec{q}}\right), \tag{2.13}$$

Since both sets of normal modes (and their conjugates) must be able to express all solutions to the Klein-Gordon equation (i.e., be complete), they must be able to express one another. Therefore we can write

$$g_{\vec{q}} = \int d^3k \left(\alpha_{\vec{q},\vec{k}} f_{\vec{k}} + \beta_{\vec{q},\vec{k}} f^*_{\vec{k}}\right), \tag{2.14}$$

and

$$f_{\vec{k}} = \int d^3q \left(\alpha^*_{\vec{q},\vec{k}} g_{\vec{q}} - \beta_{\vec{q},\vec{k}} g^*_{\vec{q}}\right). \tag{2.15}$$

[I] A Killing field ξ^μ is such that $\nabla_{(\mu}\xi_{\nu)} = 0$, where $()$ is the symmetrization procedure.

[II] We take this opportunity to highlight the fact that particles are a *global* concept, depending on the solutions of the field equation *over all spacetime.*

[III] I.e., non-observer dependent.

The complex numbers $\alpha_{\vec{q},\vec{k}}$ and $\beta_{\vec{q},\vec{k}}$ are termed *Bogoliubov coefficients*. By use of the orthonormality relations of the modes, Eqs. (2.6) and (2.7), we can express them in terms of Klein-Gordon products between the different sets of modes. This gives

$$\alpha_{\vec{q},\vec{k}} = (g_{\vec{q}}, f_{\vec{k}}), \tag{2.16}$$

$$\beta_{\vec{q},\vec{k}} = -(g_{\vec{q}}, f^*_{\vec{k}}). \tag{2.17}$$

Using Eq. (2.13) we can relate both sets of expansion coefficients $a_{\vec{k}}$ and $b_{\vec{q}}$. In terms of their respective annihilation operators, we have

$$\hat{a}_{\vec{k}} = \int d^3q \left(\alpha_{\vec{q},\vec{k}}\hat{b}_{\vec{q}} + \beta^*_{\vec{q},\vec{k}}\hat{b}^\dagger_{\vec{q}}\right), \tag{2.18}$$

$$\hat{b}_{\vec{q}} = \int d^3k \left(\alpha^*_{\vec{q},\vec{k}}\hat{a}_{\vec{k}} - \beta^*_{\vec{q},\vec{k}}\hat{a}^\dagger_{\vec{k}}\right), \tag{2.19}$$

with the relation for creation operators being easily obtained by complex conjugation. For completeness, we note that from the orthonormality relations we can also obtain two constraints on the Bogoliubov coefficients, namely

$$\int d^3k \left(\alpha_{\vec{q},\vec{k}}\alpha^*_{\vec{q}',\vec{k}} - \beta_{\vec{q},\vec{k}}\beta^*_{\vec{q}',\vec{k}}\right) = \delta_{\vec{q},\vec{q}'}, \tag{2.20}$$

$$\int d^3k \left(\alpha_{\vec{q},\vec{k}}\alpha_{\vec{q}',\vec{k}} - \beta_{\vec{q},\vec{k}}\beta_{\vec{q}',\vec{k}}\right) = 0. \tag{2.21}$$

Notice that annihilation operators associated with one set of modes are written in terms of *both* creation and annihilation operators of the other set. *If* any of the $\beta_{\vec{q},\vec{k}}$ coefficients is non-zero then both sets of annihilation operators *do not* annihilate the same vacuum state. Putting it in another way, if there is any mixing between negative and positive frequency modes, the vacuum states associated with these modes are inequivalent and, as explained above, so is the definition of what is a particle. As the set $\left\{f_{\vec{k}}, f^*_{\vec{k}}\right\}$ is naturally associated with inertial observers (by being eigenfunctions of ∂_t), the set $\left\{g_{\vec{q}}, g^*_{\vec{q}}\right\}$ may, perhaps, be naturally associated with a different class of observers. If this is the case, then, *particles are an observer dependent concept*. This gives credence to the adage that *quantum field theory really is a theory of fields, not particles*.

This fact, although following directly from the mathematical structure of free quantum field theory, is not as widely known as one may expect. Historically, QFT arose to explain phenomena seen from the point of view of (approximately) inertial observers on Earth. As it so happens, *all inertial observers agree on their vacuum and particle definitions* (thanks to Poincaré invariance), rendering the previous discussion innocuous. However, changing the background spacetime or considering different classes of observers forces us again to think carefully about how we define particles.

The formalism presented here is applicable to a wide range of different phenomena such

as superconductivity [27][IV], inflation [10] and, most famously, the Hawking effect [16]. Although both in inflationary scenarios and in the Hawking effect we deal with curved spacetimes, as we shall see now, even in the simpler setting of flat spacetime the concept of a particle may be treacherous, being dependent on the state of motion of the observer. This leads us directly to the Unruh effect.

2.2 The Unruh effect in flat spacetime

Here we focus on deriving the Unruh effect in flat spacetime since it is in this arena we will work on in later chapters. The Unruh effect [17], succinctly, expresses the fact that *while inertial observers see no particles in their vacuum state, uniformly accelerated observers (Rindler observers) see a thermal bath of particles with a temperature proportional to their proper acceleration a, i.e., $T_U = a/2\pi$.*

This thermal bath can be interpreted as a specific type of particle-populated quantum state, which must be related to the no-particles Minkowski vacuum state somehow. Finding what is this relation amounts to finding what is the Bogoliubov transformation between normal modes associated with Rindler observers and inertial ones.

Since we already presented the normal modes obtained by inertial observers in flat spacetime, given by Eq. (2.3) (along with their complex conjugates), we shall concern us here with modes associated with observers following uniformly accelerated trajectories. For this reason we begin by writing the Klein-Gordon equation in coordinates more appropriate to them. The trajectories of Rindler observers are given by the orbits generated by the four-velocity

$$u^\mu(\tau) = (az(\tau,\xi), 0, 0, at(\tau,\xi)), \tag{2.22}$$

with

$$t(\tau,\xi) = a^{-1}e^{a\xi}\sinh(a\tau), \tag{2.23}$$

$$z(\tau,\xi) = a^{-1}e^{a\xi}\cosh(a\tau), \tag{2.24}$$

where $\tau \in (-\infty,+\infty)$ is proportional to the proper time of these observers, $\xi \in (-\infty,+\infty)$ characterizes the trajectory and a is an acceleration scale, fixed by being the proper acceleration of the observer at $\xi = 0$. We can invert Eqs. (2.23) and (2.24) to obtain

$$\tau(t,z) = a^{-1}\tanh^{-1}(t/z), \tag{2.25}$$

$$\xi(t,z) = (2a)^{-1}\ln[(az)^2 - (at)^2]. \tag{2.26}$$

Note that the (τ,ξ) set of coordinates only covers the region $|t| < z$. This region is called

[IV] In fact, although commonly used in high-energy physics, the idea of a Bogoliubov transformation arose originally in this context.

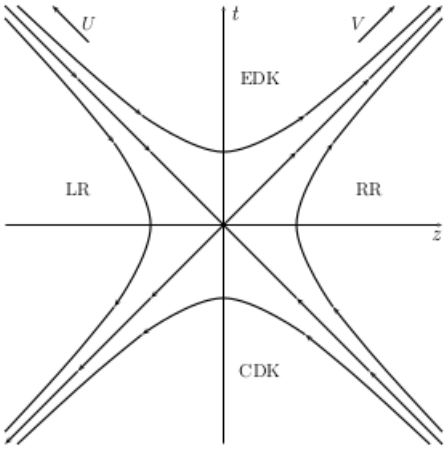

Figure 2.1: The left and right Rindler wedges (LR/RR), along with the expanding/contracting degenerate Krasner universes (EDK/CDK). Figure taken from [21] with permission.

the *right Rindler wedge*. We can cover the $|t| < -z$ region, i.e., the *left Rindler wedge*, by a similar set of coordinates, (τ',ξ'), but with the substitution $z \to -z$ in Eq. (2.24). Both wedges are needed to obtain a Cauchy surface for the whole Minkowski spacetime, allowing us to quantize the field over the whole spacetime and compare it with the quantization made by inertial observers over a Cauchy surface $t = 0$. The remaining regions of Minkowski spacetime (called *expanding/contracting degenerate Krasner universes*) cannot contain uniformly accelerated time-like trajectories as the ones generated by the four-velocity given in Eq. (2.22). A depiction of these regions is shown in Fig. 2.1. Let us focus on the right Rindler wedge for now.

In the (τ,ξ) coordinates, the four-velocity of our observers is simply ∂_τ. The line element is given by

$$ds^2 = e^{2a\xi}(d\tau^2 - d\xi^2) - dx^2 - dy^2, \tag{2.27}$$

and the Klein-Gordon equation, Eq. (2.2), can be written as

$$\left[\partial_\tau^2 - \partial_\xi^2 - e^{2a\xi}(\partial_x^2 + \partial_y^2 - m^2)\right]\Phi(\tau,\xi,\vec{x}_\perp) = 0, \tag{2.28}$$

where we have denoted (x, y) as $\vec{x}_\perp$. The symmetries of Eq. (2.28) suggest an ansatz of the form

$$g_{\vec{q}}(\tau,\xi,\vec{x}_\perp) \propto h_{\vec{q}}(\xi)e^{ik_x x + ik_y y - i\varpi\tau}, \tag{2.29}$$

where $\vec{q} \equiv (\varpi, k_x, k_y)$, $\varpi \in [0,\infty)$. Inserting it in Eq. (2.28) we obtain

$$\left[\partial_\xi^2 - (e^{2a\xi}l^2 - \varpi^2)\right]h_{\vec{q}}(\xi) = 0, \tag{2.30}$$

where we have defined $l \equiv \sqrt{k_x^2 + k_y^2 + m^2} \equiv \sqrt{|\vec{k}_\perp|^2 + m^2}$, with $\vec{k}_\perp = (k_x, k_y)$.

To find an unique solution to the above equation we impose two additional conditions: first that $h_{\vec{q}}(\xi)$ should not diverge as $\xi \to \infty$ and second that it must be normalized according

to the Klein-Gordon scalar product, Eq. (2.5), in such a way that $(g_{\vec{q}}, g_{\vec{q}'}) = \delta^3(\vec{q} - \vec{q}')$. This final condition requires us to choose a Cauchy surface to define $d\Sigma^\mu$. We can do so by defining $g_{\vec{q}} = 0$ on the left Rindler wedge and consider the $t = 0$ surface. Eventually, we extend the modes to cover the whole spacetime as explained in [8] or [21]. Imposing these conditions, the transformation $p = (l/a)e^{a\xi}$ reduces Eq. (2.30) to Eq. (8.494.1) of Ref. [28], giving us

$$g_{\vec{q}}(\tau, \xi, \vec{x}_\perp) = \left[\frac{\sinh(\pi\varpi/a)}{4\pi^4 a}\right]^{1/2} K_{i\varpi/a}\left(\frac{l}{a}e^{a\xi}\right) e^{i\vec{k}_\perp\cdot\vec{x}_\perp - i\varpi\tau}, \tag{2.31}$$

where the term in brackets comes from normalizing $g_{\vec{q}}$. In the same way that the modes given by Eq. (2.3) are positive frequency modes with respect to ∂_t, the modes $g_{\vec{q}}$ are positive frequency modes with respect to the generator of Rindler observers' trajectories, i.e., they satisfy

$$i\partial_\tau g_{\vec{q}} = +\varpi g_{\vec{q}}. \tag{2.32}$$

Another noteworthy feature of the modes $g_{\vec{q}}$ is that Eq. (2.28) *does not* impose a dispersion relation between ϖ and the transverse momentum $\vec{k}_\perp$. Since ϖ is the energy measured by a Rindler observer for a particle with quantum numbers $\vec{q} = (\varpi, \vec{k}_\perp)$, we can have a mode with arbitrarily low energy and arbitrary transverse momenta, *independent* from one another. In particular, a Rindler particle may have *zero* energy with *non-zero* momenta[V]. Although this may sound very counter-intuitive, the existence of such particles have profound physical consequences as we shall explore in more detail in Chapter 4.

Rindler modes on the left wedge, $g'_{\vec{q}}$, can be obtained from Eq. (2.31) by the substitution $(\tau, \xi) \to (\tau', \xi')$. Both sets $g_{\vec{q}}$ and $g'_{\vec{q}}$ taken together enable us to expand $\hat{\Phi}$ as

$$\hat{\Phi} = \int_0^\infty d\varpi \int d^2k_\perp \left[g_{\vec{q}}\hat{b}_{\vec{q}} + g^*_{\vec{q}}\hat{b}^\dagger_{\vec{q}} + g'_{\vec{q}}\hat{b}'_{\vec{q}} + g'^*_{\vec{q}}\hat{b}'^\dagger_{\vec{q}}\right], \tag{2.33}$$

where the creation and annihilation operators satisfy the usual commutation relations, with commutators between primed and unprimed operators vanishing. In the same way as the Minkowski vacuum state, the *Rindler vacuum* state, $|0_R\rangle$, is defined as the state which satisfies

$$\hat{b}_{\vec{q}}|0_R\rangle = 0, \quad \forall\vec{q}, \tag{2.34}$$

$$\hat{b}'_{\vec{q}}|0_R\rangle = 0, \quad \forall\vec{q}. \tag{2.35}$$

We emphasize that although we are quantizing the same field, *in principle*, $|0_M\rangle \neq |0_R\rangle$. This can only be decided by computing the Bogoliubov coefficients, a task to which we turn now.

First, we note that we have four types of coefficients, $\alpha_{\vec{q},\vec{k}}$, $\alpha'_{\vec{q},\vec{k}}$, $\beta_{\vec{q},\vec{k}}$ and $\beta'_{\vec{q},\vec{k}}$. Let us focus first on the unprimed ones (relative to the right Rindler wedge modes). Since both sets of modes contain exponentials of the type $e^{\pm ik_x x}$ and $e^{\pm ik_y y}$, we see that $\alpha_{\vec{q},\vec{k}}$ (and $\beta_{\vec{q},\vec{k}}$) are

[V] Note that this is independent of the mass.

zero unless the transverse momenta is the same for $\vec{k}$ and $\vec{q}$. Because of this, we simplify our notation for the coefficients to $\alpha_{\omega,k_z;\vec{k}_\perp}$ and $\beta_{\omega,k_z;\vec{k}_\perp}$. From Eq. (2.14) we obtain

$$g_{\vec{q}} = \left[\frac{\sinh(\pi\omega/a)}{4\pi^4 a}\right]^{1/2} K_{i\omega/a}\left(\frac{l}{a}e^{a\xi}\right) e^{i\vec{k}_\perp\cdot\vec{x}_\perp - i\omega\tau} = \tag{2.36}$$
$$\int dk_z \frac{e^{i\vec{k}_\perp\cdot\vec{x}_\perp}}{2\pi}\left[\alpha_{\omega,k_z;\vec{k}_\perp}\frac{e^{-i\omega t+ik_z z}}{\sqrt{4\pi\omega}} + \beta_{\omega,k_z;\vec{k}_\perp}\frac{e^{i\omega t-ik_z z}}{\sqrt{4\pi\omega}}\right].$$

To obtain the coefficients it is useful to study the behavior of the preceding equation at the $t \to z$ surface. Note that in this limit $\tau \to \infty$ and $\xi \to -\infty$. Being both divergent they are not the best set of coordinates to analyze Eq. (2.36). To this end, we introduce *light-cone* type coordinates $u = \tau - \xi$ and $v = \tau + \xi$. In the limit above, we have that $u \to \infty$ and v may have any finite value $v \to a^{-1}\ln(2az)$. Using the small argument limit of the modified Bessel function (Eq. (A10) of Ref. [21]), we obtain that

$$\frac{i}{2[a\sinh(\pi\omega/a)]^{1/2}}\left[\frac{(l/2a)^{i\omega/a}e^{-i\omega u}}{\Gamma(1+i\omega/a)} - \frac{(l/2a)^{-i\omega/a}e^{-i\omega v}}{\Gamma(1-i\omega/a)}\right]\Bigg|_{u\to\infty, v\to a^{-1}\ln(2az)} = \tag{2.37}$$
$$\int dk_z\left[\alpha_{\omega,k_z i;\vec{k}_\perp}\frac{e^{-i(\omega-k_z)z}}{\sqrt{4\pi\omega}} + \beta_{\omega,k_z;\vec{k}_\perp}\frac{e^{i(\omega-k_z)z}}{\sqrt{4\pi\omega}}\right].$$

The first term on the left-hand side is zero in a distributional sense due to its infinitely many oscillations. Multiplying both sides by $e^{i(\omega'-k'_z)z}$, where $\omega'^2 = l^2 + k_z'^2$ and integrating over z we obtain (after getting rid of the primes)

$$\alpha_{\omega,k_z;\vec{k}_\perp} = -\frac{i(\omega-k_z)}{2\left[\omega a\sinh(\pi\omega/a)\right]^{1/2}}\int_0^\infty dz\left[\frac{(l/2a)^{-i\omega/a}e^{i(\omega-k_z)z}e^{-i\omega a^{-1}\ln(2az)}}{\Gamma(1-i\omega/a)}\right], \tag{2.38}$$

where we have used the fact that the right Rindler modes have no support in the $z<0$ region. Eliminating l in favor of ω and k_z, we can solve the integral and find that

$$\alpha_{\omega,k_z;\vec{k}_\perp} = e^{\pi\omega/2a}(4\pi\omega a\sinh(\pi\omega/a))^{-1/2}\left(\frac{\omega+k_z}{\omega-k_z}\right)^{-i\omega/2a}. \tag{2.39}$$

A similar procedure gives us

$$\beta_{\omega,k_z;\vec{k}_\perp} = -e^{-\pi\omega/2a}(4\pi\omega a\sinh(\pi\omega/a))^{-1/2}\left(\frac{\omega+k_z}{\omega-k_z}\right)^{-i\omega/2a}. \tag{2.40}$$

To obtain the primed Bogoliubov coefficients (i.e., between f and g'), we use that the integrals for calculating them are the same as the previous ones if we make the substitution $k_z \to -k_z$. Therefore, $\alpha'_{\omega,k_z;\vec{k}_\perp} = \alpha_{\omega,-k_z;\vec{k}_\perp}$ and $\beta'_{\omega,k_z;\vec{k}_\perp} = \beta_{\omega,-k_z;\vec{k}_\perp}$. From the form of the Bo-

goliubov coefficients, we note that they satisfy the relations

$$\alpha'_{\omega,k_z;\vec{k}_\perp} = -e^{\pi\omega/a}\beta^*_{\omega,k_z;\vec{k}_\perp}, \tag{2.41}$$

$$\alpha_{\omega,k_z;\vec{k}_\perp} = -e^{\pi\omega/a}\beta'^*_{\omega,k_z;\vec{k}_\perp}. \tag{2.42}$$

By using the above relations, together with Eq. (2.36) and its primed counterpart, and noticing that the Bogoliubov coefficients are the same for $\vec{k}_\perp$ and $-\vec{k}_\perp$, we see that

$$u_{\omega,\vec{k}_\perp} = g_{\omega,\vec{k}_\perp} + e^{-\pi\omega/a}g'^*_{\omega,-\vec{k}_\perp}, \tag{2.43}$$

and

$$u'_{\omega,\vec{k}_\perp} = g'_{\omega,\vec{k}_\perp} + e^{-\pi\omega/a}g^*_{\omega,-\vec{k}_\perp}, \tag{2.44}$$

are both positive frequency modes with respect to ∂_t. Inverting the above relations, we can expand Eq. (2.33) in terms of the u and u' modes and see that the Minkowski vacuum is annihilated by the following combinations of Rindler annihilation and creation operators:

$$\left[\hat{b}_{\omega,\vec{k}_\perp} - e^{-\pi\omega/a}\hat{b}'^\dagger_{\omega,-\vec{k}_\perp}\right]|0_M\rangle = 0, \tag{2.45}$$

$$\left[\hat{b}'_{\omega,\vec{k}_\perp} - e^{-\pi\omega/a}\hat{b}^\dagger_{\omega,-\vec{k}_\perp}\right]|0_M\rangle = 0. \tag{2.46}$$

By multiplying by the left the first equation above by a right Rindler wedge creation operator, multiplying also by the left the second equation by a left Rindler wedge creation operator and considering it for $\vec{k}_\perp \to -\vec{k}_\perp$, after subtracting one from the other we obtain

$$\left[\hat{b}^\dagger_{\omega,\vec{k}_\perp}\hat{b}_{\omega,\vec{k}_\perp} - \hat{b}'^\dagger_{\omega,-\vec{k}_\perp}\hat{b}'_{\omega,-\vec{k}_\perp}\right]|0_M\rangle = 0. \tag{2.47}$$

This equation says that the Minkowski vacuum can be expanded in terms of the Rindler Fock space as a state with an equal number of left and right particles, i.e.,

$$|0_M\rangle = \bigotimes_{\omega,\vec{k}_\perp}\sum_{n=0}^{\infty} C^n_{\omega,\vec{k}_\perp}|n_{\omega,\vec{k}_\perp}, n'_{\omega,-\vec{k}_\perp}\rangle. \tag{2.48}$$

By plugging this *ansatz* in Eqs. (2.45) and (2.46) and taking into account the normalization condition $\langle 0_M|0_M\rangle = 1$, we find explicitly that

$$C^n_{\omega,\vec{k}_\perp} = \sqrt{1-e^{-2\pi\omega/a}}\,e^{-n\pi\omega/a}. \tag{2.49}$$

The state given by Eq. (2.48), however, is not the state observers restricted to either the right Rindler wedge or to left Rindler wedge must use to make physical predictions. From Figure 2.1 we see that no information from the region $t > z$ can reach the right Rindler wedge.

In the same way, no information from the region $t > -z$ may reach the left Rindler wedge. Physically, this means that all phenomena restricted to one wedge must be described by tracing out information regarding the other wedge. Tracing out, for instance, the left Rindler wedge we obtain a mixed state given by

$$\hat{\rho}_R = \bigotimes_{\varpi,\vec{k}_\perp} \sum_{n=0}^{\infty} |C^n_{\varpi,\vec{k}_\perp}|^2 |n_{\varpi,\vec{k}_\perp}\rangle\langle n_{\varpi,\vec{k}_\perp}|, \tag{2.50}$$

which written in full is

$$\hat{\rho}_R = \bigotimes_{\varpi,\vec{k}_\perp} \left(1 - e^{-2\pi\varpi/a}\right) \sum_{n=0}^{\infty} e^{-2n\pi\varpi/a} |n_{\varpi,\vec{k}_\perp}\rangle\langle n_{\varpi,\vec{k}_\perp}|. \tag{2.51}$$

The same result (with n' instead of n) would be obtained by tracing out the right Rindler wedge. Thus, we arrive at the conclusion that *the Minkowski vacuum, restricted to the right (left) Rindler wedge, is seen by Rindler observers as a thermal state with a temperature*

$$T_U = \frac{a}{2\pi}. \tag{2.52}$$

This is the Unruh effect.

Since both sets of observers, inertial and uniformly accelerated, although in very different ways, describe the same quantum state, all physical phenomena (restricted to the Rindler wedges) must be consistently described by either set of observers *if the Unruh effect is taken into account*. We give a simple example of this fact in the next section, while more elaborate phenomena are treated in Chapters 3 and 4.

Before doing so, however, let us briefly show a property of thermal states we will use throughout this thesis. Consider a thermal state of a single bosonic mode with energy ϖ. Suppose that we evolve this state by an evolution operator which at first order in a perturbative expansion is of the form $\hat{I} + \hat{V}$, where $\hat{V}$ can be written as

$$\hat{V} = V_{1\to 0}\,\hat{a} + V_{0\to 1}\,\hat{a}^\dagger. \tag{2.53}$$

If $\hat{V}$ is self-adjoint, this imposes that $V_{0\to 1} = (V_{1\to 0})^*$. Also,

$$V_{0\to 1} = \langle 1|\hat{V}|0\rangle. \tag{2.54}$$

For this kind of operator, the probabilities of finding the evolved state with an additional boson or one fewer boson are given by

$$p^b_{1^+} = \sum_n p_n \langle n+1|\hat{V}|n\rangle\langle n|\hat{V}^\dagger|n+1\rangle, \tag{2.55}$$

$$p^b_{1^-} = \sum_n p_n \langle n-1|\hat{V}|n\rangle\langle n|\hat{V}^\dagger|n-1\rangle, \tag{2.56}$$

respectively, where

$$p_n = \frac{e^{-\beta n\omega}}{\sum_n e^{-\beta n\omega}}. \tag{2.57}$$

Expanding Eqs. (2.55) and (2.56) we obtain

$$p^b_{1^+} = |V_{0\to 1}|^2[1 + n_b(\omega)], \tag{2.58}$$

$$p^b_{1^-} = |V_{1\to 0}|^2 n_b(\omega) = |V_{0\to 1}|^2 n_b(\omega), \tag{2.59}$$

where

$$n_b(\omega) = \frac{1}{e^{\beta\omega} - 1} \tag{2.60}$$

is the Bose-Einstein thermal factor. From this we see that the probability of emitting one particle or absorbing one particle depends mainly on the matrix element $V_{0\to 1}$, which is the amplitude of transition from the vacuum to the first excited state, the rest being automatically obtained from the structure of the thermal state. This property will appear many times in the following chapters. For the fermionic case, a similar result can be obtained, i.e.,

$$p^f_{1^+} = |V_{0\to 1}|^2[1 - n_f(\omega)], \tag{2.61}$$

$$p^f_{1^-} = |V_{1\to 0}|^2 n_f(\omega) = |V_{0\to 1}|^2 n_f(\omega), \tag{2.62}$$

where

$$n_f(\omega) = \frac{1}{e^{\beta\omega} + 1} \tag{2.63}$$

is the Fermi-Dirac thermal factor. These results can also easily be extended for the multiple particle case (as long as the interaction is only linear in all creation/annihilation operators involved). We shall make use of this in the next chapter. Before proceeding, let us see an example where the previous concepts can be applied.

2.3 The Unruh-DeWitt detector

One important application of the Unruh effect is exemplified by the Unruh-DeWitt detector [17, 29]. This detector models a way of probing the field locally (avoiding, in principle, referring to global constructs such as particles) and also reasonably approximates the interaction of an atom with an electromagnetic field, which is useful in quantum optics. In recent years it also has become the major workhorse for studying phenomena in relativistic quantum information (see, e.g., [30, 31], for recent examples).

Although all observables regarding the detector (e.g., its excitation rate) can be derived solely applying usual inertial QFT, the Unruh effect is fundamental to understand how consistency between results obtained by inertial and accelerated observers is achieved and thus guarantee covariance of the theory. In this section we define the detector's model, calcu-

late its excitation rate from both points of view and use the opportunity to dispel a common misconception regarding the relation of the Unruh effect with thermal baths of Minkowski particles.

2.3.1 The detector as a two-level system

The Unruh-DeWitt detector is usually constructed first by defining a free two level system. The Hilbert space of this system is spanned by the ground and excited energy eigenstates, $\{|g\rangle, |e\rangle\}$, of the free Hamiltonian

$$\hat{H}_{UDW} = \Delta |e\rangle\langle e|, \tag{2.64}$$

where Δ is the detector's energy gap (and we conveniently shifted the ground state energy to zero). The next step is defining an interaction between the free system and the field. We couple both via a linear interaction action

$$\hat{S}_I = \int d\tau c(\tau) \hat{m}(\tau) \hat{\Phi}(x_0^\mu(\tau)), \tag{2.65}$$

where $c(\tau)$ is called the *switching function*, controlling for how long the detector interacts with the field, $x_0^\mu(\tau)$ is the detector's trajectory parameterized by its proper time and $\hat{m}$ is a monopole operator coupling the excited and unexcited states, i.e.,

$$\hat{m}(\tau) = e^{-i\Delta\tau}\hat{\sigma}^- + e^{i\Delta\tau}\hat{\sigma}^+, \tag{2.66}$$

where $\sigma^- = |g\rangle\langle e|$ and $\sigma^+ = \sigma^{-,\dagger}$. More complicated versions of this model may be used, such as those including smearing, which are physically more realistic [32]. For our purposes, however, the simple model presented above will suffice.

2.3.2 Excitation rate according to Minkowski observers

We will take the detector trajectory to be uniformly accelerated with proper acceleration a in Minkowski spacetime, i.e., Eqs. (2.23) and (2.24) with $\xi = 0$, located at $\vec{x}_\perp = 0$. We also assume that the interaction between the detector and the field is always turned on in such a way that $c(\tau)$ can be regarded as constant[VI]. We will comment on the consequences of this assumption shortly. If we assume the field state to be the Minkowski vacuum, $|0_M\rangle$, the only way the detector can excite according to inertial observers is by emitting a scalar particle (there is nothing to be absorbed). From their point of view, the energy for exciting the detector and emitting a particle can be easily attributed to the external agent accelerating

[VI] A realistic detector would interact with the field only for a finite amount of time. If the total time of interaction is large with respect to a^{-1} and Δ^{-1}, the expression obtained for constant c gives a reasonable approximation of this situation. See [33] for a thorough discussion about this.

the detector via the work done over it.

The amplitude for the process described above, at first order in perturbation theory, is

$$A_{I,em} = -i\langle \vec{k}; e|\hat{S}_I|0_M; g\rangle. \tag{2.67}$$

By expanding the field as in Eq. (2.4) over the detector's trajectory we obtain that

$$A_{I,em} = -\frac{ic}{(2\pi)^{3/2}\sqrt{2\omega}}\int d\tau e^{i\Delta\tau}\exp\left[\frac{i\omega}{a}\sinh(a\tau) - \frac{ik_z}{a}\cosh(a\tau)\right], \tag{2.68}$$

where for simplicity we have absorbed $\langle e|\hat{m}(0)|g\rangle$ in the definition of c. Squaring the amplitude and making the transformations $\tau = s + \sigma/2$ and $\tau' = s - \sigma/2$ gives

$$|A_{I,em}|^2 = \frac{c^2}{16\pi^3\omega}\int ds\int d\sigma e^{i\Delta\sigma}\exp\left\{\frac{2i}{a}\sinh(a\sigma/2)\left[\omega\cosh(as) - k_z\sinh(as)\right]\right\}. \tag{2.69}$$

As we are not interested in what happens to the field, we integrate over the scalar quanta tri-momenta $\vec{k}$ to obtain the total probability of excitation as

$$P_{I,exc} = \frac{c^2}{16\pi^3}\int\frac{d^3k}{\omega}\int ds\int d\sigma e^{i\Delta\sigma}\exp\left\{\frac{2i}{a}\sinh(a\sigma/2)\left[\omega\cosh(as) - k_z\sinh(as)\right]\right\}. \tag{2.70}$$

Since we assumed c to be constant, the situation is stationary and the probability of emission itself diverges due to the infinite total proper time of the interaction. The meaningful physical quantity then is the probability of excitation *per unit of proper time*. Before obtaining it we must first make the divergence in Eq. (2.70) explicit. To do so we make a boost in the z direction, i.e.,

$$\omega' = \omega\cosh(as) - k_z\sinh(as), \tag{2.71}$$

$$k_z' = k_z\cosh(as) - \omega\sinh(as). \tag{2.72}$$

This transformation is such that $dk_z'/\omega' = dk_z/\omega$, due to the dispersion relation. Therefore, the probability in Eq. (2.70) can be rewritten as

$$P_{I,exc} = \underbrace{\left(\int ds\right)}_{\Delta\tau_R}\frac{c^2}{16\pi^3}\int\frac{d^3k}{\omega}\int d\sigma e^{i\Delta\sigma}\exp\left[\frac{2i\omega}{a}\sinh(a\sigma/2)\right], \tag{2.73}$$

where we have already relabelled the prime quantities to non-primed ones. With the infinite total proper time over the accelerated trajectory $\Delta\tau_R$ extracted, the excitation *rate*, $\Gamma_{I,exc}$, can be defined as

$$\Gamma_{I,exc} \equiv \frac{P_{I,exc}}{\Delta\tau_R} = \frac{c^2}{16\pi^3}\int\frac{d^3k}{\omega}\int d\sigma e^{i\Delta\sigma}\exp\left[\frac{2i\omega}{a}\sinh(a\sigma/2)\right]. \tag{2.74}$$

Let us separate the transverse and z directions in the integration measure by writing the transverse part in polar coordinates. Since $\omega^2 = |\vec{k}_\perp|^2 + k_z^2 \equiv k_\perp^2 + k_z^2$ this gives us

$$\Gamma_{I,exc} = \frac{c^2}{8\pi^2}\int_0^\infty dk_\perp k_\perp \int \frac{dk_z}{\omega}\int d\sigma e^{i\Delta\sigma}\exp\left[\frac{2i\omega}{a}\sinh(a\sigma/2)\right]. \tag{2.75}$$

Following Ref. [21] we solve the innermost double integral by first making the substitutions $\lambda = e^{a\sigma/2}$ and $\zeta = \frac{(\omega+k_z)}{\sqrt{k_\perp^2+m^2}}$ to obtain

$$\Gamma_{I,exc} = \frac{c^2}{4\pi^2 a}\int_0^\infty dk_\perp k_\perp \int_0^\infty \frac{d\zeta}{\zeta}\int_0^\infty \frac{d\lambda}{\lambda}\lambda^{2i\Delta/a-1}\exp\left[i(k_\perp^2+m^2)^{1/2}(\lambda-\lambda^{-1})(\zeta+\zeta^{-1})/(2a)\right]. \tag{2.76}$$

Further making $\alpha = \lambda\zeta$, $\beta = \frac{\zeta}{\lambda}$ and using the residue theorem to go to the complex positive axis along with Eq. (8.432.7) of Ref. [28] we obtain the excitation rate as

$$\Gamma_{I,exc} = \frac{c^2 e^{-\pi\Delta/a}}{2\pi^2}\int_0^\infty dk_\perp k_\perp \left[K_{i\Delta/a}\left(\frac{\sqrt{k_\perp^2+m^2}}{a}\right)\right]^2. \tag{2.77}$$

Note that the result given in Eq. (2.77) goes to 0 for $a \to 0$ as it should be and also decreases with a larger Δ (the bigger the gap, the harder it is to excite the detector). More importantly, if we calculate the de-excitation rate, $\Gamma_{I,dex}$, the result is the same except for the sign in the exponential. This means that the rates satisfy the *detailed balance condition*, i.e.,

$$\frac{\Gamma_{I,exc}}{\Gamma_{I,dex}} = \exp(-2\pi\Delta/a). \tag{2.78}$$

This is also valid, as we shall see below, for a *static* detector in flat spacetime immersed in a thermal bath of field quanta (if the gap satisfies $\Delta > m$). This is a further hint at a connection between thermality and interaction rates obtained for an uniformly accelerated detector. As one may expect, from the uniformly accelerated view this can be attributed to the Unruh effect. We show this explicitly now.

2.3.3 Excitation rate according to Rindler observers

A naive expectation is that we could calculate the excitation rate of the detector in the same way as from the inertial point of view but using Rindler modes. However, it is easily seen that this cannot be the case.

Due to energy conservation in their frame (where the detector is static), differently from the inertial point of view, there cannot be simultaneously an excitation and an emission of a particle. However, Rindler observers co-accelerated with the detector, according to the Unruh effect, see a thermal bath of particles at temperature $a/2\pi$ as discussed in Section 2.2. The only available physical process, then, is for the detector to absorb a Rindler par-

ticle and excite. This is an instance of a more general result that shows that each *emission* of a Minkowski particle (i.e., seen by inertial observers) corresponds to *either* an emission *or* absorption of a Rindler particle (i.e., seen by Rindler observers) [34]. Therefore we shall calculate the amplitude

$$A_{R,abs} = -i\langle 0_R; e|\hat{S}_I|\vec{q}; g\rangle, \tag{2.79}$$

where $\vec{q} = (\varpi, \vec{k}_\perp)$. Note that, as discussed at the end of Section 2.2, here we are calculating the amplitude using the Rindler vacuum, $|0_R\rangle$, as an intermediate step to calculate the total probability of absorption (which must then be weighted by an appropriate thermal factor).

Expanding the field in terms of Rindler modes, Eq. (2.31), and remembering that $l = +\sqrt{k_\perp^2 + m^2}$, we write the amplitude as

$$A_{R,abs} = -2\pi i c \left[\frac{\sinh(\pi\varpi/a)}{4\pi^4 a}\right]^{1/2} K_{i\varpi/a}\left(\frac{l}{a}\right)\delta(\varpi - \Delta), \tag{2.80}$$

where we have again absorbed $\langle e|\hat{m}(0)|g\rangle$ in the definition of c. The same caveat as before regarding the total duration of the interaction applies, so instead of calculating the probability of excitation we calculate the *rate* of excitation. Using the prescription

$$2\pi\delta(0) = \int_{-\infty}^{+\infty} d\tau = \Delta\tau_R, \tag{2.81}$$

we can write

$$\frac{|A_{R,abs}|^2}{\Delta\tau_R} = c^2\left[\frac{\sinh(\pi\varpi/a)}{2\pi^3 a}\right]\left|K_{i\varpi/a}\left(\frac{l}{a}\right)\right|^2\delta(\omega - \Delta), \tag{2.82}$$

which, taking into account the existence of the Unruh thermal bath in the uniformly accelerated frame, allow us to write the total rate of excitation according to Rindler observers as

$$\Gamma_{R,exc} \equiv \int_0^\infty d\varpi \int d^2k_\perp \frac{|A_{R,abs}|^2}{\Delta\tau_R} n_b(\varpi), \tag{2.83}$$

where $n_b(\varpi)$ is given in Eq. (2.60). Plugging Eq. (2.82) into Eq. (2.83), going to polar coordinates in the transverse momenta and integrating we have

$$\Gamma_{R,exc} = \frac{c^2 e^{-\pi\Delta/a}}{2\pi^2}\int_0^\infty dk_\perp k_\perp \left[K_{i\Delta/a}\left(\frac{\sqrt{k_\perp^2 + m^2}}{a}\right)\right]^2, \tag{2.84}$$

which is exactly the same as Eq. (2.77), i.e., $\Gamma_{I,exc} = \Gamma_{R,exc} \equiv \Gamma_{exc}$. This is true *only due to the Unruh effect being taken into account in the uniformly accelerated frame* via $n_b(\varpi)$. Were this not the case, the excitation rate would be identically zero according to Rindler observers, which would be a contradiction, since the excitation rate is a physical observable. It is also interesting to note how the calculation is drastically easier in the uniformly accelerated frame due to the presence of the δ function.

Before going to the next chapter, let us highlight an important point. Taking the $m \to 0$ limit, a nice closed expression can be found by using Eq. (6.521.3) of [28] (in the $a \to b$ limit), giving

$$\Gamma_{exc,m=0} = \frac{c^2}{2\pi} \frac{\Delta}{e^{2\pi\Delta/a} - 1}. \tag{2.85}$$

Let us now briefly calculate the excitation rate of an *inertial detector* immersed in a thermal bath at a temperature *numerically equal to* $T_U = a/2\pi$. It is a common misconception that this result will be the same as the one obtained using the Unruh effect, Eq. (2.84). As we shall see, this is not true in general.

The excitation rate in this case can be obtained *ab initio* by using the trajectory $x_0^\mu(\tau) = (t = \tau, \vec{x} = 0)$ and repeating the same procedure as in Section 2.3.2. It can also be quickly obtained as the $a \to 0$ limit of Eq. (2.74) with a thermal factor, Eq. (2.60), to account for the different field state and the substitution $\Delta \to -\Delta$ since now we must absorb a particle to excite the detector. This gives

$$\begin{aligned} \Gamma_{exc,T_U} &= \frac{c^2}{8\pi^2} \int \frac{d^3k}{\omega} \frac{\delta(\Delta - \omega)}{e^{2\pi\omega/a} - 1} \\ &= \frac{c^2}{2\pi} (\Delta^2 - m^2)^{1/2} \frac{\theta(\Delta - m)}{e^{2\pi\Delta/a} - 1}, \end{aligned} \tag{2.86}$$

which is clearly different from Eq. (2.84), *except* in the limit $m \to 0$, giving Eq. (2.85). This is enough to show that, in general, the Unruh effect does *not* say that an uniformly accelerated detector behaves in the same way as an inertial detector in a thermal bath at temperature $T_U = a/2\pi$, although some aspects of both situations are clearly the same due to the thermal character involved.

This ends our exposition of the basics regarding the Unruh effect. In the following chapters we apply this formalism to study two situations. First, whether the Unruh effect can be applied to mixing neutrino fields, a point of contention in the recent literature [25]. The study of the relation between the Unruh effect and Bremsstrahlung comes next.

CHAPTER 3

The Unruh effect for mixing neutrinos

In the preceding chapter we derived the Unruh effect for a free massive scalar field. However, the result is much more general: it is valid for any "reasonable" interacting QFT[I]. The equivalence between physical observables such as detector excitation rates has also been shown in more general settings, in particular for neutrino fields without mixing [35].

The behavior of neutrinos is probably the surest hint we have for physics beyond the Standard Model (SM). This rests on the fact that in the SM neutrinos are massless, while experiments, however, give resounding evidence that they are *massive* [36, 37]. When extending the SM to account for these experiments, however, we must also guarantee that this extension is also compatible with previous results from different areas of physics such as, of particular interest to us, the Unruh effect.

In this chapter we discuss a controversy sparked in the literature when trying to understand particle decays from the accelerated observers' point of view when mixing neutrinos are involved [25, 38]. We begin by laying out the interaction process we will be interested on, namely, the inverse beta decay. Then, we discuss what states we must use to describe neutrinos involved in the process. Finally, we show that when due care is taken, there is no incompatibility between inertial and accelerated observers' conclusions regarding the interaction rate for the inverse beta decay with multiple neutrinos.

3.1 The inverse beta decay

An important phenomenon in particle physics is the beta decay, namely

$$n^0 \to p^+ + e^- + \bar{\nu}_e, \tag{3.1}$$

where n^0, p^+, e^- and $\bar{\nu}_e$ stand for the neutron, proton, electron and electron neutrino (usually taken to be massless in calculations) respectively, since it was responsible for the discovery of the neutrino and for the development of one of the first models of the weak interaction, namely Fermi theory (later supplanted by electroweak theory) [5].

A less known process is the inverse beta decay,

$$p^+ \to n^0 + e^+ + \nu_e. \tag{3.2}$$

This decay, in contrast to Eq. (3.1), is not kinematically allowed if the proton is at rest, as the mass of the proton is smaller than the mass of the neutron. This process may happen, however, if the proton is uniformly accelerated, since an external agent may do work over the proton and this work ensures energy conservation.

It is interesting to analyze this process from the point of view of an observer riding along with the proton. In this case there is no work done (there is no displacement from this ob-

[I] Where by reasonable we mean satisfying the Wightman axioms.

server's point of view: the proton is always at rest). Since a decay is an event in spacetime and all observers must agree if it happened or not, how does this observer explains the decay?

This is exactly the same behavior seen with the Unruh-deWitt detector model presented in Section 2.3. By analogy, we see that the Unruh effect must come to the rescue: an uniformly accelerated observer sees the proton interacting with a thermal bath of particles (in this case, of electrons and neutrinos) in such a way that the total interaction rate from this point of view is exactly the same as the one that an inertial observer would obtain. Despite a completely different physical description, both sets of observers *must* agree regarding any physical observable.

This has been shown previously by Ref. [35] using numerical methods and later on, building over this work, analytically in Ref. [39]. All calculations were done using the (reasonably) approximation where only the electron neutrino is involved.

We know from experimental observations, however, that there are at least three different types of neutrinos and, moreover, none of them can be considered in isolation if we want to include neutrino mixing in our description of reality. Attempts to extend the above mentioned calculations to the case with multiple neutrinos, where mixing occurs, obtained, at first, strange results. For instance, Ref. [25] declares that rates obtained by both set of observers disagree when multiple mixing neutrinos are taken into account and this characterizes a paradox that can only be experimentally solved. Later on, Ref. [38] tried to better understand this result, but in their framework they obtain strange conclusions such as the vacuum states associated with flavor and massive neutrinos being orthogonal to one another. This implies that a massive neutrino detector would, in principle, be able to see a flavor neutrino in its vacuum state and vice versa, which seems non-physical. This point has already been previously debated, see, e.g., Ref. [40].

The correct way out of this conundrum is to be careful when working with neutrino fields. By careful here we mean focusing mainly on *massive* neutrino fields, which satisfy the massive Dirac equation. Flavor neutrinos have properties difficult to associate with fundamental particles (e.g., they do not have a definite mass, not being able to exist "on-shell"). Also, they only arise in specific experiments (such as neutrino oscillations), where there is uncertainty regarding energy and momentum which is comparably large with respect to the neutrinos' masses, requiring a wave-packet treatment to make sense [41].

For this reasons flavor neutrinos should not be seen as fundamental fields. Since, as we showed in the previous chapters, the Unruh effect is defined for fundamental fields having a well-defined equation of motion, we must try not to incur into the Procrustean mistake of fitting phenomenological definitions in this framework. Let us discuss this now.

3.2 Fermi theory and the decay rate for the inverse beta decay

We consider the proton and the neutron as a semi-classical two-state system similar to the one describing the Unruh-deWitt detector of Section 2.3. Their Hamiltonian satisfy

$$\hat{H}|p\rangle = m_p|p\rangle, \tag{3.3}$$
$$\hat{H}|n\rangle = m_n|n\rangle, \tag{3.4}$$

with $m_p < m_n$, where m_p and m_n are the proton and neutron masses respectively. For simplicity, we also define $\Delta m \equiv m_n - m_p$. Being semi-classical, the proton-neutron system has a well-defined trajectory and can be described by a semi-classical current

$$\hat{j}^\mu(\tau) = \frac{\hat{q}(\tau)}{\sqrt{-g}u^0} u^\mu(\tau)\delta^3(\vec{x} - \vec{x}_0(\tau)), \tag{3.5}$$

where $\hat{q}(\tau)$ is given by

$$\hat{q}(\tau) = e^{i\hat{H}\tau}\hat{q}(0)e^{-i\hat{H}\tau}, \tag{3.6}$$

$u^0(\tau)$ is the time component of the proton four-velocity and $\vec{x}_0(\tau)$ is the spatial trajectory of the proton, everything being parameterized by the proton's proper time τ. We identify the Fermi constant, G_F, in this model with $|\langle n|\hat{q}(0)|p\rangle|$, giving a measure of the strength of the weak interaction, and take the proton-neutron trajectory to be the same as in Sec. 2.3.

The Fermi action we consider is given by

$$\begin{aligned}\hat{S}_I &= \int d^4x\sqrt{-g}\frac{1}{\sqrt{2}}\left(\sum_{\alpha=e,\mu,\tau}\hat{\bar{\nu}}_\alpha\gamma^\mu\left(1-\gamma^5\right)\hat{l}_\alpha\hat{j}_\mu + h.c.\right) \\ &\equiv \int d^4x\sqrt{-g}\frac{1}{\sqrt{2}}\left(\sum_{\alpha=e,\mu,\tau}\sum_{i=1,2,3}U^*_{\alpha,i}\hat{\bar{\nu}}_i\gamma^\mu\left(1-\gamma^5\right)\hat{l}_\alpha\hat{j}_\mu + h.c.\right),\end{aligned} \tag{3.7}$$

where $U_{\alpha,i}$ is an element of the Pontecorvo–Maki–Nakagawa–Sakata (PMNS) matrix [42, 43], ν_i is the neutrino-field with mass m_i, l_α is an electrically charged lepton field with flavor α (and mass m_α), $\bar{\psi}_\alpha = \psi^\dagger_\alpha\gamma^0$, and γ^μ are given by

$$\gamma^0 = \begin{pmatrix} I & 0 \\ 0 & -I \end{pmatrix}; \quad \gamma^i = \begin{pmatrix} 0 & \sigma_i \\ -\sigma_i & 0 \end{pmatrix}; \quad \gamma^5 = i\gamma^0\gamma^1\gamma^2\gamma^3 = \begin{pmatrix} 0 & I_{2x2} \\ I_{2x2} & 0 \end{pmatrix}. \tag{3.8}$$

Note that we have *defined* the flavor neutrino field

$$\hat{\nu}_\alpha \equiv \sum_{i=1,2,3} U_{\alpha,i}\hat{\nu}_i \tag{3.9}$$

as a simple mathematical shortcut for writing the Fermi action. In particular, we *do not*

quantize the field $\hat{\nu}_\alpha$ nor associate quanta to it. As discussed in Appendix A, this procedure does not lead to a physically meaningful Fock space. One may wonder, then, what state we associate to the end particle present in a decay such as the one given in Eq. (3.2) and how can we calculate the interaction rate. We present how to construct this state explicitly in Appendix A, but highlight a few relevant points here:

- For our purposes, as proven by Eq. (A.15), it is important to notice that, when due care is taken, the inverse beta decay interaction rate will be given as an *incoherent* sum over the three different massive neutrino channels, i.e.,

$$\Gamma^{\,p^+\to n\,\bar{l}_\alpha^+\,\nu_\alpha} = \sum_{i=1,2,3} \Gamma^{\,p^+\to n\,\bar{l}_\alpha^+\,\nu_i}. \tag{3.10}$$

- This is not in conflict with neutrino mixing experiments as explained in the aforementioned appendix. The main reason this is so is that these experiments are localized in space and time, which inherently means uncertainty in the energy and momenta of the resulting neutrino, both in the source and in the detector. This means that only a wave-packet description makes sense in this setting [41, 44]. In fact, observing particle decays with higher precision in determining energy and momenta is one way to pinpoint the mass of a single *massive* neutrino (see, e.g., [44] for mentions of this type of experiments).

For this reason, we focus on calculating the decay rate for one massive neutrino, with the total rate being obtained by summing over the three channels.

3.3 Inertial point of view

Our first step will be to calculate the inverse β-decay rate as seen by inertial observers. We follow here the notational conventions adopted in Ref. [39]. The fermionic fields (the electron and massive neutrino fields) can be expanded in terms of plane waves as

$$\hat{\psi} = \sum_{\sigma=\pm} \int d^3k \left(\hat{a}_{\vec{k},\sigma} u^{+\omega}_{\vec{k},\sigma} + \hat{b}^\dagger_{\vec{k},\sigma} u^{-\omega}_{\vec{k},-\sigma} \right), \tag{3.11}$$

where the normal modes $u^{\pm\omega}_{\vec{k},\sigma}$, solutions of the standard Dirac equation,

$$\left(i\gamma^\mu \partial_\mu - m\right)\psi = 0, \tag{3.12}$$

are given by

$$u^{\pm\omega}_{\vec{k},\sigma} = \frac{e^{\mp i k_\mu x^\mu}}{(2\pi)^{3/2}} v^{\pm\omega}_\sigma(\vec{k}), \tag{3.13}$$

where

$$v^{\pm\omega}_\sigma(\vec{k}) = \frac{(k_\mu \gamma^\mu \pm mI)}{[2\omega(\omega \pm m)]^{1/2}} \hat{v}_\sigma, \tag{3.14}$$

with

$$\hat{v}_+ = \begin{pmatrix} 1 \\ 0 \\ 0 \\ 0 \end{pmatrix}; \qquad \hat{v}_- = \begin{pmatrix} 0 \\ 1 \\ 0 \\ 0 \end{pmatrix}. \tag{3.15}$$

In inertial coordinates, Eq. (3.5) reduces to

$$j^\mu(\tau) = \frac{\hat{q}(\tau)}{az} u^\mu(\tau)\delta(x)\delta(y)\delta\left(z - \sqrt{t^2 - a^{-2}}\right), \tag{3.16}$$

with $u^\mu(\tau)$, $t(\tau)$ and $z(\tau)$ being given in Eqs. (2.22), (2.23) and (2.24) with $\xi = 0$, respectively. By inspection of Eq. (3.7) we see that the inverse β-decay from the inertial point of view happens via only one type of interaction, namely

$$p^+ \to n + \bar{l}^+_\alpha + \nu_i, \tag{3.17}$$

with $\alpha = e, \mu, \tau$, labelling the flavor, and $i = 1,2,3$, labelling the mass. We start by calculating the amplitude

$$A_{I,i} = -i\langle \bar{l}^+_\alpha \nu_i; n|\hat{S}_I|0; p\rangle, \tag{3.18}$$

which when expanded using Eqs. (3.7), (3.16) and (3.11) gives

$$\begin{aligned} A_{I,i} = \frac{-iG_F U^*_{\alpha,i}}{(2\pi)^3\sqrt{2}} \int_{-\infty}^{\infty} d\tau\, e^{i\Delta m\tau} \exp\left\{\frac{i}{a}(\omega_\alpha + \omega_i)\sinh(a\tau) - \frac{i}{a}(k^3_\alpha + k^3_i)\cosh(a\tau)\right\} \\ \times \left[\cosh(a\tau)\,\bar{u}^{+\omega_i}_{k_i,\sigma_i} M_1 u^{-\omega_\alpha}_{k_\alpha,-\sigma_\alpha} - \sinh(a\tau)\,\bar{u}^{+\omega_i}_{k_i,\sigma_i} M_2 u^{-\omega_\alpha}_{k_\alpha,-\sigma_\alpha}\right], \end{aligned} \tag{3.19}$$

where, for simplicity, we have defined the matrices

$$M_1 = \begin{pmatrix} 1 & 0 & -1 & 0 \\ 0 & 1 & 0 & -1 \\ 1 & 0 & -1 & 0 \\ 0 & 1 & 0 & -1 \end{pmatrix}, \qquad M_2 = \begin{pmatrix} -1 & 0 & 1 & 0 \\ 0 & 1 & 0 & -1 \\ -1 & 0 & 1 & 0 \\ 0 & 1 & 0 & -1 \end{pmatrix}. \tag{3.20}$$

The differential probability of decay will be given by

$$\frac{dP^{\,p^+ \to n\, \bar{l}^+_\alpha\, \nu_i}}{d^3k_\alpha\, d^3k_i} = \sum_{\sigma_\alpha,\sigma_i} |A_{I,i}|^2. \tag{3.21}$$

After squaring Eq. (3.19) we perform the spin-sums in Mathematica[©II]. For the same reasons as discussed in Sec. 2.3 we must extract a divergence in the total proper time of the probability and obtain an interaction rate instead. To do so, we first make a standard change of

[II] The code is shown in Appendix B.

coordinates

$$s = (\tau + \tau')/2, \tag{3.22}$$

$$2\xi = \sigma = \tau - \tau' \tag{3.23}$$

and perform a boost in the z direction [Eqs. (2.71) and (2.72)] with regard to both the neutrino and the electron momenta. After dividing by the total proper time and cleaning up the resulting expression, we obtain a differential interaction rate given by

$$\begin{aligned}\frac{d\Gamma^{\,p^+\to n\,\bar{l}_\alpha^+\,\nu_i}}{d^3k_\alpha\, d^3k_i} = \frac{2G_F^2|U_{\alpha,i}|^2}{(2\pi)^6}\int_{-\infty}^{\infty} d\xi \exp\{\big(2i[\Delta m\xi + a^{-1}(\omega_\alpha+\omega_i)\sinh a\xi]\big)\} \\ \times(\omega_i\omega_\alpha)^{-1}[k_i^z k_\alpha^z + \omega_i\omega_\alpha + f(k_{i,\alpha}^x, k_{i,\alpha}^y)],\end{aligned} \tag{3.24}$$

where $f(k_{i,\alpha}^x, k_{i,\alpha}^y)$ is an odd function of each of its arguments which will not contribute to the decay rate when integrated over the momenta. Let us use spherical coordinates for both the neutrino (indexed by i) and charged lepton (indexed by α) momenta and make an additional coordinate change for ξ, i.e.,

$$k_{i,\alpha}^x = k_{i,\alpha}\sin\theta_{i,\alpha}\cos\phi_{i,\alpha}, \tag{3.25}$$

$$k_{i,\alpha}^y = k_{i,\alpha}\sin\theta_{i,\alpha}\sin\phi_{i,\alpha}, \tag{3.26}$$

$$k_{i,\alpha}^z = k_{i,\alpha}\cos\theta_{i,\alpha}, \tag{3.27}$$

$$\lambda = e^{a\xi}, \tag{3.28}$$

with $\omega_{i,\alpha} = \sqrt{|\vec{k}|_{i,\alpha}^2 + m_{i,\alpha}^2}$. Integrating over the angular variables we get

$$\begin{aligned}\Gamma^{\,p^+\to n\,\bar{l}_\alpha^+\,\nu_i} = \frac{G_F^2|U_{\alpha,i}|^2}{2\pi^4 a}\int_0^\infty d\lambda\int_0^\infty dk_\alpha\int_0^\infty dk_i \\ \times\lambda^{\frac{2i\Delta m}{a}-1}e^{a^{-1}(\omega_\alpha+\omega_i)(\lambda-\lambda^{-1})}k_\alpha^2 k_i^2.\end{aligned} \tag{3.29}$$

Performing the λ-integral (Eq. (8.432.7) of Ref. [28]) we are left with

$$\begin{aligned}\Gamma^{\,p^+\to n\,\bar{l}_\alpha^+\,\nu_i} = \frac{G_F^2|U_{\alpha,i}|^2}{\pi^4 a}e^{\frac{-\pi\Delta m}{a}}\int_0^\infty dk_\alpha\, k_\alpha^2\int_0^\infty dk_i\, k_i^2 \\ \times K_{2i\Delta m/a}\left(\frac{2}{a}(\omega_\alpha+\omega_i)\right).\end{aligned} \tag{3.30}$$

For comparison with the accelerated result it proves useful to use the same techniques of Ref. [39] to transform this integral in a double integral over complex variables. To this end, we begin by expressing the modified Bessel function $K_\mu(x)$ as

$$K_\mu(x) = \frac{1}{2}\int_{C_s}\frac{ds}{2\pi i}\Gamma(-s)\Gamma(-s-\mu)\left(\frac{x}{2}\right)^{2s+\mu}, \tag{3.31}$$

where in our case $\mu = 2i\Delta m/a$, $x = \frac{2}{a}\left(\sqrt{k_\alpha^2+m_\alpha^2}+\sqrt{k_i^2+m_i^2}\right)$ and the counter C_s is such that all poles of the Γ functions are inside it (see Ref. [39] for a derivation of this formula).

Therefore, we write the decay rate as

$$\Gamma^{\,p^+\to n\,\bar{l}_\alpha^+\,\nu_i} = \frac{G_F^2|U_{\alpha,i}|^2}{2\pi^4 a}e^{\frac{-\pi\Delta m}{a}}\int_0^\infty dk_\alpha\,k_\alpha^2\int_0^\infty dk_i\,k_i^2\int_{C_s}\frac{ds}{2\pi i}\Gamma(-s) \times\Gamma\left(-s-\frac{2i\Delta m}{a}\right)\left(\frac{1}{a}\left(\sqrt{k_\alpha^2+m_\alpha^2}+\sqrt{k_i^2+m_i^2}\right)\right)^{2s+\frac{2i\Delta m}{a}}. \tag{3.32}$$

Now we express the term inside the parenthesis as

$$\left(\frac{1}{a}\left(\sqrt{k_\alpha^2+m_\alpha^2}+\sqrt{k_i^2+m_i^2}\right)\right)^{2s+\frac{2i\Delta m}{a}} = \int_{C_t}\frac{dt}{2\pi i}\frac{\Gamma(-t)\Gamma(t-2s-\frac{2i\Delta m}{a})}{\Gamma(-2s-\frac{2i\Delta m}{a})}a^{-2s-\frac{2i\Delta m}{a}} \times\left(k_i^2+m_i^2\right)^{-\frac{t}{2}+s+\frac{i\Delta m}{a}}\left(k_\alpha^2+m_\alpha^2\right)^{\frac{t}{2}}, \tag{3.33}$$

where the contour C_t is such that it separates the poles of the Γ functions in the numerator (see Ref. [39] for details). The contours used in these integrals allow us to make the substitution $s\to s-\frac{i\Delta m}{a}$ without altering the results. Therefore

$$\begin{aligned}\Gamma^{\,p^+\to n\,\bar{l}_\alpha^+\,\nu_i} = {}& \frac{G_F^2|U_{\alpha,i}|^2}{2\pi^4 a}e^{\frac{-\pi\Delta m}{a}}\int_0^\infty dk_\alpha\,k_\alpha^2\int_0^\infty dk_i\,k_i^2 \\ &\times\int_{C_s}\frac{ds}{2\pi i}\Gamma\left(-s+\frac{i\Delta m}{a}\right)\Gamma\left(-s-\frac{i\Delta m}{a}\right) \\ &\times\int_{C_t}\frac{dt}{2\pi i}\frac{\Gamma(-t)\Gamma(t-2s)}{\Gamma(-2s)}a^{-2s} \\ &\times\left(k_i^2+m_i^2\right)^{-\frac{t}{2}+s}\left(k_\alpha^2+m_\alpha^2\right)^{\frac{t}{2}}\end{aligned} \tag{3.34}$$

Similarly, we make a sequence of transformations (a) $t\to 2t$, (b) $s\to s+t$ and (c) $s\to s-3/2$, $t\to t-3/2$ to arrive at

$$\begin{aligned}\Gamma^{\,p^+\to n\,\bar{l}_\alpha^+\,\nu_i} = {}& \frac{G_F^2 a^5|U_{\alpha,i}|^2}{\pi^4}e^{\frac{-\pi\Delta m}{a}}\int_0^\infty dk_\alpha\,k_\alpha^2\int_0^\infty dk_i\,k_i^2 \\ &\times\int_{C_s}\frac{ds}{2\pi i}\int_{C_t}\frac{dt}{2\pi i}\Gamma\left(-s-t+\frac{i\Delta m}{a}+3\right)\Gamma\left(-s-t-\frac{i\Delta m}{a}+3\right) \\ &\times\frac{\Gamma(-2t+3)\Gamma(-2s+3)}{\Gamma(-2s-2t+6)}a^{-2s-2t} \\ &\times\left(k_i^2+m_i^2\right)^{s-3/2}\left(k_\alpha^2+m_\alpha^2\right)^{t-3/2}.\end{aligned} \tag{3.35}$$

Using the integral identity (which holds here by an appropriate choice of the countours)

$$\int_0^\infty k^2(k^2+m^2)^{s-3/2} = \frac{\sqrt{\pi}}{4}\frac{m^{2s}\Gamma(-s)}{\Gamma(3/2-s)}, \tag{3.36}$$

we obtain

$$\begin{aligned}\Gamma^{\,p^+\to n\,\bar{l}_\alpha^+\,\nu_i} = &\frac{G_F^2 a^5 |U_{\alpha,i}|^2}{2^4\pi^3} e^{\frac{-\pi\Delta m}{a}} \\ &\times \int_{C_s}\frac{ds}{2\pi i}\int_{C_t}\frac{dt}{2\pi i}\Gamma\left(-s-t+\frac{i\Delta m}{a}+3\right)\Gamma\left(-s-t-\frac{i\Delta m}{a}+3\right) \\ &\times \frac{\Gamma(-2t+3)\Gamma(-2s+3)}{\Gamma(-2s-2t+6)\Gamma(3/2-s)\Gamma(3/2-t)} a^{-2s-2t} \\ &\times (m_\alpha)^{2t}(m_i)^{2s}\Gamma(-s)\Gamma(-t).\end{aligned} \tag{3.37}$$

Finally we use one of the properties of the Γ function, i.e.,

$$\Gamma(2x) = 2^{2x-1}(\pi)^{-1/2}\Gamma(x)\Gamma(x+1/2), \tag{3.38}$$

to write

$$\begin{aligned}&\frac{\Gamma(2(-t+3/2))\Gamma(2(-s+3/2))}{\Gamma(2(-s-t+3))\Gamma(3/2-s)\Gamma(3/2-t)} \\ &= \frac{\Gamma(2-t)\Gamma(2-s)}{2\sqrt{\pi}\Gamma(-s-t+3)\Gamma(-s-t+7/2)}.\end{aligned} \tag{3.39}$$

Also, using that $\Gamma(x)^* = \Gamma(x^*)$, we arrive at the final form for the decay rate

$$\begin{aligned}\Gamma^{\,p^+\to n\,\bar{l}_\alpha^+\,\nu_i} = &\frac{G_F^2 a^5 |U_{\alpha,i}|^2}{2^5\pi^{7/2}} e^{\frac{-\pi\Delta m}{a}} \\ &\times \int_{C_s}\frac{ds}{2\pi i}\int_{C_t}\frac{dt}{2\pi i}\left|\Gamma\left(-s-t+\frac{i\Delta m}{a}+3\right)\right|^2 \\ &\times \frac{\Gamma(-s)\Gamma(-t)\Gamma(-t+2)\Gamma(-s+2)}{\Gamma(-s-t+3)\Gamma(-s-t+7/2)} \\ &\times (m_\alpha/a)^{2t}(m_i/a)^{2s}\end{aligned} \tag{3.40}$$

We note that this result correctly reproduces the ones given in Ref. [35] in the massless limit and is the same as in Ref. [39] in the case of a single massive neutrino. As we have noted before, the total rate for the process

$$p^+ \to n + e^+ + \nu_e \tag{3.41}$$

is given by the *incoherent* sum of Eq. (3.40) with $\alpha = e$ over the rates obtained for ν_i, i.e.,

$$\begin{aligned}\Gamma^{\,p^+\to n\,e^+\,\nu_e} = \frac{G_F^2 a^5}{2^5\pi^{7/2}} e^{\frac{-\pi\Delta m}{a}} \\ \times \int_{C_s}\frac{ds}{2\pi i}\int_{C_t}\frac{dt}{2\pi i}\left|\Gamma\left(-s-t+\frac{i\Delta m}{a}+3\right)\right|^2 \\ \times \frac{\Gamma(-s)\Gamma(-t)\Gamma(-t+2)\Gamma(-s+2)}{\Gamma(-s-t+3)\Gamma(-s-t+7/2)} \\ \times (m_e/a)^{2t}\left(\sum_{i=1,2,3}|U_{e,i}|^2\,(m_i/a)^{2s}\right),\end{aligned} \tag{3.42}$$

The semi-classical Feynman diagrams associated with this decay are shown below in Figure 3.1.

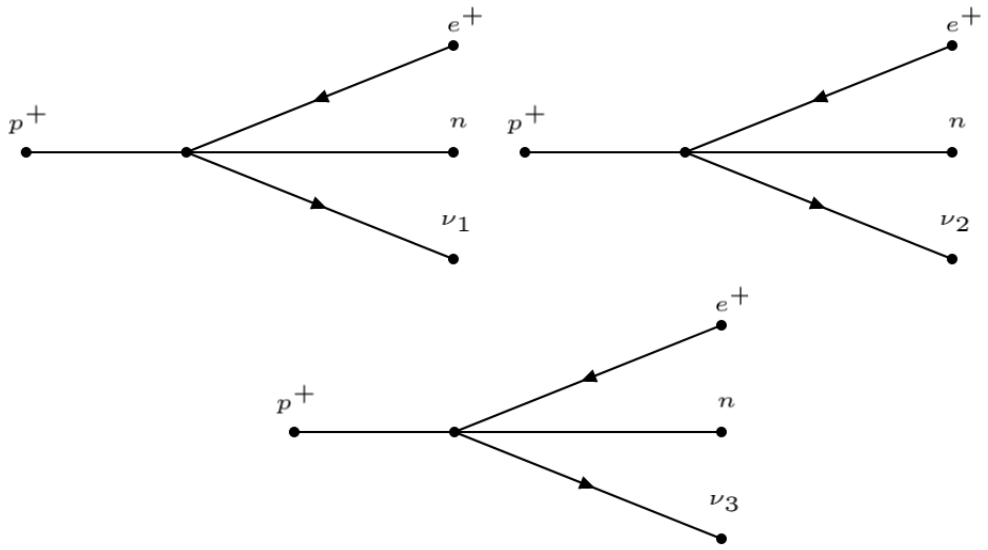

Figure 3.1: Feynman diagrams for the semi-classical inverse β-decay according to inertial observers.

This is the result that all other observers must ascribe to the total interaction rate for the inverse beta decay process, as demanded by the covariance of quantum field theory. We shall see now how this happens from the accelerated point of view.

3.4 Accelerated point of view

In the same way that for the Unruh-deWitt detector we had to consider a different type of process (an absorption) in the Rindler frame as opposed to a simple emission in the inertial frame, we must now see what kind of processes correspond to the decay channels seen by inertial observers.

From the form of the interaction action given Eq. (3.7) we see that energy for the decay can only come from absorbing a charged lepton, an anti-neutrino or both. Therefore, each

decay of the type $p^+ \rightarrow n + \bar{l}_\alpha^+ + \nu_i$ seen by inertial observers will correspond to three processes from the Rindler point of view, which are

- (a) $p^+ + l_\alpha^- \rightarrow n + \nu_i$,
- (b) $p^+ + \bar{\nu}_i \rightarrow n + \bar{l}_\alpha^+$,
- (c) $p^+ + l_\alpha^- + \bar{\nu}_i \rightarrow n$.

The total interaction rate for the inverse beta decay, then, is obtained by summing over all three channels above for each massive neutrino. We must calculate then nine different amplitudes, again following the conventions of Ref. [39]. Let us start with the amplitude for process (a) for the i neutrino. It will be given by

$$A_{R,i}^{(a)} = -i\langle \nu_{i;\vec{q}_i,\sigma_i}; n|\hat{S}_I|l_{\alpha;\vec{q}_\alpha,\sigma_\alpha}; p\rangle, \tag{3.43}$$

where we have again used the shorthand $\vec{q} = (\varpi, \vec{k}_\perp)$ for each Rindler particle, with ϖ standing for the Rindler frequency. To calculate this amplitude we must expand the lepton fields using Rindler modes, i.e.,

$$\hat{\psi} = \sum_{\sigma=\pm} \int d^3q \left(\hat{c}_{\varpi,\vec{k}_\perp,\sigma} g^{+\varpi}_{\vec{k}_\perp,\sigma} + \hat{d}^\dagger_{\varpi,\vec{k}_\perp,\sigma} g^{-\varpi}_{\vec{k}_\perp,-\sigma} \right), \tag{3.44}$$

with

$$g^{\pm\varpi}_{\vec{k}_\perp,\sigma} = \frac{e^{\mp i\varpi\tau + i\vec{k}_\perp\cdot\vec{x}_\perp}}{(2\pi)^{3/2}} h_\sigma(\pm\varpi, \vec{k}_\perp), \tag{3.45}$$

where

$$\begin{aligned} h_\sigma(\pm\varpi, \vec{k}_\perp) = &\left[\frac{\cosh(\varpi\pi/a)}{\pi a l}\right]^{1/2} \\ &\times \gamma^0 \left[\left(\vec{k}_\perp\cdot\vec{\gamma}_\perp + m\mathbb{I}\right) K_{\pm i\varpi/a+1/2}\left(\frac{l}{a}e^{a\xi}\right) \right. \\ &\left. + il\gamma^3 K_{\pm i\varpi/a-1/2}\left(\frac{l}{a}e^{a\xi}\right) \right] \hat{h}_\sigma, \end{aligned} \tag{3.46}$$

with

$$\hat{h}_+ = \begin{bmatrix} 1 \\ 0 \\ 1 \\ 0 \end{bmatrix}, \quad \hat{h}_- = \begin{bmatrix} 0 \\ 1 \\ 0 \\ -1 \end{bmatrix}, \tag{3.47}$$

$l = \sqrt{|\vec{k}_\perp|^2 + m^2}$ and $\vec{\gamma}_\perp \equiv (\gamma^1, \gamma^2)$. Expanding Eq. (3.43) we obtain

$$A_{R,i}^{(a)} = \frac{iG_F}{(2\pi)^2\sqrt{2}} U^*_{\alpha,i}\delta(\varpi_\alpha - \varpi_i - \Delta m)\left[\bar{u}^{+\varpi_i}_{\vec{q}_i,\sigma_i}\gamma^0(\hat{I} - \gamma^5)u^{+\varpi_\alpha}_{\vec{q}_\alpha,\sigma_\alpha}\right]. \tag{3.48}$$

Similarly, for process (b) and (c) we obtain

$$A^{(b)}_{R,i} = \frac{iG_F}{(2\pi)^2\sqrt{2}} U^*_{\alpha,i}\delta(\varpi_i - \varpi_\alpha - \Delta m)\left[\bar{u}^{-\varpi_i}_{\vec{q}_i,-\sigma_i}\gamma^0(\hat{I}-\gamma^5)u^{-\varpi_\alpha}_{\vec{q}_\alpha,-\sigma_\alpha}\right], \tag{3.49}$$

$$A^{(c)}_{R,i} = \frac{iG_F}{(2\pi)^2\sqrt{2}} U^*_{\alpha,i}\delta(\varpi_i + \varpi_\alpha - \Delta m)\left[\bar{u}^{-\varpi_i}_{\vec{q}_i,-\sigma_i}\gamma^0(\hat{I}-\gamma^5)u^{+\varpi_\alpha}_{\vec{q}_\alpha,\sigma_\alpha}\right]. \tag{3.50}$$

To obtain the decay rates we square the amplitudes, multiply them by the thermal fermionic factor (as discussed at the end of Sec. 2.2), divide them by the total proper time using Eq. (2.81) and sum over the spins to obtain

$$\begin{aligned}\frac{d\Gamma^{(a)}}{d^3q_i\, d^3q_\alpha} &= \frac{G_F^2|U_{\alpha,i}|^2\delta(\varpi_\alpha - \varpi_i - \Delta m)}{2(2\pi)^5} n_f(\varpi_\alpha)(1-n_f(\varpi_i)) \\ &\times \sum_{\sigma_i,\sigma_\alpha}\left|\left[\bar{u}^{+\varpi_i}_{\vec{q}_i,\sigma_i}\gamma^0(I-\gamma^5)u^{+\varpi_\alpha}_{\vec{q}_\alpha,\sigma_\alpha}\right]\right|^2 \\ &= \frac{G_F^2|U_{\alpha,i}|^2\delta(\varpi_\alpha - \varpi_i - \Delta m)}{2^3(2\pi)^5 e^{\pi\Delta m/a}\cosh(\pi\omega_\alpha/a)\cosh(\pi\omega_i/a)} \\ &\times \sum_{\sigma_i,\sigma_\alpha}\left|\left[\bar{u}^{+\varpi_i}_{\vec{q}_i,\sigma_i}\gamma^0(I-\gamma^5)u^{+\varpi_\alpha}_{\vec{q}_\alpha,\sigma_\alpha}\right]\right|^2,\end{aligned} \tag{3.51}$$

where $n_f(x)$ is given by Eq. (2.63). Similarly for the other processes we have

$$\begin{aligned}\frac{d\Gamma^{(b)}}{d^3q_i\, d^3q_\alpha} &= \frac{G_F^2|U_{\alpha,i}|^2\delta(\varpi_i - \varpi_\alpha - \Delta m)}{2(2\pi)^5} n_f(\varpi_i)(1-n_f(\varpi_\alpha)) \\ &\times \sum_{\sigma_i,\sigma_\alpha}\left|\left[\bar{u}^{-\varpi_i}_{\vec{q}_i,-\sigma_i}\gamma^0(I-\gamma^5)u^{-\varpi_\alpha}_{\vec{q}_\alpha,-\sigma_\alpha}\right]\right|^2 \\ &= \frac{G_F^2|U_{\alpha,i}|^2\delta(\varpi_i - \varpi_\alpha - \Delta m)}{2^3(2\pi)^5 e^{\pi\Delta m/a}\cosh(\pi\omega_\alpha/a)\cosh(\pi\omega_i/a)} \\ &\times \sum_{\sigma_i,\sigma_\alpha}\left|\left[\bar{u}^{-\varpi_i}_{\vec{q}_i,-\sigma_i}\gamma^0(I-\gamma^5)u^{-\varpi_\alpha}_{\vec{q}_\alpha,-\sigma_\alpha}\right]\right|^2,\end{aligned} \tag{3.52}$$

$$\begin{aligned}\frac{d\Gamma^{(c)}}{d^3q_i\, d^3q_\alpha} &= \frac{G_F^2|U_{\alpha,i}|^2\delta(\varpi_\alpha + \varpi_i - \Delta m)}{2(2\pi)^5} n_f(\varpi_i)n_f(\varpi_\alpha) \\ &\times \sum_{\sigma_i,\sigma_\alpha}\left|\left[\bar{u}^{-\varpi_i}_{\vec{q}_i,-\sigma_i}\gamma^0(I-\gamma^5)u^{+\varpi_\alpha}_{\vec{q}_\alpha,\sigma_\alpha}\right]\right|^2 \\ &= \frac{G_F^2|U_{\alpha,i}|^2\delta(\varpi_\alpha + \varpi_i - \Delta m)}{2^3(2\pi)^5 e^{\pi\Delta m/a}\cosh(\pi\omega_\alpha/a)\cosh(\pi\omega_i/a)} \\ &\times \sum_{\sigma_i,\sigma_\alpha}\left|\left[\bar{u}^{-\varpi_i}_{\vec{q}_i,-\sigma_i}\gamma^0(I-\gamma^5)u^{+\varpi_\alpha}_{\vec{q}_\alpha,\sigma_\alpha}\right]\right|^2.\end{aligned} \tag{3.53}$$

Let us focus only on the spin sums for the moment. Using the code provided in Appendix B, disregarding odd terms in the transverse momenta (which will not contribute when integrated over all transverse momenta) and also using that $K^*_{1/2+ix}(y) = K_{-1/2+ix}(y)$ (for $y \in \mathbb{R}$)

to simplify the expressions, we obtain that in all three cases they are equal to

$$\frac{32\cosh(\pi\varpi_\alpha/a)\cosh(\pi\varpi_i/a)\,l_\alpha\,l_i}{a^2\pi^2}\left|K_{\frac{1}{2}+i\frac{\varpi_i}{a}}(l_i/a)\right|^2\left|K_{\frac{1}{2}+i\frac{\varpi_\alpha}{a}}(l_\alpha/a)\right|^2 \tag{3.54}$$

where $l_{i,\alpha}=\sqrt{k^2_{x;i,\alpha}+k^2_{y;i,\alpha}+m^2_{i,\alpha}}$. In this way we obtain for the rates

$$\begin{aligned}\frac{d\Gamma^{(a)}}{d^3q_i\,d^3q_\alpha}&=\frac{G_F^2|U_{\alpha,i}|^2\delta(\varpi_\alpha-\varpi_i-\Delta m)}{a^2 2^3\pi^7 e^{\pi\Delta m/a}}\\&\times l_i l_\alpha\left|K_{\frac{1}{2}+i\frac{\varpi_i}{a}}(l_i/a)\right|^2\left|K_{\frac{1}{2}+i\frac{\varpi_\alpha}{a}}(l_\alpha/a)\right|^2,\end{aligned} \tag{3.55}$$

$$\begin{aligned}\frac{d^2\Gamma^{(b)}}{d^3q_i\,d^3q_\alpha}&=\frac{G_F^2|U_{\alpha,i}|^2\delta(\varpi_i-\varpi_\alpha-\Delta m)}{a^2 2^3\pi^7 e^{\pi\Delta m/a}}\\&\times l_i l_\alpha\left|K_{\frac{1}{2}+i\frac{\varpi_i}{a}}(l_i/a)\right|^2\left|K_{\frac{1}{2}+i\frac{\varpi_\alpha}{a}}(l_\alpha/a)\right|^2,\end{aligned} \tag{3.56}$$

$$\begin{aligned}\frac{d\Gamma^{(c)}}{d^3q_i\,d^3q_\alpha}&=\frac{G_F^2|U_{\alpha,i}|^2\delta(\varpi_\alpha+\varpi_i-\Delta m)}{a^2 2^3\pi^7 e^{\pi\Delta m/a}}\\&\times l_i l_\alpha\left|K_{\frac{1}{2}+i\frac{\varpi_i}{a}}(l_i/a)\right|^2\left|K_{\frac{1}{2}+i\frac{\varpi_\alpha}{a}}(l_\alpha/a)\right|^2.\end{aligned} \tag{3.57}$$

Now we must integrate over the remaining leptonic quantum numbers. First we get rid of the δ-functions by integrating over ϖ_i, therefore

$$\begin{aligned}\Gamma^{(a)}=&\frac{G_F^2|U_{\alpha,i}|^2}{a^2 2^3\pi^7 e^{\pi\Delta m/a}}\int_{\Delta m}^{\infty}d\omega_\alpha\int dk_{x;i}\int dk_{x;\alpha}\int dk_{y;i}\int dk_{y;\alpha}\\&\times l_i l_\alpha\left|K_{\frac{1}{2}+i\frac{\omega_\alpha-\Delta m}{a}}(l_i/a)\right|^2\left|K_{\frac{1}{2}+i\frac{\omega_\alpha}{a}}(l_\alpha/a)\right|^2.\end{aligned} \tag{3.58}$$

We do the same procedure for the other rates . Now, taking into account the integration ranges and the fact that we must compare the *total* interaction rate for each i neutrino with the one obtained by inertial observers (and then sum them all), we must sum over all processes resulting in

$$\begin{aligned}\Gamma^{(tot)}=&\frac{G_F^2|U_{\alpha,i}|^2}{a^2 2^3\pi^7 e^{\pi\Delta m/a}}\int_{-\infty}^{\infty}d\varpi_\alpha\int dk_{x;i}\int dk_{x;\alpha}\int dk_{y;i}\int dk_{y;\alpha}\\&\times l_i l_\alpha\left|K_{\frac{1}{2}+i\frac{\varpi_\alpha-\Delta m}{a}}(l_i/a)\right|^2\left|K_{\frac{1}{2}+i\frac{\varpi_\alpha}{a}}(l_\alpha/a)\right|^2.\end{aligned} \tag{3.59}$$

Now we use the identity

$$(l/a)K_{1/2+i\omega/a}(l/a)K_{-1/2+i\omega/a}(l/a)=\frac{\sqrt{\pi}}{2}G^{40}_{24}\left((l/a)^2\,\middle|\,\begin{matrix}1/2, & 1\\ i\omega/a+1/2, & +1, \quad 0, \quad -i\omega/a+1/2\end{matrix}\right) \tag{3.60}$$

$$=\frac{\sqrt{\pi}}{2}\int_{C_s}\frac{ds}{2\pi i}(l/a)^{2s-1}\frac{\Gamma(i\omega/a+1-s)\Gamma(-s+1/2)\Gamma(-i\omega/a+1-s)}{\Gamma(1-s)},$$

where we used the definition of the Meijer-G function, Eq. (9.301) of [28], along with a contour change in the contour C_s, which encloses all poles of the Γ functions (in a similar way to what was done in the inertial case). Going to polar coordinates in the transverse momenta and noting that in the range of s covered by C_s

$$\int_0^\infty d\rho\,\rho\left(\frac{\rho^2+m^2}{a^2}\right)^{s-1/2} = -\frac{a^{1-2s}m^{2s+1}}{1+2s}, \tag{3.61}$$

we obtain, after making $\varpi_\alpha/a \to \varpi_\alpha$ and using Eq. (3.60) twice,

$$\begin{aligned}\Gamma^{tot} = &\frac{a^3G_F^2|U_{\alpha,i}|^2}{2^3\pi^4 e^{\pi\Delta m/a}}\int_{-\infty}^{\infty}d\varpi_\alpha\int_{C_s}\frac{ds}{2\pi i}\int_{C_t}\frac{dt}{2\pi i} \\ &\times\frac{a^{-2s}m_\alpha^{2s+1}a^{-2t}m_i^{2t+1}}{(1+2s)(1+2t)\Gamma(-s+1)\Gamma(-t+1)} \\ &\times\Gamma(-s+1/2)\Gamma(-t+1/2)|\Gamma(i\varpi_\alpha+1-t)|^2|\Gamma(i\varpi_\alpha-i\Delta m/a+1-s)|^2.\end{aligned} \tag{3.62}$$

Now we make $i\varpi_\alpha = x$ and use that

$$\int_{-i\infty}^{i\infty}dx\,\Gamma(a+x)\Gamma(b+x)\Gamma(c-x)\Gamma(d-x) = 2\pi i\frac{\Gamma(a+c)\Gamma(a+d)\Gamma(b+c)\Gamma(b+d)}{\Gamma(a+b+c+d)}, \tag{3.63}$$

where in our case $a=c=1-t$, $b=-i\Delta m/a+1-s$, and $d=i\Delta m/a+1-s$. After making (a) $s\to s-1/2$ and (b) $t\to t-1/2$, this leads us to

$$\begin{aligned}\Gamma^{tot} = &\frac{a^5G_F^2|U_{\alpha,i}|^2}{2^2\pi^3 e^{\pi\Delta m/a}}\int_{C_s}\frac{ds}{2\pi i}\int_{C_t}\frac{dt}{2\pi i}\frac{a^{-2s}m_\alpha^{2s}a^{-2t}m_i^{2t}}{(2s)(2t)\Gamma(-s+3/2)\Gamma(-t+3/2)} \\ &\times\Gamma(-s+1)\Gamma(-t+1)|\Gamma(3-t-s+i\Delta m/a)|^2 \\ &\times\frac{\Gamma(3-2t)\Gamma(3-2s)}{\Gamma(6-2t-2s)}\end{aligned} \tag{3.64}$$

We apply again the identity given in Eq. (3.38) obtaining that

$$\frac{\Gamma(2(3/2-t))\Gamma(2(3/2-s))}{\Gamma(2(3-t-s))} = (\pi)^{-1/2}\frac{2^{-1}\Gamma(3/2-t)\Gamma(-t+2)\Gamma(3/2-s)\Gamma(-s+2)}{\Gamma(3-t-s)\Gamma(7/2-t-s)}, \tag{3.65}$$

so, finally,

$$\begin{aligned}\Gamma^{tot} = &\frac{a^5G_F^2|U_{\alpha,i}|^2}{2^5\pi^{7/2}e^{\pi\Delta m/a}}\int_{C_s}\frac{ds}{2\pi i}\int_{C_t}\frac{dt}{2\pi i}a^{-2s}m_\alpha^{2s}a^{-2t}m_i^{2t}\Gamma(-t+2)\Gamma(-s+2)\Gamma(-t)\Gamma(-s) \\ &\times\frac{|\Gamma(3-t-s+i\Delta m/a)|^2}{\Gamma(3-t-s)\Gamma(7/2-t-s)}.\end{aligned} \tag{3.66}$$

Again taking into account an incoherent sum over the different neutrinos and fixing the end particle to be a positron in the same way as before we obtain the decay rate (after a relabelling

$s \leftrightarrow t$)

$$\begin{aligned}\Gamma^{\,p^+ \to n\, e^+\, \nu_e} = & \frac{G_F^2 a^5}{2^5 \pi^{7/2}} e^{\frac{-\pi \Delta m}{a}} \\ & \times \int_{C_t} \frac{dt}{2\pi i} \int_{C_s} \frac{ds}{2\pi i} \left| \Gamma\left(-s-t+\frac{i\Delta m}{a}+3\right)\right|^2 \\ & \times \frac{\Gamma(-s)\Gamma(-t)\Gamma(-t+2)\Gamma(-s+2)}{\Gamma(-s-t+3)\Gamma(-s-t+7/2)} \\ & \times (m_e/a)^{2t} \left(\sum_{i=1,2,3} |U_{e,i}|^2 \, (m_i/a)^{2s} \right).\end{aligned} \tag{3.67}$$

which is exactly the same rate obtained from the inertial point of view, despite the drastically different description of the decay (the Feynman diagrams from the Rindler point of view are shown below in Figure 3.2).

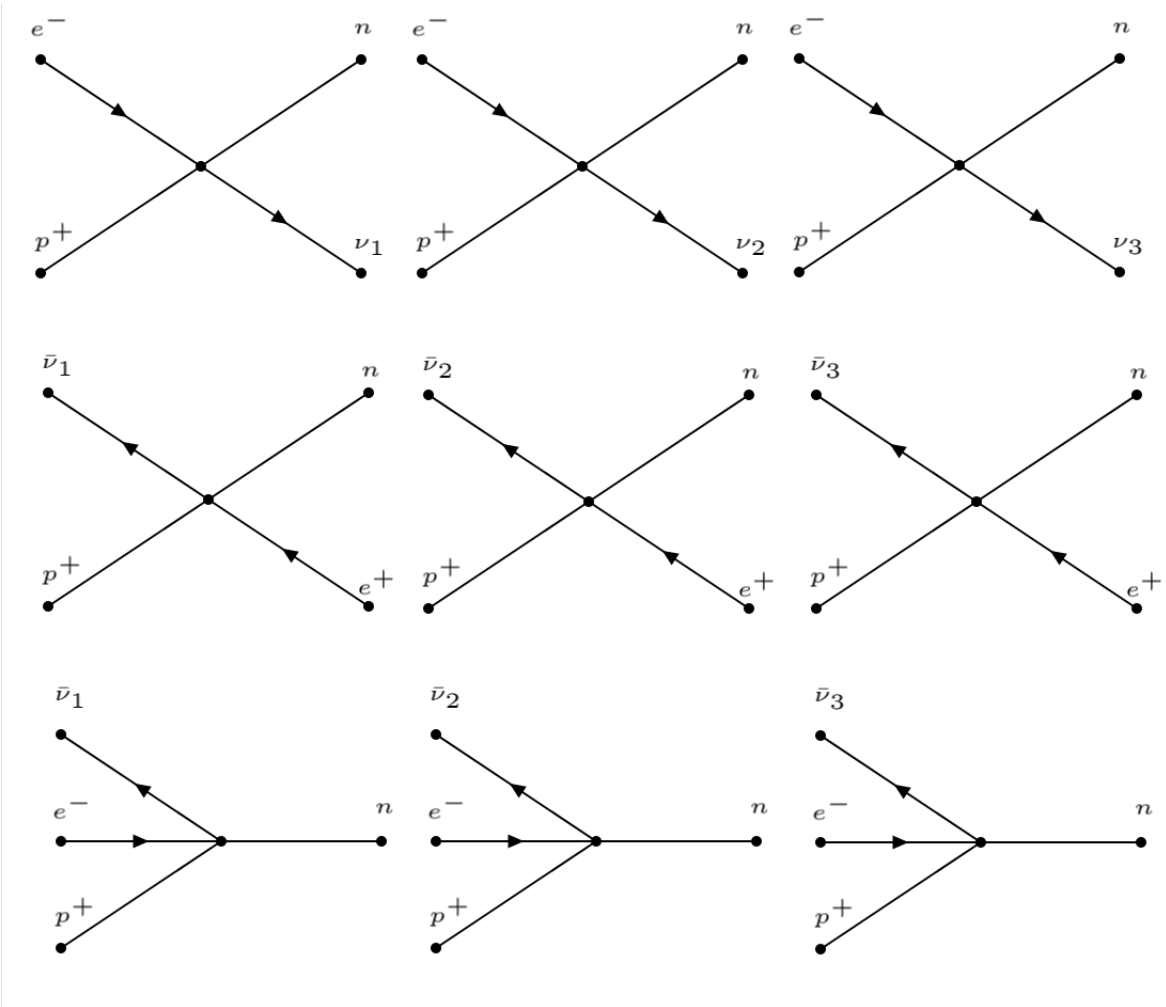

Figure 3.2: Feynman diagrams for the semi-classical inverse β-decay according to Rindler observers.

This shows that there is no paradox regarding the Unruh effect and mixing neutrinos, in contrast to what was obtained in Ref. [25].

As a final aside, note that our calculations involve no approximation whatsoever (as those of Ref. [38]). We owe this due to the fact that we used fields which have a well-defined quantization (i.e., massive neutrino ones) in our calculations.

Our result is not a surprising one, since we should expect it from the general covariance of QFT. It is, nonetheless, reassuring, given the existing discussion in the literature. Despite not posing any paradox to be solved experimentally, the inverse beta decay could be used, in principle at least, as a way to test the Unruh effect. For reasons we discuss in the next chapter, it is not possible to do so and we must search for a different way of probing the effect. A promising platform is the use of electromagnetic radiation, the subject to which we turn now.

CHAPTER 4

Proposal for observing the Unruh effect with classical electrodynamics

In the previous chapter we have seen that by taking into account the thermal bath in the accelerated frame, along with a careful examination of how to quantize neutrinos when there is flavor mixing, we obtain consistency between inertial and accelerated observers' results. As mentioned in Chapter 1, besides neutrinos, a similar reasoning can be applied to different observables of different types of fields. Despite being derived from basic principles and its fundamental role in guaranteeing consistency of the QFT framework, some people remain skeptical of the existence of the Unruh effect.

A point of contention regarding the Unruh effect is the nature of particles seen in the Rindler frame: are they real or not? Is it possible to observe them in the laboratory? In this chapter we discuss such questions and also show how the Unruh effect can be virtually confirmed by an experiment involving mainly classical electromagnetism.

4.1 Rindler particles

As we have seen in Chapter 2, Rindler particles are defined by uniformly accelerated observers in the same way that inertial observers define particles in their frame, as excitations of a vacuum state via the action of creation operators. Different particle concepts come from using different vacua and creation operators.

Although particles seen by Rindler observers have counter-intuitive properties (e.g., not having an "usual" dispersion relation between energy and momenta, possibly having zero energy), there is no reason to doubt their existence since they follow from basic principles of QFT. In fact, a recurring theme in the preceding chapters has been that *the existence of Rindler particles, in the form of the Unruh thermal bath, is paramount for the consistency of QFT*. An useful analogy here is the concept of inertial forces in classical mechanics: they are required for consistency of description between different sets of observers.

We saw this briefly in the case of the Unruh-deWitt detector in Chapter 2 and in much more detail in the case of the inverse beta decay rate for accelerated protons in Chapter 3. Leaving aside the complications brought by mixing neutrinos, this could be regarded as an experimental idea for "observing" the Unruh effect. However, the proton lifetime obtained from these decay rates precludes this from being a realistic possibility. As an estimate, under typical accelerations obtainable with the LHC the accelerated proton lifetime would be of order $10^{3\times10^8}$ years, being much larger than the lifetime of the universe.

An important scale existing in both these problems associated with this problem is the gap between the proton and neutron masses. If the gap were smaller, observing the decay would be easier (although not necessarily *easy*). This motivates us to look for another system where this "energy gap" could be arbitrarily small. One system fitting this criterion is a charged radiating particle, since it can emit photons with any frequency.

The connection between electromagnetic radiation and the Unruh effect was already studied before [20]. Although equality between interaction rates was already obtained there,

the fact that in the Rindler frame the charge (without a regularization procedure) only interacted with (an infinite number of) zero-energy photons, was seen by skeptics as a problem.

With these two points in mind we proceed now to discuss a variant of this previous work where this problem is avoided. This is done via addition of transversal motion to the charge. In particular, we consider that the charge not only accelerates uniformly in the z direction but that it also rotates in the $x-y$ plane with a constant acceleration with respect to Rindler observers. This type of motion makes the situation stationary from the accelerated point of view, which allow us to study it analytically and also makes the charge interact with non-zero energy particles in the Rindler frame. As we shall see, the Unruh effect is *still* fundamental for obtaining consistent results, no matter if these results involve particles with zero or non-zero energy in the Rindler frame.

With regards to observing the Unruh effect experimentally, an important point to notice is that we *will not* consider an observer co-moving with the charge. It is known that the Unruh effect cannot be derived for uniformly rotating observers, since the Killing field generating their trajectory is not globally timelike [21] . This is the main reason the experimental proposal made in Ref. [24] for observing the Unruh effect only achieves partial success. In the last years there have been many other proposals for observing the Unruh effect experimentally, both directly (e.g., Ref. [45]) and using analogue models (e.g., Ref. [23]).

We will also propose an experiment to obtain an observable which can be directly interpreted in terms of the Unruh effect with some notable advantages: firstly, we calculate the expected result in both inertial and accelerated frames, which is something that some proposals only hint on being able to do. Secondly, our experiment involve mainly *classical* quantities, with only one quantum ingredient added. Although this may sound a bit surprising, we will show this explicitly. We believe that our experiment may be doable with current technology, but comment on some of the challenges involved at the end of this chapter.

4.2 Observing the Unruh effect with electromagnetic radiation

4.2.1 Rindler observers' proposal

Here we describe the setup for our experiment in detail. To this end, we consider a semi-classical electromagnetic current j^μ and ask Rindler observers to predict the interaction rate for the charge immersed in the Unruh thermal bath of photons. Later we will see that it is easy to generalize the result to a thermal state at an arbitrary temperature. Keeping the thermal state general allow us to also see how deviations from the Unruh temperature (which would indicate something wrong with the derivation of the Unruh effect) affect our results. Afterwards, these observers propose a setup for inertial experimenters to confirm their prediction. Since this setup involves only classical electrodynamics, we can use Maxwell's the-

ory to predict the expected interaction rate.

Rindler observers cover spacetime with coordinates (λ, ξ, r, ϕ) such that the spacetime length element is given by

$$ds^2 = e^{2a\xi}\left(d\lambda^2 - d\xi^2\right) - dr^2 - r^2 d\phi^2, \tag{4.1}$$

where $\lambda \in (-\infty, +\infty)$[I], $\xi \in (-\infty, \infty)$, $r \in [0, \infty)$ and $\phi \in [0, 2\pi)$. The current we want to describe is one that is uniformly rotating with respect to Rindler observers. It is given by

$$j^\mu = \frac{q\, u^\mu}{u^0 \sqrt{-g}} \delta^3(\vec{x} - \vec{x}_0) \tag{4.2}$$

$$= \frac{q\, u^\mu}{R\, u^0} \delta(\xi)\delta(\phi - \Omega\lambda)\delta(r - R), \tag{4.3}$$

where q is electric charge, R is the radius of movement in the transversal plane, Ω is the angular velocity (with respect to Rindler observers) and the four-velocity u^μ is given by

$$u^\mu = \gamma\,(1, 0, 0, \Omega)\,, \quad \gamma = \left(1 - R^2\Omega^2\right)^{-1/2}. \tag{4.4}$$

Rindler observers must quantize the electromagnetic field, A_μ, but now we shall use polar coordinates, which are more adequate to the symmetry of our setup. Let us consider initially the scalar Klein-Gordon equation [Eq. (2.2)], which we will use as a stepping stone for constructing the solutions of the vector one. In the above coordinates, it can be written as

$$\left[e^{-2a\xi}(\partial_\lambda^2 - \partial_\xi^2) - r^{-1}\partial_r(r\partial_r) - r^{-2}\partial_\phi^2\right]\Phi = 0. \tag{4.5}$$

Due to the time and axial symmetries of the problem we try an *ansatz* proportional to $e^{-i\varpi\lambda + im\phi}$. The same method presented in Chapter 2, together with the definition of the Bessel J function leads us to

$$g_{\vec{q}} = C_\varpi K_{i\varpi/a}\left(\frac{k_\perp}{a} e^{a\xi}\right) J_m(k_\perp r) e^{im\phi} e^{-i\varpi\lambda}, \tag{4.6}$$

where $\vec{q} = (\varpi, k_\perp, m)$, the normalization constant C_ϖ is

$$C_\varpi = \left[\sinh\left(\pi\varpi/a\right)/(2\pi^3 a)\right]^{1/2}, \tag{4.7}$$

and the quantum numbers are such that $m \in \mathbb{Z}$, $k_\perp \in [0, \infty)$ and $\varpi \in [0, \infty)$. Again we note that there is no dispersion relation between any of the quantum numbers.

[I] We use λ here in place of τ since as the charge will be rotating with respect to Rindler observers, their proper time ($\propto \lambda$) will not coincide with the charge proper time, τ.

For the electromagnetic field we consider the usual Lagrangian

$$\mathscr{L} = -\sqrt{-g}\left[(1/4)F_{\mu\nu}F^{\mu\nu} + (2\alpha)^{-1}(\nabla_\mu A^\mu)^2\right], \tag{4.8}$$

with the Feynman gauge ($\alpha = 1$) and where, as usual, $F_{\mu\nu} = \partial_\mu A_\nu - \partial_\nu A_\mu$. This leads to the wave equation

$$\nabla^\mu \nabla_\mu A_\nu = 0. \tag{4.9}$$

The physical modes of the electromagnetic field, which also satisfy the Lorenz condition $\nabla_\mu A^\mu = 0$ and are not pure gauge modes, can then be written in terms of Eq. (4.6) as

$$A^{(\epsilon=1)}_{\mu,\vec{q}} = k_\perp^{-1}\left(\partial_\xi g_{\vec{q}}, \partial_\lambda g_{\vec{q}}, 0, 0\right), \tag{4.10}$$

$$A^{(\epsilon=2)}_{\mu,\vec{q}} = k_\perp^{-1}\left(0, 0, -mr^{-1} g_{\vec{q}}, -ir\partial_r g_{\vec{q}}\right). \tag{4.11}$$

Together with the non-physical modes, $A^{(\epsilon=3,4)}_{\mu,\vec{q}}$, whose form shall not concern us here (since no physical particle state will have such polarizations), we can expand the field as

$$\hat{A}_\mu = \sum_m \int_0^\infty dk_\perp k_\perp \int_0^\infty d\omega \sum_{\epsilon=1}^{4}\left(\hat{b}_{\epsilon,\vec{q}} A^{(\epsilon)}_{\mu,\vec{q}} + c.c.\right). \tag{4.12}$$

For calculating the interaction rate we work perturbatively to first order in the charge q with the interaction action given by

$$\hat{S}_I = \int d^4x\sqrt{-g}\; j^\mu \hat{A}_\mu. \tag{4.13}$$

The procedure is similar to the cases treated in Chapter 2 and 3: we calculate the interaction amplitudes, both for emission and absorption, square them, divide them by the total proper time of the interaction to obtain a finite result, multiply them by the appropriate thermal factors coming from the Unruh thermal bath and integrate non-invariant quantum numbers. The extra detail is that we must sum over both polarizations incoherently (since they give rise to different final states).

We begin with emission for the $\epsilon = 1$ case. In this case, the amplitude is given by

$$\begin{aligned} A_{R,em,\epsilon=1} &= -i\langle\vec{q}|\hat{S}_I|0_R\rangle_{\epsilon=1} \\ &= -i\int \mathrm{d}^4x\sqrt{-g}\; j^\mu\left(\hat{A}^{(\epsilon=1)}_{\mu,\vec{q}}\right)^* \\ &= -2\pi i q J_m(k_\perp R)\left[\frac{\sinh\pi\omega/a}{2\pi^3 a}\right]^{1/2} K'_{\frac{i\omega}{a}}\left(\frac{k_\perp}{a}\right)\delta(\omega - m\Omega), \end{aligned} \tag{4.14}$$

where the prime indicates differentiation with respect to the argument of the modified Bessel function. Note that we are calculating the amplitude using the Rindler vacuum state, $|0_R\rangle$ as explained at the end of Chapter 2. Another important point to notice here is the presence of

the $\delta(\varpi_R - m\Omega)$ term. For $m \neq 0$ the particles interacting with the semi-classical current *do not have zero energy with respect to Rindler observers.* As mentioned in the introduction to this chapter, this has been a point of debate in the literature and the existence of the rotational movement in the current was inserted specifically to address such criticism.

Using Eq. (2.81) we obtain

$$\frac{|A_{R,em,\epsilon=1}|^2}{\Delta\tau_R} = \frac{q^2}{\pi^2 a}|J_m(k_\perp R)|^2 \sinh(\pi\varpi/a)\left|K'_{\frac{i\varpi}{a}}\left(\frac{k_\perp}{a}\right)\right|^2 \delta(\varpi - m\Omega). \tag{4.15}$$

Integrating the Rindler frequency and multiplying by the appropriate thermal factor we obtain the interaction rate for emission as

$$\frac{d\Gamma^{m,\epsilon=1}_{R,em}}{k_\perp dk_\perp} \equiv \frac{1}{\Delta\tau_R}\frac{dN^{m,\epsilon=1}_{R,em}}{k_\perp dk_\perp} = \int_0^\infty \mathrm{d}\varpi \frac{|A_{R,em,\epsilon=1}|^2}{\Delta\tau_R}\left(\frac{1}{e^{2\pi\varpi/a}-1}+1\right) \tag{4.16}$$

$$= \begin{cases} 0 & \text{if } m<0, \\ \frac{q^2}{2\pi^2 a}\left(\left|K'_{\frac{i\Omega m}{a}}\left(\frac{k_\perp}{a}\right)\right|^2 |J_m(k_\perp R)|^2 e^{\pi m\Omega/a}\right) & \text{if } m>0. \end{cases}$$

The same procedure can be followed for the absorption part of the interaction rate. Noting that the probability for absorption and for emission are the same, the only difference is the thermal factor (which does not include the spontaneous emission term). This gives

$$\frac{d\Gamma^{m,\epsilon=1}_{R,abs}}{k_\perp dk_\perp} = \int_0^\infty \mathrm{d}\varpi \frac{|A_{R,em,\epsilon=1}|^2}{\Delta\tau_R}\left(\frac{1}{e^{2\pi\varpi/a}-1}\right) \tag{4.17}$$

$$= \begin{cases} 0 & \text{if } m<0, \\ \frac{q^2}{2\pi^2 a}\left(\left|K'_{\frac{i\Omega m}{a}}\left(\frac{k_\perp}{a}\right)\right|^2 |J_m(k_\perp R)|^2 e^{-\pi m\Omega/a}\right) & \text{if } m>0. \end{cases}$$

The remaining case, $m = 0$ (the zero-energy mode), is dealt by considering both emission and absorption together[II]

$$\frac{d\Gamma^{m=0,\epsilon=1}_{R,em+abs}}{k_\perp dk_\perp} = \frac{q^2}{2\pi^2 a}\left(\left|K'_0\left(\frac{k_\perp}{a}\right)\right|^2 |J_0(k_\perp R)|^2\right). \tag{4.18}$$

[II] This is not strictly needed, but avoids a lengthy regularization procedure. See, e.g., Ref. [20] for a discussion.

With the first polarization being taken care of, let us look at $\epsilon = 2$. In this case,

$$\begin{aligned} A_{R,em,\epsilon=2} &= -i\langle \vec{q}|\hat{S}_I|0_R\rangle_{\epsilon=2} \\ &= -i\int \mathrm{d}^4x\sqrt{-g}\; j^\mu\left(\hat{A}^{(\epsilon=2)}_{\mu,\vec{q}}\right)^* \\ &= 2\pi qR\Omega\left[\frac{\sinh(\pi\varpi/a)}{2\pi^3 a}\right]^{1/2} J'_m(k_\perp R)\,K_{\frac{i\varpi}{a}}\left(\frac{k_\perp}{a}\right)\delta(\varpi - m\Omega)\,, \end{aligned} \tag{4.19}$$

where a prime again denotes differentiation with respect to the argument. Following the same steps as the previous case, we obtain the emission rate as

$$\begin{aligned} \frac{d\Gamma^{m,\epsilon=2}_{R,em}}{k_\perp dk_\perp} &= \int_0^\infty \mathrm{d}\varpi \frac{|A_{R,em,\epsilon=2}|^2}{\Delta\tau_R}\left(\frac{1}{e^{2\pi\varpi/a}-1}+1\right) \\ &= \begin{cases} 0 & \text{if } m<0, \\ \frac{(R\Omega)^2q^2}{2\pi^2 a}\left(\left|K_{\frac{i\Omega m}{a}}\left(\frac{k_\perp}{a}\right)\right|^2|J'_m(k_\perp R)|^2 e^{\pi m\Omega/a}\right) & \text{if } m>0. \end{cases} \end{aligned} \tag{4.20}$$

The absorption rate, on the other hand, is given by

$$\begin{aligned} \frac{d\Gamma^{m,\epsilon=2}_{R,abs}}{k_\perp dk_\perp} &= \int_0^\infty \mathrm{d}\varpi \frac{|A_{R,em,\epsilon=2}|^2}{\Delta\tau_R}\left(\frac{1}{e^{2\pi\varpi/a}-1}\right) \\ &= \begin{cases} 0 & \text{if } m<0, \\ \frac{(R\Omega)^2q^2}{2\pi^2 a}\left(\left|K_{\frac{i\Omega m}{a}}\left(\frac{k_\perp}{a}\right)\right|^2|J'_m(k_\perp R)|^2 e^{-\pi m\Omega/a}\right) & \text{if } m>0. \end{cases} \end{aligned} \tag{4.21}$$

Finally, the $m = 0$ case for $\epsilon = 2$ gives

$$\frac{d\Gamma^{m=0,\epsilon=2}_{R,em+abs}}{k_\perp dk_\perp} = \frac{(R\Omega)^2q^2}{2\pi^2 a}\left(\left|K_0\left(\frac{k_\perp}{a}\right)\right|^2|J'_0(k_\perp R)|^2\right). \tag{4.22}$$

The total interaction rate per transverse momenta seen by Rindler observers then is given by the sum over m of the previous expressions for the individual rates. We will not show the full expression here since we will write this result in a more general way shortly below.

There are two interesting things to note in the above results: firstly, considering the $\Omega \to 0$ case and summing over m, we can see that these are the same results obtained in Ref. [20] [if we make $dk_x dk_y \to k_\perp dk_\perp d\phi_k$ and integrate in ϕ_k in their Eq. (31)], as expected. Secondly, the charge only interacts with $m > 0$ from the accelerated point of view. This will not be the case from the inertial point of view and we shall see that this is related to conservation of angular momentum.

Up until now we have considered a thermal bath at the Unruh temperature $T_U = a/2\pi$. Since it is our interest to consider how inertial observers can verify the properties of the Unruh thermal bath, we consider a general thermal state seen by Rindler observers at an arbitrary temperature T (including the possibility that both inertial and uniformly accelerated

vacuum are equal, i.e., $T = 0$). We can easily generalize the above calculations for this case by making the substitution $2\pi\varpi/a \to \varpi/T$ in the thermal factors of Eqs. (4.16), (4.17), (4.20), (4.21) (the same caveats regarding the $m = 0$ mode also apply).

We obtain then

$$\begin{aligned}\frac{d\Gamma^m_{R,tot}}{k_\perp dk_\perp} &\equiv \frac{1}{\Delta\tau_R}\frac{dN^m_{R,tot}}{k_\perp dk_\perp} = \\ &= \Theta(m)\frac{q^2}{\pi^2 a}\sinh\left(\frac{\pi m\Omega}{a}\right)\coth\left(\frac{m\Omega}{2T}\right)\times \\ &\left[|K'_{im\Omega/a}(k_\perp/a)|^2|J_m(k_\perp R)|^2 + (R\Omega)^2|K_{im\Omega/a}(k_\perp/a)|^2|J'_m(k_\perp R)|^2\right].\end{aligned} \tag{4.23}$$

where $\Theta(m)$ is the Heaviside function with $\Theta(0) = 1/2$. This expression, summed over m, is plotted for different values of T in Figure 4.1. With these results, Rindler observers predict that the total interaction rate seen by inertial observers (which from their point of view is comprised only of photon emission) if the Unruh effect is valid, i.e., if $T = T_U = a/2\pi$ is the one given by Eq. (4.23) precisely for this temperature (the blue middle curve).

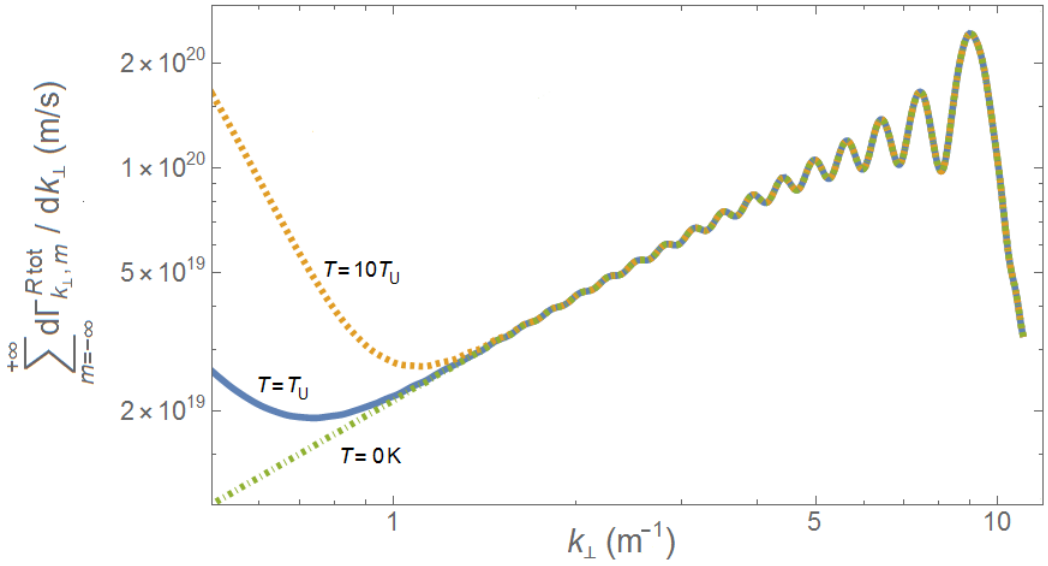

Figure 4.1: Interaction rate per transverse momenta for different temperatures of the Rindler thermal bath. The values of the chosen parameters are explained in Sec. 4.3.

To confirm Rindler observers predictions, inertial observers must set up an experiment. They consider a charged bunch of electrons which propagates along a cylinder with an opening in the middle where appropriate electromagnetic fields have been set up. This opening is surrounded by a sphere of electromagnetic detectors which we assume are able to discern the energy and angle of arrival of the radiation. A conceptual picture of this setup is shown in Figure 4.2. Note that the information we require inertial observers to gather is purely "classical", i.e., it does not involve quantum observables. We discuss the experimental parameters of this setup and how reasonable they are at the end of this chapter.

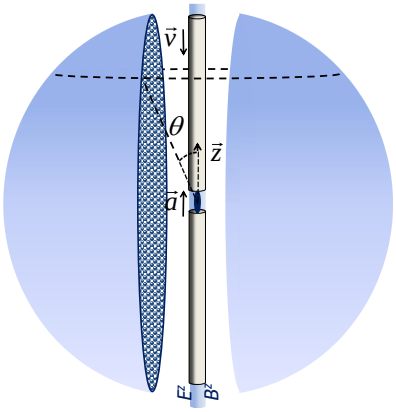

Figure 4.2: Experiment representation. After setting appropriate electric and magnetic fields to create the described 4-current, we inject a bunch of electrons into the cylinder with an opening in the middle, from where radiation is collected by a sphere of electromagnetic detectors.

4.2.2 Inertial observers' confirmation

Now we will show that using only classical electrodynamics and the usual quantization of energy (i.e., $\mathscr{E} = N_M\omega$, where N_M is the number of photons seen by Minkowski observers and $\omega = |\vec{k}|$) we can predict the experimental result from the inertial point of view. To this end, let us consider the angular-resolved spectral density of the emitted radiation, i.e.,

$$I(\omega,\theta,\phi) \equiv \frac{d\mathscr{E}(\omega,\theta,\phi)}{d\omega\, d(\cos\theta)\, d\phi}. \tag{4.24}$$

We obtain the infinitesimal number of photons dN emitted with energy $d\mathscr{E}$ as

$$dN_M = d\mathscr{E}/\omega = I(\omega,\theta,\phi)\omega^{-1} d\omega\, d(\cos\theta)\, d\phi. \tag{4.25}$$

Using the geometry shown in Figure 4.2 we see that $k_z = \omega\cos\theta$ and $k_\perp = \omega\sin\theta$. After integrating with respect to non-invariant quantities between both sets of observers we can write the number of emitted photons per transverse momenta seen by Minkowski observers as

$$\frac{dN_M}{k_\perp dk_\perp} = \int_0^{2\pi} d\phi \int_{-\infty}^{\infty} \frac{dk_z}{(k_\perp^2 + k_z^2)^{3/2}} I(\omega,\theta,\phi). \tag{4.26}$$

The spectral density defined in Eq. (4.24) depends only on the properties of the radiating electric field $\vec{E}_{rad}$. It can be written as a Fourier transform of this field, i.e.,

$$I(\omega,\theta,\phi) = \frac{R_S^2}{\pi}\left|\int dt \vec{E}_{rad}(t,\theta,\phi)e^{-i\omega t}\right|^2, \tag{4.27}$$

where R_S is the radius of the sphere of the detectors. Since the properties of the electric field in the radiating zone can be expressed in terms of the current j^μ, we can reduce the above

equation to (see, e.g., [46])

$$I(\omega,\theta,\phi) = \frac{q^2\omega^2}{4\pi^2}|\vec{F}(\omega,\theta,\phi)|^2, \tag{4.28}$$

with

$$\vec{F}(\omega,\theta,\phi) = (F_x,F_y,F_z) = \hat{r}\times\int d\lambda \frac{d\vec{r}_q}{d\lambda} f(\lambda), \tag{4.29}$$

where

$$\vec{r}_q(\lambda) = \left(R\cos(\Omega\lambda), R\sin(\Omega\lambda), a^{-1}\cosh(a\lambda)\right) \tag{4.30}$$

is the charged bunch spatial trajectory,

$$\hat{r} = \left(\sin(\theta)\cos(\phi), \sin(\theta)\sin(\phi), \cos(\theta)\right) \tag{4.31}$$

gives the observation direction, and

$$f(\lambda) \equiv \exp\left[-i\omega\left(\hat{r}\cdot\vec{r}_q(\lambda) - a^{-1}\sinh(a\lambda)\right)\right]. \tag{4.32}$$

Expanding $f(\lambda)$ we get

$$f(\lambda) = \exp\left[-i\omega(R\sin(\theta)\cos\left(\phi-\Omega\lambda\right) + a^{-1}(\cos(\theta)\cosh(a\lambda) - \sinh(a\lambda)))\right]. \tag{4.33}$$

If we expand Eq. (4.28) we see that each component is given in terms of a similar integral. We shall show how F_x is calculated explicitly, with F_y and F_z being obtained by applying very similar ideas. Therefore, let us expand F_x as

$$F_x = \int d\lambda f(\lambda)\left[\sinh(a\lambda)\sin(\theta)\sin\left(\phi\right) - \Omega R\cos(\theta)\cos(\Omega\lambda)\right] \tag{4.34}$$

Before proceeding, however, we will derive a series of useful mathematical building blocks for doing the integrals which will appear. To allow a comparison with the result obtained by Rindler observers, the first step we must take is to make the m quantum number appear in the formulas above, as it is not immediately obvious why it does so. To this end, we expand the ϕ-dependent part using the Rayleigh formula, Eq. [8.511.4(2)] of Ref. [28],

$$e^{-i\omega R\sin(\theta)\cos\left(\phi-\Omega\lambda\right)} = \sum_m i^m J_m(-R\underbrace{\omega\sin(\theta)}_{k_\perp})e^{im(\phi-\Omega\lambda)}. \tag{4.35}$$

Since in the spectral density formula we have terms with cosines and sines multiplying the exponential function it will be useful to derive some other identities from Eq. (4.35) by differentiation with respect to $-k_\perp R$ and ϕ. Firstly, deriving Eq. (4.35) with respect to $-Rk_\perp$, we have

$$\cos\left(\phi-\Omega\lambda\right)e^{-ik_\perp R\cos\left(\phi-\Omega\lambda\right)} = -i\sum_m i^m J'_m(-k_\perp R)e^{im(\phi-\Omega\lambda)}, \tag{4.36}$$

where the $'$ means differentiation with respect to the argument. Differentiating Eq. (4.35)

with respect to ϕ, on the other hand, gives us

$$Rk_\perp \sin(\phi-\Omega\lambda)e^{-ik_\perp R\cos(\phi-\Omega\lambda)} = \sum_m i^m m J_m(-k_\perp R)e^{im(\phi-\Omega\lambda)}. \tag{4.37}$$

Both identities above can be written alternatively as

$$\begin{aligned}\sin(\phi)\sin(\Omega\lambda)e^{-ik_\perp R\cos(\phi-\Omega\lambda)} = &-i\sum_m\left(i^m J_m'(-k_\perp R)e^{im(\phi-\Omega\lambda)}\right)\\ &-\cos(\phi)\cos(\Omega\lambda)e^{-ik_\perp R\cos(\phi-\Omega\lambda)},\end{aligned} \tag{4.38}$$

and

$$\begin{aligned}\sin(\phi)\cos(\Omega\lambda)e^{-ik_\perp R\cos(\phi-\Omega\lambda)} = &\frac{1}{k_\perp R}\sum_m\left(m\, i^m J_m(-k_\perp R)e^{im(\phi-\Omega\lambda)}\right)\\ &+\cos(\phi)\sin(\Omega\lambda)e^{-ik_\perp R\cos(\phi-\Omega\lambda)}.\end{aligned} \tag{4.39}$$

Using Eq. (4.35) then we can write F_x as

$$\begin{aligned}F_x = a^{-1}&\left[\sum_m i^m e^{im\phi}J_m(-k_\perp R)\times\right.\\ &\left.\left(\sin(\theta)\sin(\phi)\int_{-\infty}^{+\infty}d\lambda\sinh(\lambda)e^{-im\Omega\lambda/a}e^{-i\omega a^{-1}\cos(\theta)\cosh(\lambda)}e^{i\omega a^{-1}\sinh(\lambda)}\right)\right]\\ &-\cos(\theta)a^{-1}R\Omega\int_{-\infty}^{+\infty}d\lambda\cos\left(\frac{\Omega\lambda}{a}\right)f(\lambda/a),\end{aligned} \tag{4.40}$$

where we have made $\lambda\to\lambda/a$. Identities (4.38) and (4.39) can be used to express the integral appearing in F_x, i.e.,

$$\int_{-\infty}^{+\infty}d\lambda\cos\left(\frac{\Omega\lambda}{a}\right)f(\lambda/a), \tag{4.41}$$

in terms of another integral whose general form is similar to the first term in the expression above (and also similar to integrals appearing in the F_y and F_x components). Applying Eqs. (4.38) and (4.39) we have

$$\begin{aligned}\int_{-\infty}^{+\infty}d\lambda\cos\left(\frac{\Omega\lambda}{a}\right)f(\lambda/a) &= \frac{\csc(\phi)}{k_\perp R}\sum_m m\, i^m e^{im\phi}C_m(\omega,\theta)\\ &+\cot(\phi)\int_{-\infty}^{+\infty}d\lambda\sin\left(\frac{\Omega\lambda}{a}\right)f(\lambda/a)\\ &= \frac{\csc(\phi)}{k_\perp R}\sum_m m\, i^m e^{im\phi}J_m(-k_\perp R)C_m(\omega,\theta)\\ &-i\frac{\cos(\phi)}{\sin^2(\phi)}\sum_m i^m e^{im\phi}J_m'(-k_\perp R)C_m(\omega,\theta)\\ &-\frac{\cos^2(\phi)}{\sin^2(\phi)}\int_{-\infty}^{+\infty}d\lambda\cos\left(\frac{\Omega\lambda}{a}\right)f(\lambda/a)\end{aligned} \tag{4.42}$$

giving finally

$$\int_{-\infty}^{+\infty} \mathrm{d}\lambda \cos\left(\frac{\Omega\lambda}{a}\right) f(\lambda/a) = \frac{\sin(\phi)}{k_\perp R} \sum_m m\, i^m e^{im\phi} J_m(-k_\perp R) C_m(\omega,\theta) \\ - i\cos(\phi) \sum_m i^m e^{im\phi} J'_m(-k_\perp R) C_m(\omega,\theta), \tag{4.43}$$

where

$$C_m(\omega,\theta) = \int_{-\infty}^{+\infty} \mathrm{d}\lambda\; e^{-im\Omega\lambda/a} e^{-i\omega a^{-1}\cos(\theta)\cosh(\lambda)} e^{i\omega a^{-1}\sinh(\lambda)}. \tag{4.44}$$

All remaining integrals can be written in a general form (after making the change of variables $t = e^\lambda$) as

$$I = 2^{-1} \int_0^\infty \mathrm{d}t (t^\alpha + \epsilon t^{-\alpha}) t^{-ib-1} \exp\left\{\left[\frac{ci}{2}\left(dt - f/t\right)\right]\right\}, \tag{4.45}$$

where $\epsilon = \pm 1$, $\alpha = 0$ or 1, $b = m\Omega/a$, $c = a^{-1}\omega$, $d = 1-\cos\theta$, $f = 1+\cos\theta$. Using the residue theorem with a quarter-circle contour to go to the positive imaginary axis of the complex plane and using Eq. (8.432.7) of Ref. [28] we obtain the result

$$I = e^{\frac{\pi m\Omega}{2a}} (\tan(\theta/2))^{\frac{im\Omega}{a}} \left[i^\alpha (\tan(\theta/2))^{-\alpha} K_{\frac{im\Omega}{a}-\alpha}\left(\frac{k_\perp}{a}\right) + \epsilon(\alpha \Leftrightarrow -\alpha)\right], \tag{4.46}$$

where $(\alpha \Leftrightarrow -\alpha)$ means making the indicated substitution in the preceding term of the bracket. Using the result given by Eq. (4.46) with $\alpha = \epsilon = 0$, we can solve the integral defining $C_m(\omega,\theta)$ and write the integral in the second term of Eq. (4.40) as

$$\int_{-\infty}^{+\infty} \mathrm{d}\lambda \cos\left(\frac{\Omega\lambda}{a}\right) f(\lambda/a) = \sum_m i^m e^{im\phi} e^{\frac{\pi m\Omega}{2a}} (\tan(\theta/2))^{\frac{im\Omega}{a}} \times \\ \left(\frac{2m\sin(\phi)}{k_\perp R} J_m(-k_\perp R) K_{\frac{im\Omega}{a}}\left(\frac{k_\perp}{a}\right) - 2i\cos(\phi) J'_m(-k_\perp R) K_{\frac{im\Omega}{a}}\left(\frac{k_\perp}{a}\right)\right). \tag{4.47}$$

With the second term being taken care of, we focus on the first one. Using Eq. (4.46) now with $\alpha = 1$ and $\epsilon = -1$ we get

$$\sum_m i^m e^{im\phi} J_m(-k_\perp R) a^{-1} e^{\frac{\pi m\Omega}{2a}} (\tan(\theta/2))^{\frac{im\Omega}{a}} \times \\ 2i\sin(\phi)\left[\cos^2(\theta/2) K_{\frac{im\Omega}{a}-1}\left(\frac{k_\perp}{a}\right) + \sin^2(\theta/2) K_{\frac{im\Omega}{a}+1}\left(\frac{k_\perp}{a}\right)\right]. \tag{4.48}$$

Using that $2\cos^2(\theta/2) = (1+\cos(\theta))$ and $2\sin^2(\theta/2) = (1-\cos(\theta))$ along with Eqs. (8.486.10/11) of Ref. [28] simplifies the second line of the above expression to

$$-i\sin(\phi)\left[2K'_{\frac{im\Omega}{a}}\left(\frac{k_\perp}{a}\right) + 2i\cos(\theta)\frac{m\Omega}{k_\perp} K_{\frac{im\Omega}{a}}\left(\frac{k_\perp}{a}\right)\right]. \tag{4.49}$$

Now we can write Eq. (4.40), which after simplifying everything gives

$$F_x = -2ia^{-1}\sum_m i^m e^{im\phi} e^{\pi m\Omega/2a} (\tan(\theta/2))^{\frac{im\Omega}{a}} \times \\ \left(\sin(\phi) J_m(-k_\perp R) K'_{\frac{im\Omega}{a}}\left(\frac{k_\perp}{a}\right) - R\Omega\cos(\theta)\cos(\phi) J'_m(-k_\perp R) K_{\frac{im\Omega}{a}}\left(\frac{k_\perp}{a}\right)\right). \tag{4.50}$$

This form already bears some resemblance to the result obtained by Rindler observers for the emission rate [Eq. (4.23) for $T = T_U$]. The appearance of the modified Bessel functions with the right orders and arguments is interesting, as from the Rindler frame they come directly from the quantum numbers defining the Unruh modes, while here they appear naturally. Again we note how calculating this result in the Rindler frame is much easier then doing so in the inertial one (even if we were to do so with usual QFT as is shown in Appendix C). Applying the same ideas to F_y and F_z we get

$$F_y = -2ia^{-1}\sum_m i^m e^{im\phi} e^{\pi m\Omega/2a} (\tan(\theta/2))^{\frac{im\Omega}{a}} \times \\ \left(\cos(\phi) J_m(-k_\perp R) K'_{\frac{im\Omega}{a}}\left(\frac{k_\perp}{a}\right) + R\Omega\cos(\theta)\sin(\phi) J'_m(-k_\perp R) K_{\frac{im\Omega}{a}}\left(\frac{k_\perp}{a}\right)\right) \tag{4.51}$$

and

$$F_z = -2iR\Omega a^{-1}\sin(\theta)\sum_m i^m e^{im\phi} J'_m(-k_\perp R) e^{\frac{\pi m\Omega}{2a}} (\tan(\theta/2))^{\frac{im\Omega}{a}} K_{\frac{im\Omega}{a}}\left(\frac{k_\perp}{a}\right) \tag{4.52}$$

All that remains now is to plug the results for (F_x, F_y, F_z) in Eqs. (4.28), (4.26) and integrate in ϕ. Although laborious, the calculations are much simpler than the ones above and this process results finally in

$$\frac{dN_M}{k_\perp dk_\perp} = \sum_m \int dk_z \frac{2q^2}{a^2\omega\pi} e^{\frac{\pi m\Omega}{a}} \times \\ \left(|J_m(k_\perp R)|^2 \left|K'_{\frac{im\Omega}{a}}\left(\frac{k_\perp}{a}\right)\right|^2 + (R\Omega)^2 \left|J'_m(k_\perp R)\right|^2 \left|K_{\frac{im\Omega}{a}}\left(\frac{k_\perp}{a}\right)\right|^2\right). \tag{4.53}$$

Integrating this expression with respect to k_z leads to a divergence. This is to be expected, since we have a current existing from the beginning of spacetime to its end. However, this divergence is *independent* of the transverse photon momentum $k_\perp$. We show in Appendix C that it can be identified with the total proper time of the current trajectory. Taking this fact into account we obtain that

$$\frac{dN_M}{k_\perp dk_\perp} = \underbrace{\left(\frac{4\pi}{a}\int_{-\infty}^{\infty} \frac{d\kappa_z}{(1+\kappa_z^2)^{1/2}}\right)}_{\Delta\tau_R} \sum_m \left.\frac{d\Gamma^m_{R,tot}}{k_\perp dk_\perp}\right|_{T=T_U}. \tag{4.54}$$

This shows that the inertial result is exactly the one predicted by uniformly accelerated

observers *taking into account that the inertial vacuum state is seen by them as a thermal bath with a temperature $T_U = a/2\pi$ exactly as predicted by the Unruh effect.* Plotting the resulting interaction rate gives exactly the middle curve of Figure 4.1, with $T = T_U$.

Before diving into the details of our proposed experiment, it is interesting to note some facts. Firstly, we have calculated the interaction rate using only classical electrodynamics. The fact that we can see traces of a quantum field theory effect [note the $\hbar$ in Eq. (1.1)] with a classical calculation may seem surprising at first, but it ceases to be so if one notes that $\hbar$ in T_U cancels everywhere since it is always accompanied by $\hbar m\Omega$. All "quantumness" comes from the Einstein relation between energy and frequency.

Secondly, as noted before, in the inertial frame all values of m (both negative and positive) are included in the result, while in the accelerated frame only modes with $m > 0$ contribute. The physical explanation for this is that in the accelerated frame we can have both *absorption* and *emission* of Rindler photons, which in the Minkowski frame must correspond *only* to emissions. However, an absorption of a $m > 0$ mode must then correspond to an emission of a $m < 0$ mode to preserve angular momentum. This is shown schematically in Figure 4.3.

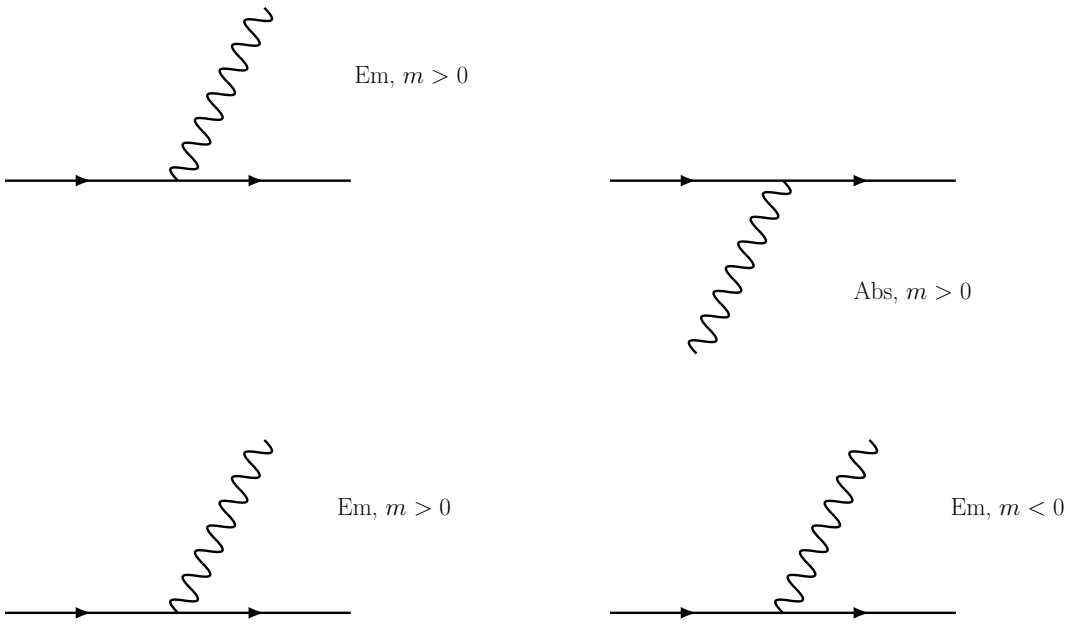

Figure 4.3: Relation between the angular quantum number m seen in the Rindler frame (above) and in the Minkowski frame (below).

4.3 Experimental proposal

The second part of the calculation in the previous section shows that the only information inertial experimenters need to recreate the result predicted by Rindler observers is the angular resolved spectral density, $I(\omega,\theta,\phi)$. Although conceptually simple, to measure such quantity we must consider various ways in which a real setup differs from the theoretical

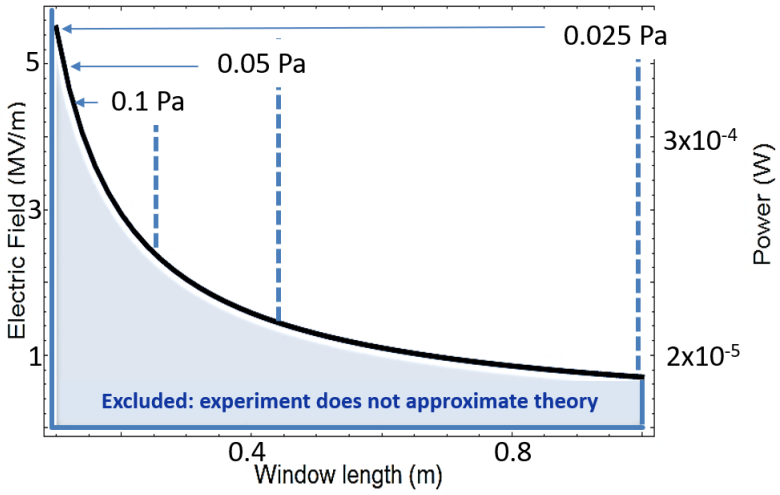

Figure 4.4: Exclusion region where the theory does not approximate the expected experimental result due to boundary effects.

proposal.

Firstly, clearly the charge q must be bigger than an elemental charge. We consider a bunch of $\approx 10^7$ electrons [47]. As seen during our calculations, we must be in the radiation zone for our predictions to be sensible. This implies that R_S must be greater than the region where the charge emits, which is the tube's opening with length L, i.e., $R_S \gg L$. Also, since we are dealing with an opening in a tube, we must require that boundary conditions are negligible.

This was not a problem in our calculation because we assumed a charge radiating from the infinite past to the infinite future. Considering a finite-time bunch, we avoid any divergence with respect to the total interaction time, but must take care with boundary conditions (i.e., the spacetime region where the charge spring into existence and where it disappears according to our radiation detectors) which in turn implies that the radiation wavelength must be smaller than the opening length L. Since the main scale determining the radiation wavelength is given by the (inverse) total charge acceleration, $a_{tot} = \gamma^2\sqrt{a^2 + R^2\Omega^4}$. This implies that we must have

$$a_{tot} \gg 10^{17}(1m/L)m/s^2. \tag{4.55}$$

In Figure 4.4 we plot the necessary electric field to achieve a total acceleration high enough in order to avoid boundary effects. We also shown the required vacuum level such as to avoid scattering by air molecules.

For estimation purposes, we consider electric and magnetic fields in the z direction such that $E^z \approx 1MV/m$ and $B^z \approx 10^{-1}T$, which are both values attainable with today's technology [48]. This gives a linear acceleration of order $a \approx 10^{17}m/s^2$ and a total acceleration $a_{tot} \approx 10^{19}m/s^2$, where we also took $R = 10^{-1}m$. These are the parameters we used to plot the curves in Figure 4.1.

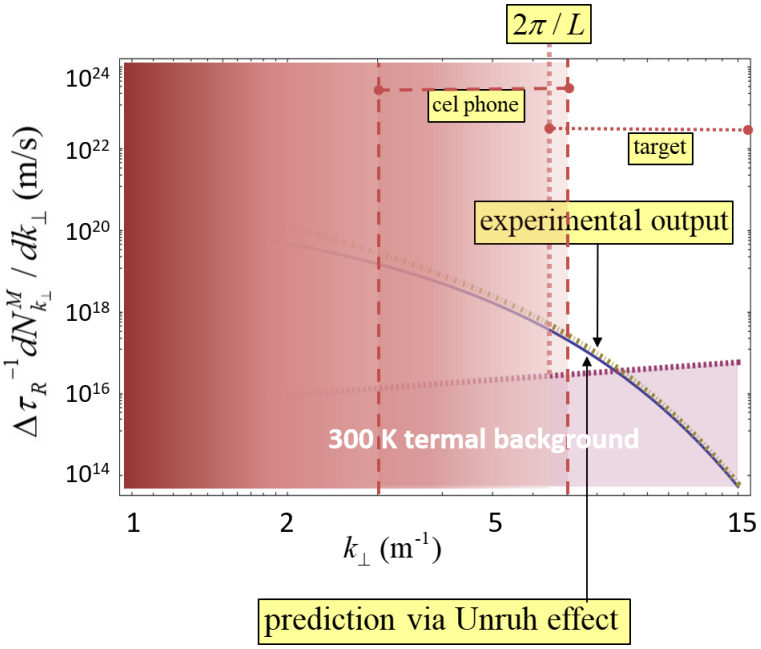

Figure 4.5: Exclusion regions due to background sources.

A final but important consideration is background noise. Experimental regions excluded by some sources of noise are shown in Figure 4.5, where we have set the magnetic field to zero for simplicity. From the plot in Figure 4.2 we see that it is easier to discern the expected result for the Unruh thermal bath the smaller $k_\perp$ we can observe. This in turn implies generally a bigger wavelength and a more challenging experimental setup to stay in the radiation zone. Note that this can be greatly ammeliorated by thermal and electromagnetical isolation. In this sense, the scenario presented here is an overly pessimistic estimate. Despite this, we still are able to see signs of the Unruh effect in this setup.

The main point of Ref. [1] was to show explicitly an observable obtainable from using mainly classical electrodynamics that could also be directly compared to an explicit prediction made based on the existence of the Unruh thermal bath. Although we believe the experiment we proposed is doable under present technology, it is still a formidable task. We hope that it or a variation based on its design can be constructed in the future, providing compelling evidence for any remaining skeptics with regards to the Unruh effect.

CHAPTER 5

Conclusion

The Unruh effect officially turned 40 years old in 2016 [17]. Although originally derived to better understand the Hawking effect, it has continuously gained more and more attention on its own during the last years. This is largely due to (i) the fact that it encapsulates in the simplest setting possible (i.e., Minkowski space-time) some important lessons learned from studying quantum field theories in curved spacetimes and (ii) that experimental technologies today are at the edge of enabling a strong and solid claim regarding an observation of the Unruh effect.

Despite being grounded purely on well-established quantum field theory constructions, a lot of mistrust has been (in our opinion, unjustly) placed on it due to it so explicitly laying bare the fact that *particles are not a fundamental concept in quantum field theory*. It could be argued that such lesson should have already been learned from condensed-matter systems (where *quasi*-particles abound), however, probably due to the non-relativistic nature of these systems, it seems this lesson was largely overlooked. The Unruh effect, however, leaves us with no doubts: *Quantum field theory is really a theory of fields and not particles*. Understanding the Unruh effect in all of its splendor still is an active area of research and we believe it will probably remain so in the mid-term future.

This thesis is our contribution to this important theme. After a brief introduction, we treated the interplay between neutrinos and the Unruh effect [3]. Mixing neutrinos have been in the spotlight in the last years due to arguably being our best bet for probing physics beyond the Standard Model. By carefully defining what a flavor neutrino is and when such a construction makes sense in the framework of QFT, we arrive at perfectly consistent predictions between inertial and Rindler observers for one observable involving mixing neutrinos, as the general covariance of QFT requires. Moreover, this is only achieved by taking into account the existence of the Unruh thermal bath.

Afterwards, we considered how a well-understood effect such as *bremsstrahlung* can be interpreted in terms of the Unruh effect. It is known that describing this phenomenon from the point of view of Rindler observers is no trivial task (as was already shown by [20]) and involve unfamiliar concepts such as zero-energy particles. This led some people to argue that the Unruh effect must be wrong (see [21] for some examples of this affirmation[I]). For this reason, we worked with a modified model where equivalence between number of photons per transverse momenta seen by both observers can be shown also for non-zero energy Rindler particles *again provided that the Unruh effect is present* [1]. Moreover, the Rindler result can be compared to a result obtained by inertial observers using only *classical* electrodynamics (plus the uncontested Einstein relation between energy and frequency). We expect that this severely weakens the case of those who argue that the Unruh effect is wrong.

[I] For more recent examples of this kind of affirmation, see *Science*, https://www.sciencemag.org/news/2017/04/does-space-heat-when-you-accelerate-physicists-propose-test-controversial-idea

Nevertheless, an experimental observation of such equivalence would be greatly appreciated. To this end we proposed a simple conceptual experiment where this could be seen and discussed some of the challenges of doing it with today's technology [2]. It is our hope that this or a similar experiment inspired by our proposal can be realized in the near future.

As discussed in the main text, despite being fundamental for the consistency of QFT in the same way as inertial forces are for classical mechanics, experiencing the Unruh effect directly in the same way as we may experience, e.g., centrifugal forces, is impossible due to the extremely high accelerations required. For this reason, two main avenues present themselves: first, the one we explored here, which is to find observable phenomena that could be easily interpreted in terms of the Unruh effect itself and, second, finding analogue models where the effect can be explored. We believe that both these venues will bear fruit in the near/mid-term future, as evidenced by a flurry of recent research on these subjects (e.g., Refs. [49, 50, 51]).

Together with the work presented in this thesis and those sprung from it (e.g., Ref. [52]), we hope to finally lay to rest any lingering doubts about the reality of the Unruh effect.

Appendices

APPENDIX A

Extending the definition of flavor neutrino states

Flavor neutrinos were proposed as a way to deal with the solar neutrino problem: the fact that the neutrino flux seen from the sun arriving at Earth was only a third of what was predicted at the time. The way out of this was to propose that neutrinos changed "flavor" in such a way that only a fraction of the original electron neutrinos would interact with the detectors on Earth. This paradigm has been phenomenologically very successful to explain neutrinos' behavior (see, e.g., [37])[I].

The usual paradigm for dealing with flavor neutrinos initially used non-relativistic quantum mechanics as a basis for the theory. Extending it to a construction based on quantum field theory was then the next natural step. However, this is not so straightforward since flavor neutrinos are not on-shell particles and, therefore, a natural Fock space cannot be associated with them [40]. The correct way to associate any state to flavor neutrinos then must be phenomenological, such as the one given in [53, 44] (which we shall review shortly).

Such definition for flavor neutrino states, however, is valid for interaction processes involving one neutrino only. This happens because to define a flavor state $|\nu_\alpha\rangle$ as a superposition of massive neutrino states one must express the amplitudes of such superposition in terms of S-matrix elements, which are well-defined for massive neutrinos only.

More care is needed for the case involving multiple neutrinos, since in this case the amplitudes used for defining the state would themselves depend on the state definition. For this reason, as explained below, we must extend the previous formalism and deal with density matrices instead of pure states. This extension is also applicable to the case of heavy and sterile neutrinos with minor modifications. In this appendix, based on [4], we briefly review the original formalism for defining flavor neutrino states and discuss how it can be extended to the case of multiple neutrinos. We focus on the main points here and refer the reader to [4] for further details that are out of the main scope of this thesis.

A.1 Flavor states for single-neutrino processes

The usual definition of a particle is given in terms of creation operators acting on the vacuum state of the field. For interacting theories, such a definition is made asymptotically, where the interactions are assumed to be negligible. For simplicity, we consider here only flat spacetime quantum field theory using Cartesian coordinates.

A massive fermionic field is described by the Lagrangian

$$\mathscr{L} = \bar{\psi}(i\gamma^\mu\partial_\mu - m)\psi, \tag{A.1}$$

where the notation is explained in the main text (Chapter 3, Sec. 3.2). Given an expansion of the field in terms of normal modes, the vacuum state of the field is then defined as the state

[I] In fact this oscillation phenomenon arose even before in the context of particle/anti-particle oscillation.

annihilated by all annihilation operators in the field expansion

$$\hat{\psi} = \sum_{\sigma=\pm} \int d^3k \left(\hat{a}_{\vec{k},\sigma} u^{+\omega}_{\vec{k},\sigma} + \hat{b}^{\dagger}_{\vec{k},\sigma} u^{-\omega}_{\vec{k},-\sigma} \right). \tag{A.2}$$

This construction is adequate for obtaining massive neutrino states. Based on these states, one may hope to construct a flavor neutrino state associated with the field $\psi_\alpha \equiv \sum_i U_{\alpha,i}\psi_i$. This should come naturally after the successful usual construction given using non-relativistic quantum theory, which is

$$|\nu_\alpha\rangle \equiv \sum_i U^*_{\alpha,i} |\nu_i\rangle. \tag{A.3}$$

However, the situation in quantum field theory is more delicate. As shown in [40] there is no physical Fock space containing such states. Moreover, they cannot be produced in fundamental interactions since, due to their ill-defined mass, they cannot hope to conserve both energy and momentum in interaction vertexes. Despite these facts, for almost all practical situations the states $|\nu_\alpha\rangle$ give correct results in calculations (such as those of neutrino oscillation phases) since one usually works in the approximation where the neutrinos can be considered either massless or with degenerate masses.

Flavor neutrino and anti-neutrino states in QFT are better understood as phenomenological superposition of massive neutrino states and not associated with any fundamental quantum field. The expression $\psi_\alpha = \sum_i U_{\alpha,i}\psi_i$ should be regarded only as a shortcut for the particular combination of fields appearing in the weak interaction Lagrangian, as discussed in Chapter 3. The states must be seen as states *associated with particular interactions*, such as

$$p^+ \to n^0 + e^+ + \nu_e, \tag{A.4}$$

and not as states coming from the action of creation operators over vacuum states. Since they are phenomenological, associating a state with a flavor neutrino depends on two hypotheses being valid: first, this state must be a superposition of massive neutrino states. Second (and more importantly), there must be uncertainty in the energy and momenta involved in the interaction such that energy-momentum conservation cannot discriminate which massive neutrino is involved [41]. We will approximate here the states by momentum eigenstates, but these manipulations must be seen formally. Fortunately, all constructions presented here generalize to the case of wave-packets where they are physically meaningful. Let us begin by considering the specific reaction described by Eq. (A.4). We define the initial and final states as

$$|i\rangle = |p^+\rangle, \tag{A.5}$$

$$|f\rangle \propto (\hat{S} - \hat{I})|i\rangle = \sum_i A^{\mathrm{P}}_{e,i} |n^0; e^+; \nu_i\rangle + ..., \tag{A.6}$$

where $A^{\mathrm{P}}_{e,i}$ are complex numbers to be calculated [not, *a priori*, elements of the PMNS matrix as in the state given by Eq. (A.3)] and "..." includes other decay channels not relevant here (they are orthogonal to the one we are considering). The initial and final states are connected by

$$|f\rangle \propto (\hat{S} - \hat{I})|i\rangle, \tag{A.7}$$

where $\hat{S}$ is the S-matrix of the process and we are excluding the possibility of no interaction by subtracting the identity $\hat{I}$ term. Using the orthonormality of the different massive neutrino states we can use the relation above to express the amplitudes as

$$A^{\mathrm{P}}_{e,i} = \langle n^0; e^+; \nu_i|\hat{S}|p^+\rangle. \tag{A.8}$$

The flavor state is then defined by projecting only onto the neutrino subspace,

$$|\nu_e\rangle \propto \langle n^0; e^+|f\rangle \tag{A.9}$$

and normalizing. We obtain then

$$|\nu_e\rangle = \frac{1}{\sqrt{\sum_i |A^{\mathrm{P}}_{e,i}|^2}} \sum_i A^{\mathrm{P}}_{e,i}|\nu_i\rangle. \tag{A.10}$$

Since experimental results concerning neutrino mixing are very well described by using the states defined in Eq. (A.3), an important question is how these are recovered in the construction presented above. To answer it, we expand the weak interaction sector of the S-matrix appearing in the amplitudes as

$$\hat{S} \approx \hat{I} - i\,\frac{G_{\mathrm{F}}}{\sqrt{2}} \int \mathrm{d}^4x\, \hat{j}^{\dagger}_{\mathrm{CC}\rho}(x)\, \hat{j}^{\rho}_{\mathrm{CC}}(x), \tag{A.11}$$

with the weak-charged current $\hat{j}^{\rho}_{\mathrm{CC}}(x)$ given by

$$\hat{j}^{\rho}_{\mathrm{CC}}(x) = \sum_{\alpha,k} U^*_{\alpha k}\, \hat{\bar{\nu}}_k(x)\gamma^{\rho}\left(1-\gamma^5\right)\hat{l}_{\alpha}(x) + \hat{h}^{\rho}_{\mathrm{CC}}(x), \tag{A.12}$$

where $\hat{h}^{\rho}_{\mathrm{CC}}(x)$ is the hadronic part of the weak charged current (which is not our main concern here). Using this expansion we can write the general form of the amplitudes given in Eq. (A.8) as $A^{\mathrm{P}}_{\alpha,i} = U^*_{\alpha,i} M^{\mathrm{P}}_i$, where

$$M^{\mathrm{P}}_i = -i\,\frac{G_{\mathrm{F}}}{\sqrt{2}} \int \mathrm{d}^4x \langle \nu_i\, l^+_{\alpha}|\hat{\bar{\nu}}_k(x)\gamma^{\rho}\left(1-\gamma^5\right)\hat{l}_{\alpha}(x)|0\rangle\; J^{P_I\to P_F}_{\rho}(x), \tag{A.13}$$

with P_I and P_F standing for the initial and final hadronic particles, l^+_{α} being the charged

anti-lepton and the hadronic transition amplitude being given by

$$J_\rho^{P_I \to P_F}(x) = \langle P_F | \hat{h}_\rho(x) | P_I \rangle. \tag{A.14}$$

Note that by approximating the hadronic part of the problem by a semi-classical current we get the proton/neutron system used in Chapter 3. This can be seen as an extra justification for the treatment we used there. Now, in the approximation that all neutrino masses m_i are degenerate or zero, we have no i-index dependence in the M_i^{P} terms and we can denote them all M^{P} . This allow us to factor them out of the sum in Eq. (A.10). From the unitarity of the PMNS matrix, we see that the denominator is M^{P} up to an (irrelevant) phase, recovering the states defined in Eq. (A.3).

We stress again that the states given by Eq. (A.10) and their approximation in the degenerate mass/massless limit are physically reasonable approximations for real flavor neutrino states, which must necessarily be wave packets with energy-momentum uncertainty.

With the definition of weak states, Eq. (A.10), the whole process of neutrino emission, propagation and detection can be coherently described in the same framework (even *outside* the approximation where masses are degenerate or zero). Crucially, they imply that decay rates for flavor neutrinos are given by an *incoherent* sum over massive neutrinos. This is readily seen by calculating the probability associated with the beta decay:

$$\begin{aligned} P_{\nu_e} &= |\langle n^0; e^+; \nu_e | \hat{S} | p^+ \rangle|^2 \\ &= \left| \frac{1}{\sqrt{\sum_i |A^{\mathrm{P}}_{e,i}|^2}} \sum_i A^{*,\mathrm{P}}_{e,i} \langle n^0; e^+; \nu_i | \hat{S} | p^+ \rangle \right|^2 \\ &= \left| \frac{1}{\sqrt{\sum_i |A^{\mathrm{P}}_{e,i}|^2}} \sum_i A^{*,\mathrm{P}}_{e,i} A^{,\mathrm{P}}_{e,i} \right|^2 = \left| \frac{1}{\sqrt{\sum_i |A^{\mathrm{P}}_{e,i}|^2}} \sum_i |A^{*,\mathrm{P}}_{e,i}|^2 \right|^2 \\ &= \left| \sqrt{\sum_i |A^{\mathrm{P}}_{e,i}|^2} \right|^2 = \sum_i |A^{\mathrm{P}}_{e,i}|^2. \end{aligned} \tag{A.15}$$

Note that this discussion would follow in the same way from any point of view (inertial or accelerated). This fact was absent in the previous discussions of the Unruh effect for mixing neutrinos [25, 38], leading to the strange conclusions mentioned in Chapter 3.

A.2 Flavor states for multiple-neutrino processes

The derivations done in Sec. A.1 are well-suited for describing interactions involving one neutrino, such as the normal or inverse β decay. However, other processes may involve more

of them, e.g.,

$$\mu^+ \to e^+ + \nu_e + \bar{\nu}_\mu. \tag{A.16}$$

It is not possible to use directly the definition given in Eq. (A.10) since when projecting over the neutrino subspace we would have to project over states of the type $\langle \bar{\nu}_\mu e^+|$, which would still be not defined. The same is valid when trying to obtain the state of $\bar{\nu}_\mu$ alone. Each neutrino state, as we will show, must be described by a mixed state. We will also prove that these mixed states give the correct oscillation phase, even outside the degenerate mass approximation. We focus here on the process given by Eq. (A.16), but our considerations are valid more generally. The same caveats regarding uncertainty of the neutrinos masses and momenta still apply.

Consider first the final state of Eq. (A.16), i.e.,

$$|f\rangle \propto \left(\hat{S} - \hat{I}\right)|\mu^+\rangle = \sum_{k,j} A^{\mathrm{P}}_{\mu,e;k,j}\,|e^+, \nu_k, \bar{\nu}_j\rangle + ..., \tag{A.17}$$

The amplitudes in this case are given by

$$A^{\mathrm{P}}_{\mu,e;k,j} = \langle e^+, \nu_k, \bar{\nu}_j|\hat{S}|\mu^+\rangle = U^*_{ek} U_{\mu j} M^{\mathrm{P}}_{k,j}, \tag{A.18}$$

where

$$M^{\mathrm{P}}_{k,j} = -i\,\frac{G_{\mathrm{F}}}{\sqrt{2}} \int \mathrm{d}^4x \langle e^+, \nu_k, \bar{\nu}_j|\hat{\bar{\nu}}_k(x)\gamma^\rho\left(1-\gamma^5\right)\hat{e}(x)\hat{\bar{\mu}}(x)\gamma_\rho\left(1-\gamma^5\right)\hat{\nu}_j(x)|\mu^+\rangle. \tag{A.19}$$

The state given in Eq. (A.17) is entangled with respect to the neutrino sector. To obtain a state for each neutrino we first consider the density matrix

$$\hat{\rho} = |f\rangle\langle f| \equiv N \sum_{k,j,k',j'} A^{\mathrm{P}}_{\mu,e;k,j} A^{\mathrm{P}*}_{\mu,e;k',j'} |e^+, \nu_k, \bar{\nu}_j\rangle\langle e^+, \nu_{k'}, \bar{\nu}_{j'}|, \tag{A.20}$$

with the normalization factor

$$N = \left(\sum_{k,j} |A^{\mathrm{P}}_{\mu,e;k,j}|^2\right)^{-1} = \left(\sum_{k,j} |U_{ek}|^2 |U_{\mu j}|^2 |M^{\mathrm{P}}_{k,j}|^2\right)^{-1}, \tag{A.21}$$

guaranteeing that the density matrix has unit trace. Now we take the partial trace over the neutrino and the anti-neutrino and use Eq. (A.18) to obtain the reduced density matrices $\hat{\rho}_{\nu_e}$ and $\hat{\rho}_{\bar{\nu}_\mu}$, given by

$$\hat{\rho}_{\nu_e} = N \sum_j |U_{\mu j}|^2 \sum_{k,k'} U^*_{ek} U_{ek'} M^{\mathrm{P}}_{k,j} M^{\mathrm{P}*}_{k',j} |\nu_k\rangle\langle\nu_{k'}|, \tag{A.22}$$

$$\hat{\rho}_{\bar{\nu}_\mu} = N \sum_k |U_{ek}|^2 \sum_{j,j'} U_{\mu j} U^*_{\mu j'} M^{\mathrm{P}}_{k,j} M^{\mathrm{P}*}_{k,j'} |\bar{\nu}_j\rangle\langle\bar{\nu}_{j'}|. \tag{A.23}$$

Before continuing, we note that it is easily seen in the degenerate mass limit that these density matrices reduce to the expected ones, i.e.,

$$\hat{\rho}_{\nu_e} \simeq \left(\sum_k U^*_{ek}|\nu_k\rangle\right)\left(\sum_{k'} U_{ek'}\langle\nu_{k'}|\right), \tag{A.24}$$

$$\hat{\rho}_{\bar{\nu}_\mu} \simeq \left(\sum_j U_{\mu j}|\bar{\nu}_j\rangle\right)\left(\sum_{j'} U^*_{\mu j'}\langle\bar{\nu}_{j'}|\right), \tag{A.25}$$

since all amplitudes given in Eq. (A.18) are degenerate over the different neutrinos masses indexed by i and k.

To calculate the oscillation phase we must consider a detection process of the type

$$\nu_\mu + D_I \to \mu^- + D_F. \tag{A.26}$$

First we evolve the neutrino density matrix by a spatio-temporal translation, i.e.,

$$\mathscr{U}(T,\vec{L}) \equiv e^{-i\hat{p}_0 T + i\vec{\hat{p}}\cdot\vec{L}} \tag{A.27}$$

giving

$$\begin{aligned}\hat{\rho}_{\nu_e}(T,\vec{L}) &= \mathscr{U}(T,\vec{L})\hat{\rho}_{\nu_e}\mathscr{U}^\dagger(T,\vec{L}) \\ &= N\sum_j |U_{\mu j}|^2 \sum_{k,k'} U^*_{ek}U_{ek'}M^{\mathrm{P}}_{k,j}M^{\mathrm{P}*}_{k',j} \\ &\quad\times \exp\left[-i(E_k - E_{k'})T\right. \\ &\quad\left.+\, i(\vec{p}_k - \vec{p}_{k'})\cdot\vec{L}\right]|\nu_k\rangle\langle\nu_{k'}|,\end{aligned} \tag{A.28}$$

where T and $\vec{L}$ are the time and displacement of the neutrinos during propagation, $E_k = +\sqrt{m_k^2 + |\vec{p}_k|^2}$ and $\vec{p}_k$ is the momentum of ν_k. Now we calculate the probability of this neutrino being in the state $|\nu^{\mathrm{D}}_\mu\rangle$, i.e.,

$$P_{\nu_e\to\nu_\mu} = \mathrm{Tr}\left[\hat{\rho}_{\nu_e}(T,\vec{L})|\nu^{\mathrm{D}}_\mu\rangle\langle\nu^{\mathrm{D}}_\mu|\right], \tag{A.29}$$

where the state $|\nu^{\mathrm{D}}_\mu\rangle$ is defined by applying the procedure described in Sec. A.1 to Eq. (A.26). We also assume for simplicity that the neutrinos propagate all in the same direction (see section 8.1.3 of Ref. [44] for a discussion regarding this point) and have approximately the same momenta $\vec{p}$. In the relativistic approximation where $T \approx |\vec{L}|$, we can use that

$$-E_k T + \vec{p}_k\cdot\vec{L} \approx -m_k^2|\vec{L}|/(2E), \tag{A.30}$$

where $E \approx |\vec{p}|$, giving finally

$$P_{\nu_e \to \nu_\mu} = \sum_{j,k,k'} |U_{\mu j}|^2 \left[\frac{M^{\mathrm{D}}_k M^{\mathrm{D}*}_{k'}}{\left(\sum_i |U_{\mu i}|^2 |M^{\mathrm{D}}_{\mu,i}|^2 \right)} \right] \left[\frac{M^{\mathrm{P}}_{k,j} M^{\mathrm{P}*}_{k',j}}{\left(\sum_{a,b} |U_{ea}|^2 |U_{\mu b}|^2 |M^{\mathrm{P}}_{a,b}|^2 \right)} \right] \times U^*_{ek} U_{\mu k} U_{ek'} U^*_{\mu k'} \exp\left\{ \left(-i \frac{\Delta m^2_{kk'} |\vec{L}|}{2E} \right) \right\}, \tag{A.31}$$

which gives the correct oscillation phase. Moreover, it also reduces to the usual phase for the degenerate mass case. The concepts outlined here are also useful to define, in the QFT framework, states for reactions involving heavy or sterile neutrinos. We refer the interested reader to [4] for more details and for full calculations in these cases, which fall outside the scope of this thesis.

APPENDIX B

Mathematica© code used for calculating amplitudes of Chapter 3

Here we present the computer code used in obtaining various results throughout this thesis.

B.1 Code used for calculating Eq. (3.24)

```
(* Initialization commands *)

SetOptions[$FrontEnd, ShowCellLabel → False];

Clear[τ1, τ2, k1i, k2i, k3i, mi, ωi, k1β, k2β, k3β, mβ, ωβ];

$Conjugate[x_]:=x/.Complex[a_, b_] :→ a − Ib;

(*Definitions*)
```

$$\gamma 0 = \begin{pmatrix} 1 & 0 & 0 & 0 \\ 0 & 1 & 0 & 0 \\ 0 & 0 & -1 & 0 \\ 0 & 0 & 0 & -1 \end{pmatrix}; \gamma 1 = \begin{pmatrix} 0 & 0 & 0 & 1 \\ 0 & 0 & 1 & 0 \\ 0 & -1 & 0 & 0 \\ -1 & 0 & 0 & 0 \end{pmatrix};$$

$$\gamma 2 = \begin{pmatrix} 0 & 0 & 0 & -I \\ 0 & 0 & I & 0 \\ 0 & I & 0 & 0 \\ -I & 0 & 0 & 0 \end{pmatrix}; \gamma 3 = \begin{pmatrix} 0 & 0 & 1 & 0 \\ 0 & 0 & 0 & -1 \\ -1 & 0 & 0 & 0 \\ 0 & 1 & 0 & 0 \end{pmatrix};$$

```
γ5 = IDot[γ0, Dot[γ1, Dot[γ2, γ3]]];
```

$$W[\omega\_, k1\_, k2\_, k3\_]:= \begin{pmatrix} \omega & 0 & -k3 & -k1 + ik2 \\ 0 & \omega & -k1 - ik2 & k3 \\ k3 & k1 - ik2 & -\omega & 0 \\ k1 + ik2 & -k3 & 0 & -\omega \end{pmatrix}; up = \begin{pmatrix} 1 \\ 0 \\ 0 \\ 0 \end{pmatrix}; ud = \begin{pmatrix} 0 \\ 1 \\ 0 \\ 0 \end{pmatrix};$$

```
Ubarpwps[ω_, k1_, k2_, k3_, m_]:=Dot[ConjugateTranspose[Dot[(W[ω, k1, k2, k3]
+mIdentityMatrix[4]), up]], γ0]/Sqrt[(2ω(ω + m))];
FullSimplify[%];
Ubarpwms[ω_, k1_, k2_, k3_, m_]:=Dot[ConjugateTranspose[Dot[(W[ω, k1, k2, k3]
+mIdentityMatrix[4]), ud]], γ0]/Sqrt[(2ω(ω + m))];
FullSimplify[%];
```

```
Umwps[ω_,k1_,k2_,k3_,m_]:=Dot[(W[ω,k1,k2,k3]
−mIdentityMatrix[4]),up]/Sqrt[(2ω(ω−m))];
FullSimplify[%];
Umwms[ω_,k1_,k2_,k3_,m_]:=Dot[(W[ω,k1,k2,k3]
−mIdentityMatrix[4]),ud]/Sqrt[(2ω(ω−m))];
FullSimplify[%];
```

$$M1 = \begin{pmatrix} 1 & 0 & -1 & 0 \\ 0 & 1 & 0 & -1 \\ 1 & 0 & -1 & 0 \\ 0 & 1 & 0 & -1 \end{pmatrix}; M2 = \begin{pmatrix} -1 & 0 & 1 & 0 \\ 0 & 1 & 0 & -1 \\ -1 & 0 & 1 & 0 \\ 0 & 1 & 0 & -1 \end{pmatrix};$$

```
(* Calculating amplitudes and probabilities *)

Ipp[τ1_]:=2^(−1)Refine[Flatten[Exp[aτ1]Dot[Ubarpwps[ωi,k1i,k2i,k3i,mi],
Dot[(M1−M2),Umwms[ωβ,k1β,k2β,k3β,mβ]]]
+Exp[−aτ1]Dot[Ubarpwps[ωi,k1i,k2i,k3i,mi],
Dot[(M1+M2),Umwms[ωβ,k1β,k2β,k3β,mβ]]],1][[1]],
Element[{ωi,k1i,k2i,k3i,mi,ωβ,k1β,k2β,k3β,mβ},Reals]];
P1 = Ipp[τ1] * $Conjugate[Ipp[τ2]]//FullSimplify;

Ipm[τ1_]:=2^(−1)Refine[Flatten[Exp[aτ1]Dot[Ubarpwps[ωi,k1i,k2i,k3i,mi],
Dot[(M1−M2),Umwps[ωβ,k1β,k2β,k3β,mβ]]]
+Exp[−aτ1]Dot[Ubarpwps[ωi,k1i,k2i,k3i,mi],
Dot[(M1+M2),Umwps[ωβ,k1β,k2β,k3β,mβ]]],1][[1]],
Element[{ωi,k1i,k2i,k3i,mi,ωβ,k1β,k2β,k3β,mβ},Reals]];
P2 = Ipm[τ1] * $Conjugate[Ipm[τ2]]//FullSimplify;

Imp[τ1_]:=2^(−1)Refine[Flatten[Exp[aτ1]Dot[Ubarpwms[ωi,k1i,k2i,k3i,mi],
Dot[(M1−M2),Umwms[ωβ,k1β,k2β,k3β,mβ]]]
+Exp[−aτ1]Dot[Ubarpwms[ωi,k1i,k2i,k3i,mi],
Dot[(M1+M2),Umwms[ωβ,k1β,k2β,k3β,mβ]]],1][[1]],
Element[{ωi,k1i,k2i,k3i,mi,ωβ,k1β,k2β,k3β,mβ},Reals]];
```

```
P3 = Imp[τ1] * $Conjugate[Imp[τ2]]//FullSimplify;

Imm[τ1_]:=2^(-1)Refine[Flatten[Exp[aτ1]Dot[Ubarpwms[ωi,k1i,k2i,k3i,mi],
Dot[(M1 - M2),Umwps[ωβ,k1β,k2β,k3β,mβ]]]
+Exp[-aτ1]Dot[Ubarpwms[ωi,k1i,k2i,k3i,mi],
Dot[(M1 + M2),Umwps[ωβ,k1β,k2β,k3β,mβ]]],1][[1]],
Element[{ωi,k1i,k2i,k3i,mi,ωβ,k1β,k2β,k3β,mβ},Reals]];
P4 = Imm[τ1] * $Conjugate[Imm[τ2]]//FullSimplify;

(* Summing over the spins *)

Result = (P1 + P2 + P3 + P4)//FullSimplify;

(* Making coordinate changes and boosting both the neutrino and the positron *)

τ1 = s + (σ/2); τ2 = s - (σ/2);

k1i = Sqrt[ωi^2 - k2i^2 - k3i^2 - mi^2];
k1β = Sqrt[ωβ^2 - k2β^2 - k3β^2 - mβ^2];

(*pstandsforprime," ' "*)

ωi = ωipCosh[as] + k3ipSinh[as];
k3i = ωipSinh[as] + k3ipCosh[as];
ωβ = ωβpCosh[as] + k3βpSinh[as];
k3β = ωβpSinh[as] + k3βpCosh[as];

(* Final result *)

FullSimplify[Result]
```

B.2 Code used for obtaining the spin sums in Eq. (3.51) and subsequent similar calculations

```
SetOptions[$FrontEnd, ShowCellLabel → False];

$Conjugate[x_]:=x/.Complex[a_, b_] :→ a − Ib;

Clear[l];

γ0 = {{1, 0, 0, 0}, {0, 1, 0, 0}, {0, 0, −1, 0}, {0, 0, 0, −1}};
γ1 = {{0, 0, 0, 1}, {0, 0, 1, 0}, {0, −1, 0, 0}, {−1, 0, 0, 0}};
γ2 = {{0, 0, 0, −I}, {0, 0, I, 0}, {0, I, 0, 0}, {−I, 0, 0, 0}};
γ3 = {{0, 0, 1, 0}, {0, 0, 0, −1}, {−1, 0, 0, 0}, {0, 1, 0, 0}};
γ5 = IDot[γ0, Dot[γ1, Dot[γ2, γ3]]];


l[k1_, k2_, m_] = Sqrt[k1^2 + k2^2 + m^2];


Ord[ω_]:=Iω/a;

SI = Dot[γ0, (IdentityMatrix[4] − γ5)];

γ0R = u^(−1)γ0;

up = {{1}, {0}, {1}, {0}};
um = {{0}, {1}, {0}, {−1}};

Upwps[ω_, k1_, k2_, m_]:=Sqrt[(aCosh[πω/a])/(πl[k1, k2, m])] *

Dot[((−(k1/a) * Dot[γ0, γ1] − (k2/a) * Dot[γ0, γ2]+

(m/a) * γ0)BesselK[Ord[ω] + 1/2, l[k1, k2, m] * u]+

I(l[k1, k2, m]/a)Dot[γ0, γ3]BesselK[Ord[ω] − 1/2, l[k1, k2, m] * u]), up];
```

```
Umwps[ω_,k1_,k2_,m_]:=Sqrt[((aCosh[πω/a])/(πl[k1,k2,m]))]*
Dot[((-(k1/a)*Dot[γ0,γ1]-(k2/a)*Dot[γ0,γ2]
+(m/a)*γ0)BesselK[Ord[-ω]+1/2,l[k1,k2,m]*u]
+I(l[k1,k2,m]/a)Dot[γ0,γ3]BesselK[Ord[-ω]-1/2,l[k1,k2,m]*u]),up];

Upwms[ω_,k1_,k2_,m_]:=Sqrt[((aCosh[πω/a])/(πl[k1,k2,m]))]*
Dot[((-(k1/a)*Dot[γ0,γ1]-(k2/a)*Dot[γ0,γ2]
+(m/a)*γ0)BesselK[Ord[ω]+1/2,l[k1,k2,m]*u]
+I(l[k1,k2,m]/a)Dot[γ0,γ3]BesselK[Ord[ω]-1/2,l[k1,k2,m]*u]),um];

Umwms[ω_,k1_,k2_,m_]:=Sqrt[((aCosh[πω/a])/(πl[k1,k2,m]))]*
Dot[((-(k1/a)*Dot[γ0,γ1]-(k2/a)*Dot[γ0,γ2]
+(m/a)*γ0)BesselK[Ord[-ω]+1/2,l[k1,k2,m]*u]
+I(l[k1,k2,m]/a)Dot[γ0,γ3]BesselK[Ord[-ω]-1/2,l[k1,k2,m]*u]),um];

Ubar[v_]:=Dot[$Conjugate[Transpose[v]],γ0]

(*Processa)*)


Dot[Dot[Ubar[Upwps[ωi,k1i,k2i,mi]],SI],Upwps[ωβ,k1β,k2β,mβ]]*
$Conjugate[Dot[Dot[Ubar[Upwps[ωi,k1i,k2i,mi]],SI],Upwps[ωβ,k1β,k2β,mβ]]]+
Dot[Dot[Ubar[Upwps[ωi,k1i,k2i,mi]],SI],Upwms[ωβ,k1β,k2β,mβ]]*
$Conjugate[Dot[Dot[Ubar[Upwps[ωi,k1i,k2i,mi]],SI],Upwms[ωβ,k1β,k2β,mβ]]]+
Dot[Dot[Ubar[Upwms[ωi,k1i,k2i,mi]],SI],Upwps[ωβ,k1β,k2β,mβ]]*
$Conjugate[Dot[Dot[Ubar[Upwms[ωi,k1i,k2i,mi]],SI],Upwps[ωβ,k1β,k2β,mβ]]]+
Dot[Dot[Ubar[Upwms[ωi,k1i,k2i,mi]],SI],Upwms[ωβ,k1β,k2β,mβ]]*
$Conjugate[Dot[Dot[Ubar[Upwms[ωi,k1i,k2i,mi]],SI],Upwms[ωβ,k1β,k2β,mβ]]]//Simplify

(*Processb)*)


Dot[Dot[Ubar[Umwms[ωi,k1i,k2i,mi]],SI],Umwms[ωβ,k1β,k2β,mβ]]*
$Conjugate[Dot[Dot[Ubar[Umwms[ωi,k1i,k2i,mi]],SI],Umwms[ωβ,k1β,k2β,mβ]]]+
Dot[Dot[Ubar[Umwps[ωi,k1i,k2i,mi]],SI],Umwms[ωβ,k1β,k2β,mβ]]*
```

```
$Conjugate[Dot[Dot[Ubar[Umwps[ωi,k1i,k2i,mi]],SI],Umwms[ωβ,k1β,k2β,mβ]]]+
Dot[Dot[Ubar[Umwms[ωi,k1i,k2i,mi]],SI],Umwps[ωβ,k1β,k2β,mβ]]
$Conjugate[Dot[Dot[Ubar[Umwms[ωi,k1i,k2i,mi]],SI],Umwps[ωβ,k1β,k2β,mβ]]]+
Dot[Dot[Ubar[Umwps[ωi,k1i,k2i,mi]],SI],Umwps[ωβ,k1β,k2β,mβ]]*
$Conjugate[Dot[Dot[Ubar[Umwps[ωi,k1i,k2i,mi]],SI],Umwps[ωβ,k1β,k2β,mβ]]]//Simplify

(*Process c)*)


Dot[Dot[Ubar[Umwms[ωi,k1i,k2i,mi]],SI],Upwps[ωβ,k1β,k2β,mβ]]*
$Conjugate[Dot[Dot[Ubar[Umwms[ωi,k1i,k2i,mi]],SI],Upwps[ωβ,k1β,k2β,mβ]]]+
Dot[Dot[Ubar[Umwms[ωi,k1i,k2i,mi]],SI],Upwms[ωβ,k1β,k2β,mβ]]*
$Conjugate[Dot[Dot[Ubar[Umwms[ωi,k1i,k2i,mi]],SI],Upwms[ωβ,k1β,k2β,mβ]]]+
Dot[Dot[Ubar[Umwps[ωi,k1i,k2i,mi]],SI],Upwps[ωβ,k1β,k2β,mβ]]*
$Conjugate[Dot[Dot[Ubar[Umwps[ωi,k1i,k2i,mi]],SI],Upwps[ωβ,k1β,k2β,mβ]]]+
Dot[Dot[Ubar[Umwps[ωi,k1i,k2i,mi]],SI],Upwms[ωβ,k1β,k2β,mβ]]*
$Conjugate[Dot[Dot[Ubar[Umwps[ωi,k1i,k2i,mi]],SI],Upwms[ωβ,k1β,k2β,mβ]]]//Simplify
```

APPENDIX C

Total proper time correspondence

In this appendix we present another way of obtaining the interaction rate for the current given in Chapter 4 using standard (i.e., from inertial observers' point of view) quantum field theory in Minkowski spacetime. This serves a two-fold purpose: firstly, it is an additional check for the results presented and, secondly and more importantly, it clarifies the interpretation of the diverging integral present in Eq. (4.54) as the total Rindler proper time, $\Delta\tau_{\mathrm{R}}$. We use the same setting and notation as presented in Chapter 4.

In the inertial reference frame, we expand the electromagnetic field $\hat{A}_\alpha$ as

$$\hat{A}_\mu = \sum_m \int_0^\infty dk_\perp k_\perp \int_{-\infty}^\infty dk_z \sum_{\epsilon=1}^4 \left(\hat{a}_{\epsilon,\vec{p}} A^{(\epsilon)}_{\mu,\vec{p}} + c.c.\right), \tag{C.1}$$

with $\vec{p} = (m, k_\perp, k_z)$, where ϵ labels the mode polarization, $m \in \mathbb{Z}$, $k_\perp \in [0, +\infty)$, $k_z \in (-\infty, +\infty)$, and we recall the existence of the dispersion relation in the inertial frame $\omega = +\sqrt{k_\perp^2 + k_z^2}$. The normalized physical modes of the electromagnetic field in polar coordinates [solutions of Eq. (4.9) in inertial polar coordinates (t, z, r, ϕ)] are

$$A^{(\epsilon=1)}_{\mu,\vec{p}} = k_\perp^{-1}\left(k_z f_{\vec{p}}, -\omega f_{\vec{p}}, 0, 0\right), \tag{C.2}$$

$$A^{(\epsilon=2)}_{\mu,\vec{p}} = k_\perp^{-1}\left(0, 0, -mr^{-1} f_{\vec{p}}, -ir\partial_r f_{\vec{p}}\right), \tag{C.3}$$

where

$$f_{\vec{p}} = (8\pi^2\omega)^{-1/2} J_m(k_\perp r)\, e^{im\phi} e^{ik_z z} e^{-i\omega t}, \tag{C.4}$$

are solutions to the Klein-Gordon equation in inertial polar coordinates. The distribution of photons seen by inertial observers as a function of the transverse momenta is given by

$$\frac{dN_M}{k_\perp dk_\perp} = \sum_{\epsilon=(1,2),m} \int_{-\infty}^\infty dk_z \, |A_{M,em,\epsilon}|^2, \tag{C.5}$$

where

$$|A_{m,em,\epsilon}| = \left| \int d^4x \sqrt{-g}\, j^\mu \langle \epsilon, \vec{p}|\hat{A}_\mu|0_M\rangle \right|, \tag{C.6}$$

and we recall that the electromagnetic current j^μ in usual inertial coordinates is given by

$$j^\mu(\lambda) = \frac{q}{u^0\sqrt{-g}} u^\mu(\lambda)\delta^3(\vec{x} - \vec{x}_0(\lambda)) \tag{C.7}$$

$$= \frac{q}{Ru^0} u^\mu(\lambda)\delta(r-R)\delta(\phi - \Omega\lambda)\delta\left(z - a^{-1}\cosh(a\lambda)\right) \tag{C.8}$$

where now

$$u^\mu = (u^t, u^x, u^y, u^z) \tag{C.9}$$

$$= \gamma\left(\cosh(a\lambda), -R\Omega\sin(\Omega\lambda), R\Omega\cos(\Omega\lambda), \sinh(a\lambda)\right).$$

We note that Eq. (C.5) [in contrast to Eqs. (4.16) and (4.17)] does not carry any thermal factor

because the Minkowski vacuum, $|0_M\rangle$, is a no-particle state according to inertial observers. The required energy for emitting a photon comes from the external agent maintaining both the linear and the circular accelerated motion. The photon emission amplitudes for both polarizations can be written as (disregarding phases, since both polarizations are summed incoherently)

$$A_{M,em,\epsilon=1} = \langle \epsilon = 1, \vec{p}|\hat{S}_I|0_M\rangle = \frac{qJ_m(k_\perp R)}{2\pi k_\perp \sqrt{2\omega}} \times \int_{-\infty}^{\infty} d\lambda\, h(\lambda)\left[k_z \cosh(a\lambda) - \omega \sinh(a\lambda)\right], \tag{C.10}$$

$$A_{M,em,\epsilon=2} = \langle \epsilon = 2, \vec{p}|\hat{S}_I|0_M\rangle = \frac{qR\Omega J'_m(k_\perp R)}{2\pi\sqrt{2\hbar\omega}} \times \int_{-\infty}^{\infty} d\lambda\, h(\lambda), \tag{C.11}$$

where

$$h(\lambda) = \exp\left\{\left(-im\Omega\lambda - \frac{i}{a}\left[k_z \cosh(a\lambda) - \omega \sinh(a\lambda)\right]\right)\right\},$$

and we recall that λ is related to the inertial time by $t = a^{-1}\sinh(a\lambda)$, i.e., λ is the proper time of a Rindler observer located at $\xi = 0$ (note that the proper time of the charge is different due to the transversal motion). Expressing everything in terms of this particular observer's proper time will allow us to factor out the total proper time $\Delta\tau_{\mathrm{R}}$ in the emitted photon number.

In order to obtain the total emitted photon number per fixed $k_\perp$, we must square the absolute values of the amplitudes (C.10) and (C.11) and insert them in Eq. (C.5). We proceed in the same way as described in Chapter 3, making the substitutions given by Eqs. (3.22) and (3.23) and boosting in the z direction. Doing so leads us to

$$\frac{dN_M}{k_\perp dk_\perp} = \Delta\tau_R \sum_m \frac{q^2}{8\pi^2}\int d\sigma \int dk_z \times \left[(\mathscr{N}_I + \mathscr{N}_{II})\exp\left[-im\Omega\sigma - 2ia^{-1}\omega\sinh(a\sigma/2)\right]\right], \tag{C.12}$$

with the total proper time being factored out and

$$\mathscr{N}_I = \frac{|J_m(k_\perp R)|^2}{\omega}\left[\left(\frac{\omega}{k_\perp}\right)^2 - \cosh^2\left(\frac{a\sigma}{2}\right)\right], \tag{C.13}$$

$$\mathscr{N}_{II} = \frac{|J'_m(k_\perp R)|^2}{\omega}(R\Omega)^2. \tag{C.14}$$

These integrals can be solved using the same techniques used in Chapter 2 and Chapter 3. Their results for a fixed value of m are

$$\frac{dN_M^{m,\epsilon=1}}{k_\perp dk_\perp} = \Delta\tau_R \frac{q^2}{2\pi^2 a}|J_m(k_\perp R)|^2\left|K'_{\frac{im\Omega}{a}}\left(\frac{k_\perp}{a}\right)\right|^2 e^{\frac{\pi m\Omega}{a}}. \tag{C.15}$$

and

$$\frac{dN_M^{m,\epsilon=2}}{k_\perp dk_\perp} = \Delta\tau_R \frac{q^2R^2\Omega^2}{2\pi^2 a}|J'_m(k_\perp R)|^2 \left|K_{\frac{im\Omega}{a}}\left(\frac{k_\perp}{a}\right)\right|^2 e^{\frac{\pi m\Omega}{a}}. \tag{C.16}$$

Summing both results and summing in m we obtain

$$\begin{aligned}\frac{dN_M}{k_\perp dk_\perp} &= \Delta\tau_{\rm R}\frac{q^2}{\pi^2 a}\sum_m \Theta(m)\left[|K'_{im\Omega/a}(k_\perp/a)|^2\right. \\ &\times|J_m(k_\perp R)|^2 + (R\Omega)^2|K_{im\Omega/a}(k_\perp/a)|^2|J'_m(k_\perp R)|^2\left.\right] \\ &\times\cosh\left[\frac{\pi m\Omega}{a}\right],\end{aligned} \tag{C.17}$$

which coincides with Eq. (4.54) provided we make the identification

$$\Delta\tau_{\rm R} \leftrightarrow \left(\frac{4\pi}{a}\int_{-\infty}^{\infty}\frac{d\kappa_z}{\left(1+\kappa_z^2\right)^{1/2}}\right). \tag{C.18}$$

As noted before, this divergence originates in the infinite duration in the accelerated part of the current spacetime trajectory. This would not be the case in a real experiment and no divergence would appear. On the other hand, the non-stationarity of the situation would make the emission rate different from the one presented above. Our results would give a good description of this situation only under the conditions discussed in the main text.

Bibliography

[1] Gabriel Cozzella, André G. S. Landulfo, George E. A. Matsas, and Daniel A. T. Vanzella. Proposal for observing the Unruh effect using classical electrodynamics. *Phys. Rev. Lett.*, 118:161102, 2017.

[2] Gabriel Cozzella, Andre G. S. Landulfo, George E. A. Matsas, and Daniel A. T. Vanzella. A quest for a "direct" observation of the Unruh effect with classical electrodynamics: In honor of Atsushi Higuchi 60th anniversary. *Int. J. Mod. Phys.*, D27(11):1843008, 2018.

[3] Gabriel Cozzella, Stephen A. Fulling, André G. S. Landulfo, George E. A. Matsas, and Daniel A. T. Vanzella. Unruh effect for mixing neutrinos. *Phys. Rev. D*, 97:105022, 2018.

[4] Gabriel Cozzella and Carlo Giunti. Mixed states for mixing neutrinos. *Phys. Rev. D*, 98:096010, 2018.

[5] M. D. Schwartz. *Quantum field theory and the standard model*. Cambridge Univ. Press, Cambridge, 2014.

[6] Alessandro Codello and Rajeev K. Jain. On the covariant formalism of the effective field theory of gravity and leading order corrections. *Classical and Quantum Gravity*, 33(22):225006, 2016.

[7] R. M. Wald. *General relativity*. Chicago Univ. Press, Chicago, 1984.

[8] N. D. Birrell and P. C. W. Davies. *Quantum fields in curved space*. Cambridge Univ. Press, Cambridge, 1982.

[9] R. M. Wald. *Quantum field theory in curved spacetime and black hole thermodynamics*. Chicago Univ. Press, Chicago, 1994.

[10] L. E. Parker and D. J. Toms. *Quantum field theory in curved spacetime: quantized fields and gravity*. Cambridge Univ. Press, Cambridge, 2009.

[11] S. A Fulling. *Aspects of quantum field theory in curved space-time*. Cambridge Univ. Press, Cambridge, 1989.

[12] V. F. Mukhanov and S. Winitzki. *Introduction to quantum effects in gravity*. Cambridge Univ. Press, Cambridge, 2007.

[13] Stefan Hollands and Robert M. Wald. Quantum fields in curved spacetime. *Physics Reports*, 574(1), 2015.

[14] Bei Lok Hu and Enric Verdaguer. Stochastic gravity: Theory and applications. *Living Reviews in Relativity*, 11(3), 2008.

[15] D. Oriti. *Approaches to quantum gravity: toward a new understanding of space, time and matter*. Cambridge University Press, Cambridge, 2009.

[16] Stephen W. Hawking. Particle creation by black holes. *Comm. Math. Phys.*, 43(3):199, 1975.

[17] William G. Unruh. Notes on black-hole evaporation. *Phys. Rev. D*, 14:870, 1976.

[18] R. Ruffini. *Proceedings of Marcel Grossmann Meeting on General Relativity, 1st, Trieste, 1975*. North-Holland Publishing Company, Amsterdam, 1977.

[19] Stephen A. Fulling. Nonuniqueness of canonical field quantization in Riemannian space-time. *Phys. Rev. D*, 7:2850–2862, 1973.

[20] Atsushi Higuchi, George E. A. Matsas, and Daniel Sudarsky. Bremssstrahlung and zero-energy Rindler photons. *Phys. Rev. D*, 45:R3308–R3311, 1992.

[21] Luis C. B. Crispino, Atsushi Higuchi, and George E. A. Matsas. The Unruh effect and its applications. *Rev. Mod. Phys.*, 80:787, 2008.

[22] Cesar A. U. Lima, Frederico Brito., José A. Hoyos, and Daniel A. T. Vanzella. Probing the Unruh effect with an accelerated extended system. *Nature Communications*, 10(3030), 2019.

[23] Ulf Leonhardt, Itay Griniasty, Sander Wildeman, Emmanuel Fort, and Mathias Fink. Classical analog of the Unruh effect. *Phys. Rev. A*, 98:022118, 2018.

[24] John S. Bell and Jon M. Leinaas. Electrons as accelerated thermometers. *Nuclear Physics B*, 212(1), 1983.

[25] Dharam V. Ahluwalia, Lance Labun, and Giorgio Torrieri. Neutrino mixing in accelerated proton decays. *Eur. Phys. J.*, A52(7):189, 2016.

[26] Larry H. Ford. Quantum field theory in curved space-time. In *Particles and fields. Proceedings, 9th Jorge Andre Swieca Summer School, Campos do Jordao, Brazil, February 16-28, 1997*, page 345, 1997.

[27] Nikolay N. Bogoliubov. On a new method in the theory of superconductivity. *Il Nuovo Cimento (1955-1965)*, 7(6):794, 1958.

[28] A. Gradshteyn, I. S. Jeffrey and I. M. Ryzhik. *Table of integrals, series, and products*. Academic Press, New York, 1980.

[29] Werner Israel and Stephen W. Hawking. *General relativity: an Einstein centenary survey*. Cambridge Univ. Press, Cambridge, 1979.

[30] Eduardo Martín-Martínez, Tales R. Perche, and Bruno de S. L. Torres. General relativistic quantum optics: Finite-size particle detector models in curved spacetimes. *Phys. Rev. D*, 101:045017, 2020.

[31] Petar Simidzija, Aida Ahmadzadegan, Achim Kempf, and Eduardo Martín-Martínez. Transmission of quantum information through quantum fields. *Phys. Rev. D*, 101:036014, 2020.

[32] Jorma Louko and Alejandro Satz. How often does the Unruh-DeWitt detector click? Regularization by a spatial profile. *Classical and Quantum Gravity*, 23(22):6321, 2006.

[33] Atsushi Higuchi, George E. A. Matsas, and Clovis B. Peres. Uniformly accelerated finite-time detectors. *Phys. Rev. D*, 48:3731, 1993.

[34] William G. Unruh and Robert M. Wald. What happens when an accelerating observer detects a Rindler particle. *Phys. Rev. D*, 29:1047, 1984.

[35] Daniel A. T. Vanzella and George E. A. Matsas. Decay of accelerated protons and the existence of the Fulling-Davies-Unruh Effec t. *Phys. Rev. Lett.*, 87:151301, 2001.

[36] Y. Fukuda et al. Evidence for oscillation of atmospheric neutrinos. *Phys. Rev. Lett.*, 81:1562, 1998.

[37] Q. R. Ahmad et al. Direct evidence for neutrino flavor transformation from neutral-current interactions in the Sudbury neutrino observatory. *Phys. Rev. Lett.*, 89:011301, 2002.

[38] Massimo Blasone, Gaetano Lambiase, Giuseppe G. Luciano, and Luciano Petruzziello. Role of neutrino mixing in accelerated proton decay. *Phys. Rev. D*, 97:105008, 2018.

[39] Hisao Suzuki and Kunimasa Yamada. Analytic evaluation of the decay rate for an accelerated proton. *Phys. Rev. D*, 67:065002, 2003.

[40] Carlo Giunti. Fock states of flavor neutrinos are unphysical. *Eur. Phys. J. C*, 39(3):377, 2005.

[41] Boris Kayser. On the quantum mechanics of neutrino oscillation. *Phys. Rev. D*, 24:110, 1981.

[42] Bruno Pontecorvo. Mesonium and antimesonium. *Sov. Phys. JETP*, 6:429, 1957.

[43] Ziro Maki, Masami Nakagawa, and Shoichi Sakata. Remarks on the unified model of elementary particles. *Prog. Theor. Phys.*, 28:870, 1962.

[44] C. Giunti and C. W. Kim. *Fundamentals of Neutrino Physics and Astrophysics*. Oxford University Press, Oxford, 2007.

[45] Ralf Schützhold, Gernot Schaller, and Dietrich Habs. Signatures of the Unruh effect from electrons accelerated by ultrastrong laser fields. *Phys. Rev. Lett.*, 97:121302, 2006.

[46] A. Zangwill. *Modern electrodynamics*. Cambridge Univ. Press, Cambridge, 2013.

[47] X. J. Wang. In *Proceedings, 1999 Particle Accelerator Conference (PAC'99)*, Piscataway, 1999. IEEE.

[48] T. P. Wangler. *RF Linear Accelerators*. Wiley-VCH, Weinheim, 2008.

[49] André G. S. Landulfo, Stephen A. Fulling, and George E. A. Matsas. Classical and quantum aspects of the radiation emitted by a uniformly accelerated charge: Larmor-Unruh reconciliation and zero-frequency Rindler modes. *Phys. Rev. D*, 100:045020, 2019.

[50] Guilherme B. Barros, João P. C. R. Rodrigues, André G. S. Landulfo, and George E. A. Matsas. Traces of the Unruh effect in surface waves. *Phys. Rev. D*, 101:065015, 2020.

[51] Ulf Leonhardt, Itay Griniasty, Sander Wildeman, Emmanuel Fort, and Mathias Fink. Classical analog of the Unruh effect. *Phys. Rev. A*, 98:022118, 2018.

[52] Kajol Paithankar and Sanved Kolekar. Role of the Unruh effect in bremsstrahlung. *Phys. Rev. D*, 101:065012, 2020.

[53] Carlo Giunti, Chung W. Kim, and Ung W. Lee. Remarks on the weak states of neutrinos. *Phys. Rev. D*, 45:2414, 1992.